University of Warsaw

Doctoral Thesis

Transition properties from the Hermitian formulation of the coupled cluster response theory

Aleksandra Tucholska

Thesis supervisor prof. Robert Moszyński

A thesis submitted in partial fulfillment
of the requirements for the degree of
Doctor of Philosophy in Chemistry

Warsaw
2018

Uniwersytet Warszawski

Praca Doktorska

Momenty przejścia w hermitowskim sformułowaniu teorii odpowiedzi sprzężonych klasterów

Aleksandra Tucholska

Promotor: prof. Robert Moszyński

Praca doktorska wykonana w Pracowni Chemii Kwantowej
Wydziału Chemii Uniwersytetu Warszawskiego
pod kierunkiem prof. dr. hab. Roberta Moszyńskiego

Warszawa
2018

Acknowledgements

First and foremost I would like to thank my supervisor Prof. Robert Moszyński for guidance, support and believing in me. Thanks to Dr. Michał Lesiuk for providing me with one- and two-electron integrals in the Slater orbital basis set. I would also like to thank my colleagues from Quantum Chemistry Laboratory in Warsaw for many insightful discussions and for creating a supportive work atmosphere, especially room 506. Last but not least, thanks to Dr. Marcin Modrzejewski for countless scientific discussions and programming guidance.

Contents

Chapter 1 Introduction

In this work I propose a complete theory for the computation of the electronic transition properties based on the coupled cluster model. The theory is presented with the use of dipole, quadrupole, and spin-orbit operators, though in general this theory is suitable for any one-electron operator. Singlet-singlet, triplet-triplet, and spin-forbidden singlet-triplet transitions are presented in the coupled cluster theory restricted to single and double excitations (CCSD) and single, double, and linear triple excitations (CC3). All the theory presented here is programmed in a standalone Fortran code that allows for an easy extension for the computation of other properties. The results are obtained with the use of both Gaussian and Slater basis sets.

1.1 Molecular properties

Physical properties of atoms and molecules are intrinsic features of matter. They describe its basic attributes like mass, electric charge, atomic radius, as well as more complex ones, like ionization energy, electron affinity, multipole moments, polarizabilities, intermolecular forces, or transition properties.

The experimental approach involves application of an external electromagnetic field on a molecule and measurement of the response of the system–scattering or absorption. As a result, one gets a deep insight into the electronic structure, time-dependent phenomena, and processes undergoing in the studied system, provided that the results are properly understood.

The development of quantum physics allowed to understand why many physical phenomena occur and how to model them. The support of computational methods is especially important in spectroscopy, where the experimental measurements can lead to rich and difficult to interpret results. Indeed, the theoretical assistance proved to be of a great help in the rotational, vibrational, ultraviolet–visible, magnetic–resonance, and other spectroscopies.

To this day numerous *ab initio* methods for modeling of the electronic structure were developed. The most widely used, configuration interaction (CI), Møller–Plesset perturbation theory (MP) also known as the many-body perturbation theory (MBPT), coupled cluster (CC), and density matrix renormalization group (DMRG) are used to describe the energetics, structure, and properties of many electron systems. Researchers can access them through the computational packages like Molpro,[1] Dalton,[2] NWChem, Gamess, KOŁOS, etc.

The starting point of most *ab initio* methods for the property computation in quantum chemistry is the response theory. This is the case since many physical observables can be derived from the response functions. Since the early works of Zubarev[3] in the field of statistical physics, the response theory has proved itself as one of the most important tools for the calculation of the molecular properties.[4–6]

Considering the system described by the time-dependent Hamiltonian $H(t)$

$$H(t) = H_0 + V(t), \tag{1.1}$$

where H_0 is an unperturbed Hamiltonian and $V(t)$ is the time-dependent perturbation, one can expand the time-dependent expectation value of an observable X in terms of the perturbation $V(t)$. The response functions are then defined as the coefficients in this expansion: linear, quadratic, cubic, and higher order response functions.

The most studied is the linear response function, as it describes properties like frequency-dependent polarizability, Van der Waals coefficients, or transition moments from the ground to the excited states. Among many valuable computational schemes for the linear response function it is worthwhile to mention: time-dependent Hartree-Fock method[7] equivalent to the random phase approximation (RPA),[8] multiconfigurational Hartree-Fock approach[9] or MP methods.[10,11] The coupled cluster approach was initiated by Monkhorst in 1977,[12,13] and later extended by Bartlett,[14] Paldus,[15] and Koch and Jørgensen.[16] This approach is referred to as time-dependent coupled cluster approach (TD-CC). In 2005 Moszynski et al.[17] proposed a novel coupled cluster approach for the computation of the linear response function. This work became the basis for the further developments: the derivation of transition moments from the ground state, done by Tucholska et al.[18] and quadratic response function and transition moments between the excited states.[19] This theory and its extension to the spin-orbit coupling matrix elements is the main subject of the present thesis.

1.2 Coupled cluster theory

The coupled cluster theory (CC)[20,21] is the gold standard among the quantum chemical wave function based methods for the description of the electronic structure of small and medium-sized systems. The hierarchy of approximations in the CC theory provides an effective description of the electron correlation while retaining the size consistency.[22]

CC theory has its origins in the many-body perturbation theory (MBPT).[23,24] It inherits the advantages of the MBPT theory, e.g., size extensivity and the computational cost lower than the configuration interaction methods, but does not rely on the assumption that the perturbation introduced by the electron correlation is small and does not suffer from poor convergence.

The coupled cluster Ansatz

$$\Psi = e^T\Phi, \tag{1.2}$$

where Φ is a reference determinantal function and T is is the coupled cluster excitation operator, was popularized in quantum chemistry by Čížek.[20] Subsequently, numerous applications of the method were reported[25] and general purpose programs[26,27] began to appear. To this day, the CC theory remains one of the most reliable *ab initio* methods. It is routinely used for the computation of correlated ground-state energies,[28] molecular properties,[29–31] excited-state properties,[32] and analytical gradients.[33] It is applied with a great success to atoms, molecules, polymers,[34,35] solids, and even nuclei.[36,37]

Most importantly, the CC theory is an invaluable tool in the computations requiring spectroscopic precision such as studies of atoms and molecules in the ultracold regime ($<$ 1 mK). Until recently, properties of the excited electronic states were not easily available in high-resolution experiments, but with the advances of new spectroscopic techniques in the hot pipe[38–42] and ultracold experiments,[43–47] more and more accurate experimental data become available and possibly need theoretical interpretation. Theoretical information about the transition moments between the excited states is also necessary to propose new routes to obtain molecules in the ground rovibrational state (see, e.g., Ref. 48). Last but not least, excited states properties define the asymptotics of the excited state interaction potentials,[49] and play an unexpectedly important role in the dynamics of nuclear motions in the presence of external fields.[50]

1.3 Spin-orbit interaction

Spin-induced radiative dipole transitions play a crucial for determining atomic and molecular lifetimes, especially for heavy atoms, where the spin-orbit interaction is very strong.[51] It is responsible for two important effects. First one, known as the fine structure splitting, lifts the degeneracies in the multiplet levels. With the increase of the nuclear charge the energy separation between multiplet levels grows, and for heavy atoms becomes comparable to the energy separation between different electronic states. The second impact on the electronic structure is the mixing of the states with different multiplicities causing radiative (phosphorescence) and nonradiative (intersystem crossing) decays. For light atoms the radiative spin-forbidden transitions are usually negligible compared to the E1 transitions, but with the increase of the atomic number, the contributions of the spin-forbidden transitions become crucial for the lifetimes computations.

The simultaneous accurate description of the spin-orbit effect and the electron correlation is challenging because the SO interaction is dominated by single excitations, and these are less important for the correlation energy. The use of the CC3 approximation allows us to overcome this problem, as the single excitation are treated in a special way in this model.

The Dirac-Coulomb-Breit Hamiltonian is a multiparticle, four-component operator, not suited for fast and effective chemical applications. The common practice is to approximate H_{DCB} by two-component operators with spin-dependent and spin-free (scalar relativistic) parts separated. This can be done on various levels, full one- and two-electron Hamiltonians, valence-only Hamiltonians or effective one-electron Hamiltonians.

In the first group, the most popular is the Breit-Pauli spin-orbit Hamiltonian. It was first derived by Pauli in 1927,[52] who considered a molecule in an external electromagnetic field. This BP Hamiltonian can only be used in a perturbation approach as it is unbounded from below and can lead to a variational collapse.[51] Although in this work we are focused on the perturbative inclusion of the spin-orbit operator, we are not using the BP Hamiltonian as it requires computation of two-electron spin-orbit integrals, which are complex, have almost no permutational symmetry, and thus cannot effectively be used for heavy element computations.[53,54]

Alternatively one can further approximate H_{DCB}, by reducing the number of electrons used in the computations. These are called frozen-core approximations, not considered in the present work.

The third group consists of the mean-field spin-orbit coupling operators, empirical one-electron operators, and spin-orbit coupling operators for effective core potential (SO ECP). The last approximation was first introduced by Pitzer[55] and Schwartz,[56] and is used in this work in a Pitzer and Winter formulation.[57] The effective Hamiltonian is given by

$$H_{\mathrm{SO}}(r) = \sum_{K}^{N_{el}} \sum_{l=1} P_l \xi_l(r_k) \vec{l} \cdot \vec{s} P_l \tag{1.3}$$

where $\xi_l(r)$ is a radial potential and $P_l = \sum_{m_l} |l, m_l\rangle \langle l, m_l|$ is the projection operator onto one electron functions with angular momentum l with respect to the given pseudopotential center.

1.4 Motivation and objectives of the thesis

In high resolution spectroscopy, the interpretation of the experimental spectra requires theory that effectively includes both the relativistic effects and electron correlation at a high level. Relativistic effects, especially the spin-orbit interaction (SO), are responsible for the fine structure splitting, existence of intercombination transitions, and phosphorescence. They also affect the shape of the potential energy surfaces of systems containing heavy atoms.

Thanks to the accuracy and universality of the coupled cluster methods, CC is a desired choice for spectroscopic applications. To this day, there is no universal *ab initio* method that can routinely be applied in a black box manner for the computation of the transition matrix elements.

Currently, there exists two coupled cluster approaches combined with the response theory. First one, developed in 1990's by Koch et al.[16,29,58,59] is formulated using the time-averaged quasi-energy Lagrangian technique. Within this approach, the authors proposed expressions for the linear, quadratic, and cubic response functions,[59] transition moments,[60] spin-orbit coupling matrix elements,[61,62] and many other properties,[63] at the CC2 level,[64,65] CCSD level,[58] CC3 level[66,67] and other approximations.

The second one of Jeziorski and Moszyński[68] was proposed in 1993, and started out with an expression for the explicitly connected commutator expression for the expectation value of an observable. Later it was extended by Moszynski et al.[17] to the computation of the polarization propagator. Subsequently, numerous works on the implementation and properties computation appeared.[30,31,69–73] Recently, this theory was applied to the computation of the transition moments for the ground to excited states[18] (Paper I), excited to excited states[19] (Paper II), and spin-orbit coupling matrix elements. CCSD and CC3 approximations were used.

The coupled cluster method based on the response theory of Koch et al.[16,29,58,59] has some drawbacks which need a brief discussion. It requires the solution of iterative equations for the coupled cluster amplitudes as well as for the Lagrange multipliers. It requires computation of both left and right eigenvectors of the CC Jacobian matrix in order to acquire excited states. And most importantly, in some cases it gives nonphysical results for the transition moments and matrix elements between the excited states due to the broken Hermitian symmetry.[17,18,30]

Although these authors try to overcome the broken-symmetry problem and propose the symmetrization[60,74] of the transition strength matrix, it does not work in all of the cases. An analysis of the problematic transitions in various systems was performed by us and can be found in Tucholska et al.[19] and in section 3.5.

In 2002 the authors of the CC response theory proposed an approach[61] for the computation of the radiative dipole transition induced by the spin-orbit coupling. They propose the use of the approximate BP Hamiltonian, and present some numerical values for light molecules. Recently the theory was added to Dalton program,[2] but only in the CCSD approximation. However, this theory cannot be used for heavier atoms, since the computation would be too demanding. Also, the triplet-triplet transitions are not implemented, so the theory does not allow for the lifetime computations in most cases.

Alternatively, one can derive the expressions required for the computation of the CC molecular properties, starting directly from the expectation value,[75] polarization propagator[17] or quadratic response function[19](Paper II). This approach will be denoted throughout this work as XCC (eXpectation value Coupled Cluster). As will become clear later, the XCC theory is much simpler and straightforward, and does not need to use complicated time-dependent formulations.

The XCC method[68] has been employed to compute numerous electronic properties: electrostatic[75] and exchange[76] contributions to the interaction energies of closed-shell systems, first-order molecular properties,[31] frequency-dependent density susceptibilities employed in coupled cluster approach to the symmetry-adapted perturbation theory,[69] static and dynamic dipole polarizabilities,[30] transition properties between the excited states developed by the us in Refs. 19 and 18 (Paper I, Paper II), and the spin-orbit coupling matrix elements, Ref. 77.

While in many cases the XCC method gives similar results to the TD-CC method, we show later in the text that for some transitions the TD-CC method fails dramatically. The different sign of the left and right transition moments results in negative transition strengths and thus lifetimes, which is obviously an unphysical result. On the contrary, the method developed by us is free from this deficiency of TD-CC, and correctly gives nearly equal left and right transition moments.

1.5 Plan of the thesis

This work is composed as follows. First we summarize the basic concepts of the coupled cluster theory for the ground and excited states, and properties computations that are crucial for the understanding how XCC transition properties are computed. Next, we present the derivation of the main XCC equations, show under which conditions the expressions for the transition moments derived in this work are Hermitian and size-intensive. In this chapter we also show how to incorporate the spin-orbit interaction into our working expressions. Next, we describe some technical details including the code for generating automatic, parallel orbital expressions for many complicated CC formulas used in this work. Finally, we show the numerical results for a selected set of atoms and molecules and compare them with the existing approaches and available measurements.

Chapter 2 Basic theory

2.1 Representation of the singly, doubly and triply excited manifold

The excited manifold is generally defined by acting with the excitation operator

$$\mu_n = \underbrace{E_{ai}E_{bj}\dots E_{fm}}_{n\ times} \tag{2.1}$$

on the reference determinant Φ

$$|\mu_n\Phi\rangle \equiv |\mu_n\rangle\,. \tag{2.2}$$

The operators E_{pq} are called generators of the unitary group,[78,79] defined by the creation and annihilation operators $a^\dagger$ and a

$$E_{pq} = a^\dagger_{p\alpha}a_{q\alpha} + a^\dagger_{p\beta}a_{q\beta}, \tag{2.3}$$

where α and β denote the spin up and spin down functions, respectively, and satisfy the following commutation relation

$$[E_{pq}, E_{rs}] = E_{ps}\delta_{rq} - E_{rq}\delta_{ps}. \tag{2.4}$$

Throughout this work we use the following convention: indices $i, j, \dots$ are reserved for the occupied orbitals, indices $a, b, \dots$ denote virtual orbitals, and $p, q, \dots$ are used for general indices. In the particular cases of single, double, and triple excitations, the excitation manifold would be denoted as

$$\begin{aligned} |\mu_1\rangle &\equiv |{}^{a}_{i}\rangle\,, \\ |\mu_2\rangle &\equiv |{}^{ab}_{ij}\rangle\,, \\ |\mu_3\rangle &\equiv |{}^{abc}_{ijk}\rangle\,, \end{aligned} \tag{2.5}$$

respectively. In our work, the ket vectors

$$|{}^{a}_{i}\rangle\,, |{}^{ab}_{ij}\rangle\,, |{}^{abc}_{ijk}\rangle \tag{2.6}$$

form a biorthonormal basis[80] with the adjoints

$$\widetilde{\langle {}^{a}_{i}|} = \frac{1}{2} \langle {}^{a}_{i}| \tag{2.7}$$
$$\widetilde{\langle {}^{ab}_{ij}|} = \frac{1}{1+\delta_{ai,bj}} \left(\frac{1}{3} \langle {}^{ab}_{ij}| + \frac{1}{6} \langle {}^{ab}_{ji}| \right) \qquad \text{for } ai \geq bj$$

The linearly independent biorthogonal singlet basis for the triple excitations is described in Table 2.1. Note that $a > b > c$ and $i > j > k$. Also in any arrangement of indices, the following relations must hold for both the bra and the ket vectors

$$\text{for } \langle {}^{abc}_{ijk}| \text{ and } |{}^{abc}_{ijk}\rangle \qquad ai \geq bj \geq ck \tag{2.8}$$
$$\text{for } \langle {}^{abc}_{jki}| \text{ and } |{}^{abc}_{jki}\rangle \qquad aj \geq bk \geq ci$$
$$\text{etc.} \ldots$$

In our implementation we distinguish four cases:

1. all indices are different ($a \neq b \neq c$ and $i \neq j \neq k$)
2. a single equality among the occupied indices (either $i = j$ or $j = k$ or $i = k$)
3. a single equality among the virtual indices (and an additional constraint on the occupied indices)
4. a single equality among the virtual indices together with a single equality among the occupied indices (and an additional constraint on the occupied indices),

The triplet basis set is spanned by the singlet and triplet excitation operators E_{pq} and T_{pq}, where the following relations are satisfied

$$T_{pq} = a^{\dagger}_{p\alpha} a_{q\alpha} - a^{\dagger}_{p\beta} a_{q\beta} \tag{2.9}$$
$$[T_{mn}, T_{pq}] = E_{mq}\delta_{pn} - E_{pn}\delta_{mq}$$
$$[T_{mn}, E_{pq}] = T_{mq}\delta_{pn} - T_{pn}\delta_{mq}$$

$$\langle\Phi|T_{ia}E_{bj}|\Phi\rangle = 0 \tag{2.10}$$
$$\langle\Phi|E_{ia}T_{bj}|\Phi\rangle = 0$$
$$\langle\Phi|T_{ia}T_{bj}|\Phi\rangle = 2\delta_{ai}\delta_{bj}$$
$$\langle\Phi|E_{ia}E_{bj}|\Phi\rangle = 2\delta_{ai}\delta_{bj}.$$

The triplet basis is given by:

$$|{}^{(3)}\mu_1\rangle = |{}^{(3)}{}^{a}_{i}\rangle = T_{ai}\,|\Phi\rangle \tag{2.11}$$
$$|\mu_{2^+}\rangle = |{}^{(+)}{}^{ab}_{ij}\rangle = (T_{ai}E_{bj} + T_{bj}E_{ai})\,|\Phi\rangle \qquad \text{for } a > cb \text{ and } i > j$$

Table 2.1: Singlet adjoints of the basis for the triple excitations.

case 1 $a \neq b \neq c$ and $i \neq j \neq k$
$\langle \widetilde{{}^{abc}_{ikj}}\| = \frac{1}{4}\langle{}^{abc}_{ikj}\| + \frac{1}{12}\langle{}^{abc}_{jik}\| + \frac{1}{6}\langle{}^{abc}_{jki}\| + \frac{1}{6}\langle{}^{abc}_{kij}\| + \frac{1}{12}\langle{}^{abc}_{kji}\|$
$\langle \widetilde{{}^{abc}_{jik}}\| = \frac{1}{12}\langle{}^{abc}_{ikj}\| + \frac{1}{4}\langle{}^{abc}_{jik}\| + \frac{1}{6}\langle{}^{abc}_{jki}\| + \frac{1}{6}\langle{}^{abc}_{kij}\| + \frac{1}{12}\langle{}^{abc}_{kji}\|$
$\langle \widetilde{{}^{abc}_{jki}}\| = \frac{1}{6}\langle{}^{abc}_{ikj}\| + \frac{1}{6}\langle{}^{abc}_{jik}\| + \frac{1}{3}\langle{}^{abc}_{jki}\| + \frac{1}{6}\langle{}^{abc}_{kij}\| + \frac{1}{6}\langle{}^{abc}_{kji}\|$
$\langle \widetilde{{}^{abc}_{kij}}\| = \frac{1}{6}\langle{}^{abc}_{ikj}\| + \frac{1}{6}\langle{}^{abc}_{jik}\| + \frac{1}{6}\langle{}^{abc}_{jki}\| + \frac{1}{3}\langle{}^{abc}_{kij}\| + \frac{1}{6}\langle{}^{abc}_{kji}\|$
$\langle \widetilde{{}^{abc}_{kji}}\| = \frac{1}{12}\langle{}^{abc}_{ikj}\| + \frac{1}{12}\langle{}^{abc}_{jik}\| + \frac{1}{6}\langle{}^{abc}_{jki}\| + \frac{1}{6}\langle{}^{abc}_{kij}\| + \frac{1}{4}\langle{}^{abc}_{kji}\|$
case 2 $a \neq b \neq c$ and $i > k$
$\langle \widetilde{{}^{abc}_{iki}}\| = \frac{1}{3}\langle{}^{abc}_{iki}\| + \frac{1}{6}\langle{}^{abc}_{kii}\|$ $\quad \langle \widetilde{{}^{abc}_{kii}}\| = \frac{1}{6}\langle{}^{abc}_{iki}\| + \frac{1}{3}\langle{}^{abc}_{kii}\|$
case 3 $a \neq b \neq c$ and $i > j > k$
$\langle \widetilde{{}^{aac}_{ikj}}\| = \frac{1}{3}\langle{}^{aac}_{ikj}\| + \frac{1}{6}\langle{}^{aac}_{jki}\|$ $\quad \langle \widetilde{{}^{aac}_{jki}}\| = \frac{1}{6}\langle{}^{aac}_{ikj}\| + \frac{1}{3}\langle{}^{aac}_{jki}\|$
$\langle \widetilde{{}^{abb}_{jik}}\| = \frac{1}{3}\langle{}^{abb}_{jik}\| + \frac{1}{6}\langle{}^{abb}_{kij}\|$ $\quad \langle \widetilde{{}^{abb}_{kij}}\| = \frac{1}{6}\langle{}^{abb}_{jik}\| + \frac{1}{3}\langle{}^{abb}_{kij}\|$
case 4 $a \neq b \neq c$ and $i > j > k$
$\langle \widetilde{{}^{aac}_{iki}}\| = \frac{1}{2}\langle{}^{aac}_{iki}\|$ $\quad \langle \widetilde{{}^{aac}_{ijj}}\| = \frac{1}{2}\langle{}^{aac}_{ijj}\|$ $\quad \langle \widetilde{{}^{abb}_{jij}}\| = \frac{1}{2}\langle{}^{abb}_{jij}\|$ $\quad \langle \widetilde{{}^{abb}_{iij}}\| = \frac{1}{2}\langle{}^{abb}_{iij}\|$

$$
\begin{aligned}
|\mu_{2^-}\rangle &= |{}^{(-)}{}^{ab}_{ij}\rangle = (T_{ai}E_{bj} - T_{bj}E_{ai})\,|\Phi\rangle \qquad \text{for } ab > ij \\
|{}^{(3)}\mu_3\rangle &= |{}^{(3)}{}^{abc}_{ijk}\rangle = E_{ai}(T_{bj}E_{ck} + T_{ck}E_{bj})\,|\Phi\rangle \qquad \text{for } b > c \text{ and } j > k
\end{aligned}
$$

The adjoints of kets: $\langle{}^{(3)}{}^{a}_{i}|$, $\langle{}^{(+)}{}^{ab}_{ij}|$ and $\langle{}^{(-)}{}^{ab}_{ij}|$ form an orthogonal basis. For the triple excitations, we took the linear combination of adjoints to achieve the orthogonality:

$$
\begin{aligned}
\langle{}^{(3)}\widetilde{{}^{abc}_{ijk}}| =& \frac{1}{8}\Big(9\,\langle{}^{(3)}{}^{abc}_{ijk}| + \langle{}^{(3)}{}^{abc}_{kji}| + \langle{}^{(3)}{}^{abc}_{jik}| \\
&+ \langle{}^{(3)}{}^{bac}_{ijk}| - \langle{}^{(3)}{}^{bac}_{kji}| - \langle{}^{(3)}{}^{bac}_{jik}| \\
&+ \langle{}^{(3)}{}^{cba}_{ijk}| - \langle{}^{(3)}{}^{cba}_{kji}| - \langle{}^{(3)}{}^{cba}_{jik}|\Big)
\end{aligned} \tag{2.12}
$$

From now on, will denote $\tilde{\mu} \equiv \mu$ for clarity and it is understood that the biorthogonal basis is used throughout the work.

2.2 Coupled cluster theory for the ground state

In the coupled cluster theory, the unnormalized wave function is represented by the Ansatz

$$\Psi = e^{T}\Phi, \tag{2.13}$$

where the cluster operator T for an N electron system is the sum of single, double, and higher excitations, $T = T_1 + T_2 + \cdots + T_N$, and Φ is the reference Hartree-Fock determinant. The n-particle cluster operator T_n can be expressed as

$$T = \sum_n \frac{1}{n!} \sum_{\mu_n} t_{\mu_n} \mu_n. \tag{2.14}$$

The ground state energy is found by inserting Eq. (2.13) into the time-independent Shrödinger equation, multiplying from left by e^{-T} and projecting on the reference determinant. Subsequently, the amplitudes are obtained by projecting the same equation on the excited determinants:

$$\begin{aligned} \langle \Phi | e^{-T} H e^{T} | \Phi \rangle &= E, \\ \langle \nu_1 | e^{-T} H e^{T} | \Phi \rangle &= 0, \\ \langle \nu_2 | e^{-T} H e^{T} | \Phi \rangle &= 0, \\ &\cdots \\ \langle \nu_N | e^{-T} H e^{T} | \Phi \rangle &= 0. \end{aligned} \tag{2.15}$$

In the case of the CCSD approximation, the operator T is truncated after double excitations. This leads to the CCSD energy correct through the third order of MBPT. The computation of the ground-state energy and amplitudes scales as N^6 where N is the size of the system, and thus can widely be used for accurate electronic structure computations. In some cases though, the lack of higher excitations can lead to serious problems.

The perfect solution would be to use a natural extension to CCSD, namely the CCSDT model.[81–83] The more accurate results as well as a better recovery of the static correlation comes with a cost of N^8, so the applicability of the CCSDT approach is very limited.

Various approaches for an approximate inclusion of the triple excitations are available in the literature, including CCSDT-1a,[84] CCSDT-1b,[85] CCSD(T),[86] and CC3.[66] In the CCSDT-1a and CCSDT-1b methods, only some terms that scale up as N^7 are selected from full equations for the triple excitations. Additionally, in CCSDT-1a single excitations are neglected in the connected contribution of the triple excitations to the equation for the double excitations. In the CCSD(T)[86] model, one does not solve the equation for T_3 and triple excitations are only included in the energy expression as the fourth and fifth order perturbation energy contributions. The CCSD(T) method is considered as the best method for molecular problems near equilibrium,[87] while CCSDT-1 works better for the description of the bond breaking. Still, there are fundamental problems with these methods. In CCSD(T) only one fifth order contribution to the energy is considered with no clear justification.[66,88] But more importantly, the CCSD(T) method cannot be used for the response properties computation due to the fact that it is a two-step procedure.

First, one computes the CCSD energy and amplitudes, and the energy correction for the triple excitations is added afterwards, making it impossible to construct a consistent scheme for the transition properties computation. In CCSDT-1, equation for T_3 needs to be iterated, enforcing the storage of the amplitudes t_3.

In the CC3[66] method, the amplitudes t_1 and t_2 are iterated until convergence as in CCSDT model,

$$\begin{aligned}\langle\mu_1|e^{-T_2}\hat{H}e^{T_2}|\Phi\rangle + \langle\mu_1|[H,T_3]|\Phi\rangle = 0 \\ \langle\mu_2|e^{-T_2}\hat{H}e^{T_2}|\Phi\rangle + \langle\mu_2|[\hat{H},T_3]|\Phi\rangle = 0.\end{aligned} \tag{2.16}$$

where $\hat{H}$ is a t_1 transformed Hamiltonian $\hat{H} = e^{-T_1}He^{T_1}$.[80] The amplitudes t_3 are computed from a modified full CCSDT equation, by taking only terms that ensure that triple excitations are correct through the second-order of the perturbation theory

$$\langle\mu_3|[F,T_3]|\Phi\rangle + \langle\mu_2|[W,T_2]|\Phi\rangle = 0. \tag{2.17}$$

Here W is the fluctuation potential, $W = H - F$, F is the Fock operator $F = \sum_p \epsilon_p E_{pp}$, and ϵ_p are the orbital energies. The computational cost of the amplitudes t_3 is N^7, and t_3 can explicitly be computed from T_1 and T_2, without iterating

$$t_3 = -\frac{\langle\mu_2|[W,T_2]|\Phi\rangle}{\epsilon_{\mu_3}}. \tag{2.18}$$

2.3 Coupled cluster equations for the excited singlet and triplet states

Equation-of-motion coupled cluster theory (EOM-CC)[89] is used for the description of excited electronic states and their properties. Energies of the excited states are found by the diagonalization of the similarity transformed Hamiltonian $e^{-T}He^{T}$. The eigenproblem is not symmetric and solutions of the left and right eigenproblems

$$\begin{aligned}\mathbf{A}R_i &= ER_i \\ L_j\mathbf{A} &= EL_j\end{aligned} \tag{2.19}$$

form a biorthogonal set

$$L_iR_j = \delta_{ij}. \tag{2.20}$$

The excited state is defined by a linear excitation operator $R = R_0 + R_1 + R_2 + \ldots + R_N$ acting on the ground state, which in our case is the CC ground state $|\Psi\rangle$, Eq. (2.13),

$$|\Psi_N\rangle = R_N|\Psi\rangle, \tag{2.21}$$

and where

$$R_N = \sum_{n=0} \frac{1}{n!}\sum_{\mu_n} r_{\mu_n,N}\mu_n \tag{2.22}$$

In the XCC theory the excited states are obtained from the coupled cluster Jacobian[14,16,80]

$$A_{\mu\nu} = \frac{d\,\langle\mu|e^{-T}He^{T}|\Phi\rangle}{d\nu} = \langle\mu|e^{-T}[H,\nu]e^{T}|\Phi\rangle \tag{2.23}$$

Due to the non-symmetric character of the Jacobian matrix, diagonalization of A leads to the set of biorthogonal left l_M and right r_K eigenvectors

$$\langle l_M|r_K\rangle = \delta_{MK}. \tag{2.24}$$

The CC3 Jacobian in Eq. (2.23) is expressed in the molecular orbital basis as

$$A^{CC3} = \begin{pmatrix} \langle\mu_1|[\hat{H}+[\hat{H},T_2],\nu_1]|\Phi\rangle & \langle\mu_1|[\hat{H},\nu_2]|\Phi\rangle & \langle\mu_1|[H,\nu_3]|\Phi\rangle \\ \langle\mu_2|[\hat{H}+[\hat{H},T_2+T_3],\nu_1]|\Phi\rangle & \langle\mu_2|[\hat{H}+[\hat{H},T_2],\nu_2]|\Phi\rangle & \langle\mu_2|[\hat{H},\nu_3]|\Phi\rangle \\ \langle\mu_3|[[\hat{H},T_2],\nu_1]|\Phi\rangle & \langle\mu_3|[\hat{H},\nu_2]|\Phi\rangle & \langle\mu_3|[F,\nu_3]|\Phi\rangle \end{pmatrix}. \tag{2.25}$$

The solution of the eigenproblem $AR=\omega R$ where $R=(R^1,R^2,R^3)$ is

$$\begin{aligned} R_1 &= \sum_{ai} r_i^a E_{ai} \\ R_2 &= \frac{1}{2}\sum_{abij} r_{ij}^{ab} E_{ai}E_{bj} \\ R_3 &= \frac{1}{6}\sum_{abcijk} r_{ijk}^{abc} E_{ai}E_{bj}E_{ck} \end{aligned} \tag{2.26}$$

The triplet Jacobian in the CC3 theory is given by the following matrix

$$\begin{pmatrix} \langle^{(3)}\mu_1|\hat{H}_1^{(1)}|\Phi\rangle & \langle^{(3)}\mu_1|\hat{H}_{2+}^{(1)}|\Phi\rangle & \langle^{(3)}\mu_1|\hat{H}_{2-}^{(1)}|\Phi\rangle & \langle^{(3)}\mu_1|[H,\nu_3]|\Phi\rangle \\ \langle\mu_{2+}|\hat{H}_1^{(1)}+\hat{H}_1^{(2)}|\Phi\rangle & \langle\mu_{2+}|\hat{H}_{2+}^{(1)}+\hat{H}_{2+}^{(2)}|\Phi\rangle & \langle\mu_{2+}|\hat{H}_{2-}^{(1)}+\hat{H}_{2-}^{(2)}|\Phi\rangle & \langle\mu_{2+}|[\hat{H},\nu_3]|\Phi\rangle \\ \langle\mu_{2-}|\hat{H}_1^{(1)}+\hat{H}_1^{(2)}|\Phi\rangle & \langle\mu_{2-}|\hat{H}_{2-}^{(1)}+\hat{H}_{2+}^{(2)}|\Phi\rangle & \langle\mu_{2-}|\hat{H}_{2-}^{(1)}+\hat{H}_{2-}^{(2)}|\Phi\rangle & \langle\mu_{2-}|[\hat{H},\nu_3]|\Phi\rangle \\ \langle^{(3)}\mu_3|\hat{H}_3^{(2)}|\Phi\rangle & \langle^{(3)}\mu_3|[\hat{H},\nu_{2+}]|\Phi\rangle & \langle^{(3)}\mu_3|[\hat{H},\nu_{2-}]|\Phi\rangle & \langle^{(3)}\mu_3|[F,\nu_3]|\Phi\rangle \end{pmatrix}, \tag{2.27}$$

where

$$\hat{H}_1^{(1)} = [\hat{H}+[\hat{H},T_2],\nu_1] \tag{2.28}$$
$$\hat{H}_1^{(2)} = [[\hat{H},T_3],\nu_1] \tag{2.29}$$
$$\hat{H}_{2\pm}^{(1)} = [\hat{H},\nu_{2\pm}] \tag{2.30}$$
$$\hat{H}_{2\pm}^{(2)} = [[\hat{H},T_2],\nu_{2\pm}] \tag{2.31}$$
$$\hat{H}_{2\pm}^{(3)} = [[\hat{H},T_2],\nu_1]. \tag{2.32}$$

The eigenvectors of the triplet Jacobian are

$$\begin{aligned} {}^{(3)}R_1 &= \sum_{ai}^{(3)} r_i^a T_{ai} \\ {}^{(+)}R_2 &= \frac{1}{2}\sum_{a>b,i>j}^{(+)} r_{ij}^{ab}(T_{ai}E_{bj}+T_{bj}E_{ai}) \end{aligned} \tag{2.33}$$

$$
{}^{(-)}R_2 = \frac{1}{2}\sum_{ai>bj}^{(-)} r_{ij}^{ab}(T_{ai}E_{bj} - T_{bj}E_{ai})
$$

$$
{}^{(3)}R_3 = \sum_{ai}\sum_{\substack{b>c \\ j>k}}^{(3)} r_{ijk}^{abc}E_{ai}(T_{bj}E_{ck} + T_{ck}E_{bj}) \tag{2.34}
$$

Alternatively, the CC Jacobian can be expressed in the basis of left l_N and right r_M eigenvectors that are later directly related to the excited states

$$
A_{NM} = \langle l_N|[e^{-T}He^T, r_M]|\Phi\rangle\,. \tag{2.35}
$$

The transformation between the two bases is given by

$$
\mu_n = \sum_N L^\star_{\mu_n N} r_N. \tag{2.36}
$$

2.4 Ground-state expectation values

The XCC theory was first proposed in 1993 by Jeziorski and Moszynski[68] as a method for the computation of the expectation value of an observable with the coupled cluster theory. In order to formulate an explicitly connected expansion for the expectation value, the authors proposed to reformulate the basic expression for the coupled cluster expectation value with the use of auxiliary cluster operator S defined as:

$$
e^S\Phi = \frac{e^{T^\dagger}e^T}{\langle e^T|e^T\rangle}\Phi, \qquad S = S_1 + S_2 + S_3 + \ldots + S_N, \tag{2.37}
$$

where ϕ is a reference state. We introduce the notation $|e^T\Phi\rangle \equiv |e^T\rangle$. Each S_n is the solution of the following set of linear equations

$$
\begin{aligned}
S_n = T_n &- \frac{1}{n}\hat{\mathcal{P}}_n\left(\sum_{k=1}\frac{1}{k!}[\widetilde{T}^\dagger, T]_k\right) \\
&- \frac{1}{n}\hat{\mathcal{P}}_n\left(\sum_{k=1}\sum_{m=0}\frac{1}{k!}\frac{1}{m!}[[\widetilde{S}, T^\dagger]_k, T]_m\right),
\end{aligned} \tag{2.38}
$$

$$
\widetilde{T} = \sum_{n=1}^{N} nT_n, \qquad \widetilde{S} = \sum_{n=1}^{N} nS_n, \tag{2.39}
$$

and $[A,B]_k$ is a k-tuply nested commutator. The superoperator $\hat{\mathcal{P}}_n(X)$ yields the n-tuple excitation part of X

$$
\hat{\mathcal{P}}_n(X) = \frac{1}{n!}\sum_{\mu_n}\langle\mu_n|X|\Phi\rangle\,\mu_n. \tag{2.40}
$$

The expansion given by Eq. (2.38) is finite but it contains terms of high order in the fluctuation potential. Moreover, finding S_n requires an iterative procedure. It was shown in Ref. 68 that equation for each S_n can efficiently be approximated by expanding S as a power series in the operator T. The hierarchy of approximations is described in details in section 3.7.

In the XCC theory the expectation value of an observable is computed with the normalized ground state wave function in the CC parametrization

$$|\Psi_0\rangle = \frac{|e^T\rangle}{\langle e^T|e^T\rangle^{\frac{1}{2}}}, \tag{2.41}$$

and thus, the explicitly connected commutator expansion for the time-independent average value of an observable X is[68]

$$\langle\Psi_0|X|\Psi_0\rangle = \frac{\langle e^T|X|e^T\rangle}{\langle e^T|e^T\rangle} = \langle e^{S^\dagger} e^{-T} X e^T e^{-S^\dagger}\rangle\,. \tag{2.42}$$

This result is used in the derivation of the expression for the quadratic response function. Note parenthetically that Ψ of Eq. (2.13) defines the unnormalized CC wave function in contrast to the normalized wave function Ψ_0 of Eq. (2.41).

2.5 Response theory

The response theory describes the response of a molecule to an external perturbation. We consider the system described by a time-dependent Hamiltonian $H(t)$

$$H(t) = H_0 + V(t) \tag{2.43}$$

where H_0 is time-independent Hamiltonian and $V(t)$ is a general time-dependent perturbation that is the sum of the products of the perturbation operators Y and perturbation strength parameters $\epsilon_Y(\omega_Y)$, at a frequency ω_Y

$$V(t) = \sum_Y \epsilon_Y(\omega_Y) Y e^{-i\omega_Y t}. \tag{2.44}$$

The perturbation strength parameter satisfies the relation:

$$\epsilon_Y(\omega_Y) = \epsilon_Y(-\omega_Y)^\star. \tag{2.45}$$

The time-dependent wave function $\Psi(t)$ is the solution of the time-dependent Schrödinger equation

$$\frac{1}{i}\frac{\partial}{\partial t}\Psi = H(t)\Psi \tag{2.46}$$

In the perturbative regime, the response functions are defined as the coefficients in the expansion of the time-dependent expectation value $\langle\Psi(t)|X|\Psi(t)\rangle$ in orders of the perturbation $V(t)$

$$\langle\Psi(t)|X|\Psi(t)\rangle = \langle\Psi|X|\Psi\rangle + \sum_{k_1} e^{-i\omega_{k_1} t} \sum_Y \langle\langle X;Y\rangle\rangle_{\omega_{k_1}} \epsilon_Y(\omega_{k_1})$$

$$+\frac{1}{2}\sum_{k_1,k_2} e^{-i(\omega_{k_1}+\omega_{k_2})t}\sum_{Y,Z}\langle\langle X;Y,Z\rangle\rangle_{\omega_{k_1},\omega_{k_2}}\epsilon_Y(\omega_{k_1})\epsilon_Z(\omega_{k_2})\ldots \quad (2.47)$$

They are called, respectively, time-independent expectation value $\langle\Psi|X|\Psi\rangle$, linear response function $\langle\langle X;Y\rangle\rangle_{\omega_{k_1}}$, quadratic response function $\langle\langle X;Y,Z\rangle\rangle_{\omega_{k_1},\omega_{k_2}}$ etc., and describe the n-th order response of an observable to the perturbation $V(t)$.

Chapter 3 XCC transition properties

3.1 General notes

The theory formulated in this thesis is based on the work of Moszynski et al.[17] The authors of Ref. 17 derived the expression for the linear response function (also known as the polarization propagator) in a time-independent approach, in contrast to the well-established time-dependent coupled cluster response theory.[16,29,58,59] The main advantage of the XCC formulation is that the linear response function is size-consistent as well as Hermitian.

Moszynski et al.[17] noticed that in the time-independent formulation the linear response function is given by

$$\langle\langle X; Y\rangle\rangle_\omega = -\langle\Psi_0|X|\Psi^{(1)}(\omega_Y)\rangle - \langle\Psi^{(1)}(\omega_X)|Y|\Psi_0\rangle \tag{3.1}$$

where the first-order perturbed wave function is defined by using the reduced resolvent

$$\Psi^{(1)}(\omega) = \mathcal{R}_\omega Y|\Psi_0\rangle \tag{3.2}$$

$$\mathcal{R}_\omega = \sum_{N>0} \frac{|N\rangle\langle N|}{\omega_N + \omega} \qquad \omega_N = E_N - E_0. \tag{3.3}$$

Eq. (3.1) is the starting point for the derivation of the CC expression for the polarization propagator. In the further steps, the authors of Ref. 17 introduced the CC parametrization of $\Psi^{(1)}(\omega)$ by the use of the excitation operator $\Omega^X(\omega)$. The last one is found from the linear response equation,[17,30] see section 3.3. After numerous algebraic manipulations represented the expression for the polarization propagator as follows

$$\langle\langle X; Y\rangle\rangle_\omega = \langle e^{-S} e^{T^\dagger} Y e^{-T^\dagger} e^S|\hat{\mathcal{P}}\left(e^{S^\dagger}\Omega^X(\omega)e^{-S^\dagger}\right)\rangle + \text{g.c.c.} \tag{3.4}$$

The generalized complex conjugation (g.c.c.) is obtained by computing the first term for $(-\omega^\star)$ and by taking the complex conjugate. The scheme for approximating the operator S, and the polarization propagator itself, was also presented in this work.[17]

While the works of Moszyński et al.[17] and Jeziorski and Moszyński[68] included only theoretical results, the XCC formalism for the ground-state properties was later implemented by Korona et al.[30,31,69] and made available in a highly-optimized form in the Molpro software package.[1] Several works containing an extensive analysis of the XCC method combined with the CCSD and CCSD(T) approaches were published.

The extension of the XCC method to compute transition matrix elements between the ground and excited states was proposed by Tucholska et al. in Ref. 18 (Paper I). In 2017, Tucholska et al.[19] (Paper II) further extended the method to compute transition matrix elements for which both bra and ket states are excited states. These two works present a complete theory for the computation of XCC transition moments at the CCSD and CC3 levels of theory. The matrix elements for the singlet-singlet and triplet-triplet transitions are discussed, the implementation is proposed, and many numerical examples are given.

In this thesis we present a full derivation of the expression for the the transition moments between excited states, and extend it with the theory for the computation of the spin-forbidden singlet-triplet transition that covers computation of the spin-orbit matrix elements, which has not been published yet and is the subject of an upcoming paper.[77]

In addition, we present an approach to the computation of the XCC transition moments between a ground and an excited state which is a better alternative to the previously published method of Ref. 18.

3.2 Exact quadratic response function and transition moments

We start from the formal definition of the quadratic response function $\langle\langle X; Y, Z\rangle\rangle_{\omega_Y,\omega_Z}$ which describes the response of an observable X to the perturbations Y and Z acting with the frequencies ω_Y and ω_Z, respectively. The explicit form of this function written as a sum over states reads[59]

$$
\begin{aligned}
&\langle\langle X; Y, Z\rangle\rangle_{\omega_Y,\omega_Z} = \qquad (3.5)\\
&= \sum_{\substack{K=1\\N=1}} \frac{\langle\Psi_0|Y|\Psi_K\rangle\left[\langle\Psi_K|X|\Psi_N\rangle - \delta_{KN}\langle\Psi_0|X|\Psi_0\rangle\right]\langle\Psi_N|Z|\Psi_0\rangle}{(\omega_K+\omega_Y)(\omega_N-\omega_Z)}\\
&+ \frac{\langle\Psi_0|Z|\Psi_K\rangle\left[\langle\Psi_K|X|\Psi_N\rangle - \delta_{KN}\langle\Psi_0|X|\Psi_0\rangle\right]\langle\Psi_N|Y|\Psi_0\rangle}{(\omega_K+\omega_Z)(\omega_N-\omega_Y)}\\
&+ \frac{\langle\Psi_0|X|\Psi_K\rangle\left[\langle\Psi_K|Y|\Psi_N\rangle - \delta_{KN}\langle\Psi_0|Y|\Psi_0\rangle\right]\langle\Psi_N|Z|\Psi_0\rangle}{(\omega_K+\omega_X)(\omega_N-\omega_Z)}
\end{aligned}
$$

$$+\frac{\langle\Psi_0|Z|\Psi_K\rangle\left[\langle\Psi_K|Y|\Psi_N\rangle-\delta_{KN}\langle\Psi_0|Y|\Psi_0\rangle\right]\langle\Psi_N|X|\Psi_0\rangle}{(\omega_K+\omega_Z)(\omega_N-\omega_X)}$$

$$+\frac{\langle\Psi_0|X|\Psi_K\rangle\left[\langle\Psi_K|Z|\Psi_N\rangle-\delta_{KN}\langle\Psi_0|Z|\Psi_0\rangle\right]\langle\Psi_N|Y|\Psi_0\rangle}{(\omega_K+\omega_X)(\omega_N-\omega_Y)}$$

$$+\frac{\langle\Psi_0|Y|\Psi_K\rangle\left[\langle\Psi_K|Z|\Psi_N\rangle-\delta_{KN}\langle\Psi_0|Z|\Psi_0\rangle\right]\langle\Psi_N|X|\Psi_0\rangle}{(\omega_K+\omega_Y)(\omega_N-\omega_X)}$$

$$=P_{XYZ}\sum_{\substack{K=1\\N=1}}\frac{\langle\Psi_0|Y|\Psi_K\rangle\left[\langle\Psi_K|X|\Psi_N\rangle-\delta_{KN}\langle\Psi_0|X|\Psi_0\rangle\right]\langle\Psi_N|Z|\Psi_0\rangle}{(\omega_K+\omega_Y)(\omega_N-\omega_Z)},$$

where the operator P_{XYZ} interchanges the indices X, Y and Z. Here, K and N run over all possible excited states with excitation energies ω_K and ω_N and Ψ_0 is the ground state. The transition moment $\mathcal{T}_{LM}$ between the excited states L and M, where $L \neq M$, is computed from the quadratic response function as a double residue:

$$\begin{aligned}
&\lim_{\omega_Y\to-\omega_L}(\omega_L+\omega_Y)\lim_{\omega_Z\to\omega_M}(\omega_M-\omega_Z)\left\langle\left\langle X;Y,Z\right\rangle\right\rangle_{\omega_Y,\omega_Z} \\
&=\lim_{\omega_Y\to-\omega_L}(\omega_L+\omega_Y)\lim_{\omega_Z\to\omega_M}(\omega_M-\omega_Z)\times \\
&\times\left(\sum_{KN}\frac{\langle\Psi_0|Y|\Psi_K\rangle\left[\langle\Psi_K|X|\Psi_N\rangle-\delta_{KN}\langle\Psi_0|X|\Psi_0\rangle\right]\langle\Psi_N|Z|\Psi_0\rangle}{(\omega_K+\omega_Y)(\omega_N-\omega_Z)}\right) \\
&=\langle\Psi_0|Y|\Psi_L\rangle\left[\langle\Psi_L|X|\Psi_M\rangle-\delta_{LM}\langle\Psi_0|X|\Psi_0\rangle\right]\langle\Psi_M|Z|\Psi_0\rangle \\
&=\langle\Psi_0|Y|\Psi_L\rangle\langle\Psi_L|X_0|\Psi_M\rangle\langle\Psi_M|Z|\Psi_0\rangle=\mathcal{T}^Y_{0L}\mathcal{T}^X_{LM}\mathcal{T}^Z_{M0}.
\end{aligned}\tag{3.6}$$

where $X_0 = X - \langle\Psi_0|X|\Psi_0\rangle$. Eq. (3.5) can be treated as a definition of the quadratic response function. It is easy to see that in order to obtain the the transition moment $\mathcal{T}^X_{LM}$, the quantity from Eq. (3.6) needs to be divided by $|\mathcal{T}^Y_{0L}\mathcal{T}^Z_{M0}| = \sqrt{|T^Y_{0L}|^2|T^Z_{M0}|^2}$.

3.3 XCC approach to the quadratic response function

To obtain transition moments between the excited states in the XCC theory we used the XCC formalism to express the quadratic response function, and subsequently computed the double residue according to Eq. (3.6).

The first step is to reformulate Eq. (3.5) so that the CC parametrization can easily be introduced. By using the first-order perturbed wave function, we get

$$\left\langle\left\langle X;Y,Z\right\rangle\right\rangle_{\omega_Y,\omega_Z}=P_{XYZ}\langle\Psi^{(1)}(\omega_Y)|X_0|\Psi^{(1)}(-\omega_Z)\rangle.\tag{3.7}$$

The normalized ground state wave function in the coupled cluster parametrization is defined through the exponential Ansatz, Eq. (2.41)

$$|\Psi_0\rangle=\frac{|e^T\rangle}{\langle e^T|e^T\rangle^{\frac{1}{2}}},\tag{3.8}$$

and the first order perturbed wave function $\Psi^{(1)}(\omega)$ in this parametrization is defined through the linear excitation operator $\Omega(\omega)$ acting on the ground state

$$|\Psi^{(1)}(\omega)\rangle = (\Omega_0 + \Omega(\omega))|\Psi_0\rangle. \tag{3.9}$$

The excitation operator $\Omega(\omega) = \Omega_1(\omega) + \Omega_2(\omega) + \ldots$, is the sum of singly, doubly, triply, etc. terms, analogously to T. The n-th cluster operator $\Omega_n(\omega)$ is represented as

$$\Omega^X(\omega) = \sum_n \frac{1}{n!} \sum_{\mu_n} O^X_{\mu_n}(\omega)\mu_n \tag{3.10}$$

The scalar term Ω_0 ensures the orthogonality of $\Psi^{(1)}$ to Ψ_0[17]

$$\Omega_0 = -\langle \Psi_0|\Omega(\omega)\Psi_0\rangle . \tag{3.11}$$

The excitation amplitudes of the operator $\Omega(\omega)$ are solutions of the linear response equation[17,30]

$$\left\langle \mu|[e^{-T}He^T, \Omega(\omega)] + \omega\Omega(\omega) + e^{-T}Xe^T \right\rangle = 0. \tag{3.12}$$

We express the excitation operator $\Omega^Y(\omega)$ in the basis of the right eigenvectors r_N of the CC Jacobian matrix $A_{\mu_n\nu_m} = \left\langle \mu_n \middle| [e^{-T}He^T, \nu_m] \right\rangle$. The molecular orbital basis μ_n written in terms of r_N is given by

$$\mu_n = \sum_N \mathcal{L}^\star_{\mu_n N} r_N \tag{3.13}$$

and thus

$$\begin{aligned} \Omega^Y(\omega) &= \sum_N \sum_{n=1} \sum_{\mu_n} \frac{1}{n!} \mathcal{L}^\star_{\mu_n N} O^Y_{\mu_n}(\omega) r_N \\ &= \sum_N O^Y_N(\omega) r_N. \end{aligned} \tag{3.14}$$

We obtain the amplitudes $O^Y_N(\omega)$ by projecting Eq. (3.12) onto the left eigenvector of the Jacobian l_N:

$$O^Y_N(\omega_Y) = -\frac{\langle l_N|e^{-T}Ye^T\rangle}{\omega_N + \omega_Y}. \tag{3.15}$$

Finally, by inserting Eqs. (3.8) and (3.9) into Eq. (3.7) we get the formula that is the starting point for the derivation of the quadratic response function in the XCC theory.

$$\langle\langle X; Y, Z\rangle\rangle_{\omega_Y,\omega_Z} = P_{XYZ}\langle(\Omega_0(\omega_Y) + \Omega(\omega_Y))\Psi_0|X_0|(\Omega_0(\omega_Z) + \Omega(-\omega_Z))\Psi_0\rangle. \tag{3.16}$$

In this section we will derive an explicit expression for the XCC quadratic response function. Let us expand Eq. (3.16), and divide it into four parts $\mathcal{A}$, $\mathcal{B}$, $\mathcal{C}$ and $\mathcal{D}$

$$\begin{aligned} \langle\langle X; Y, Z\rangle\rangle^{XCC}_{\omega_Y,\omega_Z} &= P_{XYZ}\langle(\Omega^Y_0 + \Omega^Y)\Psi_0|X_0|(\Omega^Z_0 + \Omega^Z)\Psi_0\rangle \qquad (3.17) \\ &= P_{XYZ}\Big(\underbrace{\langle\Omega^Y_0\Psi_0|X_0|\Omega^Z_0\Psi_0\rangle}_{\mathcal{A}} + \underbrace{\langle\Omega^Y\Psi_0|X_0|\Omega^Z_0\Psi_0\rangle}_{\mathcal{B}} + \underbrace{\langle\Omega^Y_0\Psi_0|X_0|\Omega^Z\Psi_0\rangle}_{\mathcal{C}} + \underbrace{\langle\Omega^Y\Psi_0|X_0|\Omega^Z\Psi_0\rangle}_{\mathcal{D}} \Big) \end{aligned}$$

$= P_{XYZ}(\mathcal{A} + \mathcal{B} + \mathcal{C} + \mathcal{D})$

The quantities $\mathcal{A}$, $\mathcal{B}$, $\mathcal{C}$ and $\mathcal{D}$ written with the explicit CC parametrization are given by the expressions

$$\begin{aligned}
\mathcal{A} &= (\Omega_0^Y)^\dagger \Omega_0^Z \frac{\langle e^T|X_0|e^T\rangle}{\langle e^T|e^T\rangle} = \frac{\langle \Omega^Y e^T|e^T\rangle}{\langle e^T|e^T\rangle}\frac{\langle e^T|\Omega^Z e^T\rangle}{\langle e^T|e^T\rangle}\frac{\langle e^T|X_0|e^T\rangle}{\langle e^T|e^T\rangle} \\
\mathcal{B} &= (\Omega_0^Y)^\dagger \frac{\langle e^T|X_0|\Omega^Z e^T\rangle}{\langle e^T|e^T\rangle} = \text{-}\frac{\langle \Omega^Y e^T|e^T\rangle}{\langle e^T|e^T\rangle}\frac{\langle e^T|X_0|\Omega^Z e^T\rangle}{\langle e^T|e^T\rangle} \\
\mathcal{C} &= \Omega_0^Z \frac{\langle \Omega^Y e^T|X_0|e^T\rangle}{\langle e^T|e^T\rangle} = \text{-}\frac{\langle e^T|\Omega^Z e^T\rangle}{\langle e^T|e^T\rangle}\frac{\langle \Omega^Y e^T|X_0|e^T\rangle}{\langle e^T|e^T\rangle} \\
\mathcal{D} &= \frac{\langle \Omega^Y e^T|X_0|\Omega^Z e^T\rangle}{\langle e^T|e^T\rangle}
\end{aligned} \tag{3.18}$$

where for clarity we denote

$$\Omega^V = \Omega(\omega_V), \qquad \Omega_0^V = \Omega_0(\omega_V) \qquad V \in \{X, Y\}. \tag{3.19}$$

The following facts are used throughout the derivation

$$\Omega^V e^T = e^T \Omega^V \tag{3.20}$$

$$e^{-S^\dagger}\Phi = \Phi \tag{3.21}$$

$$X\Phi = \langle X\rangle\Phi + \hat{\mathcal{P}}(X)\Phi \tag{3.22}$$

$$e^{-T}e^T = e^{-S}e^S = e^{-T^\dagger}e^{T^\dagger} = e^{-S^\dagger}e^{S^\dagger} = 1 \tag{3.23}$$

$$\frac{\langle e^T|X|e^T\rangle}{\langle e^T|e^T\rangle} = \langle e^{S^\dagger}e^{-T}Xe^Te^{-S^\dagger}\rangle\,, \tag{3.24}$$

where the last equality is the result of the work of Jeziorski and Moszyński.[68] Each of the terms $\mathcal{A}$, $\mathcal{B}$, $\mathcal{C}$ and $\mathcal{D}$ can further be transformed using the above facts in two alternative forms that differ only by the sequence of applying Eqs. (3.20)-(3.24). This procedure is introduced to simplify the discussion of the Hermiticity of the transition moments in section 3.5. In the following the two mathematically equivalent forms are denoted as (I) and (II). As a consequence, the XCC quadratic response function can be formulated as follows

$$\begin{aligned}
\langle\langle X; Y, Z\rangle\rangle^{(I)}_{\omega_Y,\omega_Z} &= P_{XYZ}(\mathcal{A}^{(I)} + \mathcal{B}^{(I)} + \mathcal{C}^{(I)} + \mathcal{D}^{(I)}) = \\
&= P_{XYZ}(\mathcal{A}^{(II)} + \mathcal{B}^{(II)} + \mathcal{C}^{(II)} + \mathcal{D}^{(II)}) = \langle\langle X; Y, Z\rangle\rangle^{(II)}_{\omega_Y,\omega_Z}
\end{aligned} \tag{3.25}$$

Although it is quite easy to see the equivalence between $\mathcal{A}^{(I)}$ and $\mathcal{A}^{(II)}$, $\mathcal{B}^{(I)}$ and $\mathcal{B}^{(II)}$, etc. (see below), it is not straightforward to see the equivalence between the final forms of $\langle\langle X; Y, Z\rangle\rangle^{(I)}_{\omega_Y,\omega_Z}$ and $\langle\langle X; Y, Z\rangle\rangle^{(II)}_{\omega_Y,\omega_Z}$. . The derivation of the formulas (I) and (II) for each of the terms $\mathcal{A}$, $\mathcal{B}$, $\mathcal{C}$ and $\mathcal{D}$, follows now:

$$\mathcal{A}^{(I)} = \frac{\langle \Omega^Y e^{-T^\dagger}e^{T^\dagger}e^T|e^T\rangle}{\langle e^T|e^T\rangle}\frac{\langle e^{T^\dagger}e^T|\Omega^Z\rangle}{\langle e^T|e^T\rangle}\langle e^{S^\dagger}e^{-T}X_0e^Te^{-S^\dagger}\rangle \tag{3.26}$$

$$= \langle \Omega^Y e^{-T^\dagger} e^S | e^T \rangle \langle e^S | \Omega^Z e^{-S^\dagger} \rangle \langle e^{S^\dagger} e^{-T} X_0 e^T e^{-S^\dagger} \rangle$$
$$= \langle e^{T^\dagger} \Omega^Y e^{-T^\dagger} e^S | e^{-S^\dagger} \rangle \langle e^{S^\dagger} \Omega^Z e^{-S^\dagger} \rangle \langle e^{S^\dagger} e^{-T} X_0 e^T e^{-S^\dagger} \rangle$$
$$= \langle e^{-S} e^{T^\dagger} \Omega^Y e^{-T^\dagger} e^S | \Phi \rangle \langle e^{S^\dagger} \Omega^Z e^{-S^\dagger} \rangle \langle e^{S^\dagger} e^{-T} X_0 e^T e^{-S^\dagger} \rangle$$

$$\mathcal{A}^{(II)} = \frac{\langle e^T \Omega^Y | e^T \rangle}{\langle e^T | e^T \rangle} \frac{\langle e^T | \Omega^Z e^{-T^\dagger} e^{T^\dagger} e^T \rangle}{\langle e^T | e^T \rangle} \langle e^{S^\dagger} e^{-T} X_0 e^T e^{-S^\dagger} \rangle \tag{3.27}$$
$$= \frac{\langle \Omega^Y | e^{T^\dagger} e^T \rangle}{\langle e^T | e^T \rangle} \langle e^T e^{-S^\dagger} | \Omega^Z e^{-T^\dagger} e^S \rangle \langle e^{S^\dagger} e^{-T} X_0 e^T e^{-S^\dagger} \rangle$$
$$= \langle \Omega^Y e^{-S^\dagger} | e^S \rangle \langle e^{-S} e^{T^\dagger} \Omega^Z e^{-T^\dagger} e^S \rangle \langle e^{S^\dagger} e^{-T} X_0 e^T e^{-S^\dagger} \rangle$$
$$= \langle e^{-S} (\Omega^Y)^\dagger e^S \rangle \langle e^{-S} e^{T^\dagger} \Omega^Z e^{-T^\dagger} e^S \rangle \langle e^{S^\dagger} e^{-T} X_0 e^T e^{-S^\dagger} \rangle$$

$$\mathcal{B}^{(I)} = - \langle e^{-S} e^{T^\dagger} \Omega^Y e^{-T^\dagger} e^S | \Phi \rangle \frac{\langle X_0 e^T | e^T \Omega^Z \rangle}{\langle e^T | e^T \rangle} \tag{3.28}$$
$$= - \langle e^{-S} e^{T^\dagger} \Omega^Y e^{-T^\dagger} e^S | \Phi \rangle \frac{\langle e^{T^\dagger} X_0 e^{-T^\dagger} e^{T^\dagger} e^T | \Omega^Z \rangle}{\langle e^T | e^T \rangle}$$
$$= - \langle e^{-S} e^{T^\dagger} \Omega^Y e^{-T^\dagger} e^S | \Phi \rangle \langle e^S e^{-S} e^{T^\dagger} X_0 e^{-T^\dagger} e^S | \Omega^Z e^{-S^\dagger} \rangle$$
$$= - \langle e^{-S} e^{T^\dagger} \Omega^Y e^{-T^\dagger} e^S | \Phi \rangle \langle e^{-S} e^{T^\dagger} X_0 e^{-T^\dagger} e^S | e^{S^\dagger} \Omega^Z e^{-S^\dagger} \rangle$$
$$= - \langle e^{-S} e^{T^\dagger} \Omega^Y e^{-T^\dagger} e^S | \Phi \rangle \langle e^{S^\dagger} \Omega^Z e^{-S^\dagger} \rangle \langle e^{S^\dagger} e^{-T} X_0 e^T e^{-S^\dagger} \rangle$$
$$- \langle e^{-S} e^{T^\dagger} \Omega^Y e^{-T^\dagger} e^S | \Phi \rangle \langle e^{-S} e^{T^\dagger} X_0 e^{-T^\dagger} e^S | \hat{\mathcal{P}}(e^{S^\dagger} \Omega^Z e^{-S^\dagger}) \rangle$$

$$\mathcal{B}^{(II)} = - \langle e^{-S} (\Omega^Y)^\dagger e^S \rangle \frac{\langle X_0 e^T | e^{-T^\dagger} e^{T^\dagger} \Omega^Z e^{-T^\dagger} e^{T^\dagger} e^T \rangle}{\langle e^T | e^T \rangle}$$
$$= - \langle e^{-S} (\Omega^Y)^\dagger e^S \rangle \langle e^{-T} X_0 e^T | e^S e^{-S} e^{T^\dagger} \Omega^Z e^{-T^\dagger} e^S \rangle$$
$$= - \langle e^{-S} (\Omega^Y)^\dagger e^S \rangle \langle e^{S^\dagger} e^{-T} X_0 e^T e^{-S^\dagger} | e^{-S} e^{T^\dagger} \Omega^Z e^{-T^\dagger} e^S \rangle$$
$$= - \langle e^{-S} (\Omega^Y)^\dagger e^S \rangle \langle e^{-S} e^{T^\dagger} \Omega^Z e^{-T^\dagger} e^S \rangle \langle e^{-S} e^{T^\dagger} X_0 e^{-T^\dagger} e^S \rangle$$
$$- \langle e^{-S} (\Omega^Y)^\dagger e^S \rangle \langle e^{S^\dagger} e^{-T} X_0 e^T e^{-S^\dagger} | \hat{\mathcal{P}}(e^{-S} e^{T^\dagger} \Omega^Z e^{-T^\dagger} e^S) \rangle$$

$$\mathcal{C}^{(I)} = - \langle e^{S^\dagger} \Omega^Z e^{-S^\dagger} \rangle \frac{\langle \Omega^Y e^{-T^\dagger} e^{T^\dagger} e^T | X_0 e^T \rangle}{\langle e^T | e^T \rangle} \tag{3.29}$$
$$= - \langle e^{S^\dagger} \Omega^Z e^{-S^\dagger} \rangle \langle e^{T^\dagger} X_0 e^{-T^\dagger} e^{T^\dagger} \Omega^Y e^{-T^\dagger} e^S | e^{-S^\dagger} \rangle$$
$$= - \langle e^{S^\dagger} \Omega^Z e^{-S^\dagger} \rangle \langle e^{-S} e^{T^\dagger} X_0 e^{-T^\dagger} e^S e^{-S} e^{T^\dagger} \Omega^Y e^{-T^\dagger} e^S | \Phi \rangle$$
$$= - \langle e^{S^\dagger} \Omega^Z e^{-S^\dagger} \rangle \langle (e^{-S} e^{T^\dagger} \Omega^Y e^{-T^\dagger} e^S)^\dagger \rangle \langle e^{S^\dagger} e^{-T} X_0 e^T e^{-S^\dagger} \rangle$$
$$- \langle e^{S^\dagger} \Omega^Z e^{-S^\dagger} \rangle \langle e^{-S} e^{T^\dagger} X_0 e^{-T^\dagger} e^S \hat{\mathcal{P}}(e^{-S} e^{T^\dagger} \Omega^Y e^{-T^\dagger} e^S) | \Phi \rangle$$

$$\mathcal{C}^{(II)} = - \langle e^{-S} e^{T^\dagger} \Omega^Z e^{-T^\dagger} e^S \rangle \frac{\langle e^T \Omega^Y | X_0 e^{-T^\dagger} e^{T^\dagger} e^T \rangle}{\langle e^T | e^T \rangle} \tag{3.30}$$
$$= - \langle e^{-S} e^{T^\dagger} \Omega^Z e^{-T^\dagger} e^S \rangle \langle \Omega^Y e^{-S^\dagger} | e^{T^\dagger} X_0 e^{-T^\dagger} e^S \rangle$$
$$= - \langle e^{-S} e^{T^\dagger} \Omega^Z e^{-T^\dagger} e^S \rangle \langle \Omega^Y e^{-S^\dagger} | e^S e^{-S} e^{T^\dagger} X_0 e^{-T^\dagger} e^S \rangle$$
$$= - \langle e^{-S} e^{T^\dagger} \Omega^Z e^{-T^\dagger} e^S \rangle \langle e^{S^\dagger} \Omega^Y e^{-S^\dagger} | e^{-S} e^{T^\dagger} X_0 e^{-T^\dagger} e^S \rangle$$
$$= - \langle e^{-S} e^{T^\dagger} \Omega^Z e^{-T^\dagger} e^S \rangle \langle (e^{S^\dagger} \Omega^Y e^{-S^\dagger})^\dagger \rangle \langle e^{-S} e^{T^\dagger} X_0 e^{-T^\dagger} e^S \rangle$$
$$- \langle e^{-S} e^{T^\dagger} \Omega^Z e^{-T^\dagger} e^S \rangle \langle \hat{\mathcal{P}}(e^{S^\dagger} \Omega^Y e^{-S^\dagger}) | e^{-S} e^{T^\dagger} X_0 e^{-T^\dagger} e^S \rangle$$

$$
\begin{aligned}
\mathcal{D}^{(I)} &= \frac{\langle \Omega^Y e^T | X_0 e^T e^{-T} \Omega^Z e^T \rangle}{\langle e^T | e^T \rangle} = \frac{\langle \Omega^Y e^T | X_0 e^T \Omega^Z \rangle}{\langle e^T | e^T \rangle} \\
&= \frac{\langle e^{T^\dagger} X_0 \Omega^Y e^{-T^\dagger} e^{T^\dagger} e^T | \Omega^Z \rangle}{\langle e^T | e^T \rangle} \\
&= \langle e^{T^\dagger} X_0 e^{-T^\dagger} e^{T^\dagger} \Omega^Y e^{-T^\dagger} e^S | \Omega^Z \rangle \\
&= \langle e^S e^{-S} e^{T^\dagger} X_0 e^{-T^\dagger} e^S e^{-S} e^{T^\dagger} \Omega^Y e^{-T^\dagger} e^S | \Omega^Z \rangle \\
&= \langle e^{-S} e^{T^\dagger} X_0 e^{-T^\dagger} e^S e^{-S} e^{T^\dagger} \Omega^Y e^{-T^\dagger} e^S | e^{S^\dagger} \Omega^Z e^{-S^\dagger} \rangle \\
&= \langle (e^{-S} e^{T^\dagger} \Omega^Y e^{-T^\dagger} e^S)^\dagger \rangle \, \langle e^{S^\dagger} e^{-T} X_0 e^T e^{-S^\dagger} \rangle \, \langle e^{S^\dagger} \Omega^Z e^{-S^\dagger} \rangle \\
&+ \langle (e^{-S} e^{T^\dagger} \Omega^Y e^{-T^\dagger} e^S)^\dagger \rangle \, \langle e^{-S} e^{T^\dagger} X_0 e^{-T^\dagger} e^S | \hat{\mathcal{P}}(e^{S^\dagger} \Omega^Z e^{-S^\dagger}) \rangle \\
&+ \langle e^{-S} e^{T^\dagger} X_0 e^{-T^\dagger} e^S \hat{\mathcal{P}}(e^{-S} e^{T^\dagger} \Omega^Y e^{-T^\dagger} e^S) | \Phi \rangle \, \langle e^{S^\dagger} \Omega^Z e^{-S^\dagger} \rangle \\
&+ \langle e^{-S} e^{T^\dagger} X_0 e^{-T^\dagger} e^S \hat{\mathcal{P}}(e^{-S} e^{T^\dagger} \Omega^Y e^{-T^\dagger} e^S) | \hat{\mathcal{P}}(e^{S^\dagger} \Omega^Z e^{-S^\dagger}) \rangle
\end{aligned} \tag{3.31}
$$

$$
\begin{aligned}
\mathcal{D}^{(II)} &= \frac{\langle \Omega^Y e^T | X_0 \Omega^Z e^{-T^\dagger} e^{T^\dagger} e^T \rangle}{\langle e^T | e^T \rangle} = \langle e^T \Omega^Y | X_0 \Omega^Z e^{-T^\dagger} e^S \rangle \\
&= \langle e^T \Omega^Y | X_0 e^{-T^\dagger} e^S e^{-S} e^{T^\dagger} \Omega^Z e^{-T^\dagger} e^S \rangle \\
&= \langle \Omega^Y | e^S e^{-S} e^{T^\dagger} X_0 e^{-T^\dagger} e^S e^{-S} e^{T^\dagger} \Omega^Z e^{-T^\dagger} e^S \rangle \\
&= \langle e^{S^\dagger} \Omega^Y e^{-S^\dagger} | e^{-S} e^{T^\dagger} X_0 e^{-T^\dagger} e^S e^{-S} e^{T^\dagger} \Omega^Z e^{-T^\dagger} e^S \rangle \\
&= \langle (e^{S^\dagger} \Omega^Y e^{-S^\dagger})^\dagger \rangle \, \langle e^{-S} e^{T^\dagger} \Omega^Z e^{-T^\dagger} e^S \rangle \, \langle e^{-S} e^{T^\dagger} X_0 e^{-T^\dagger} e^S \rangle \\
&+ \langle (e^{S^\dagger} \Omega^Y e^{-S^\dagger})^\dagger \rangle \, \langle e^{-S} e^{T^\dagger} X_0 e^{-T^\dagger} e^S \hat{\mathcal{P}}(e^{-S} e^{T^\dagger} \Omega^Z e^{-T^\dagger} e^S) \rangle \\
&+ \langle e^{-S} e^{T^\dagger} \Omega^Z e^{-T^\dagger} e^S \rangle \, \langle \hat{\mathcal{P}}(e^{S^\dagger} \Omega^Y e^{-S^\dagger}) | e^{-S} e^{T^\dagger} X_0 e^{-T^\dagger} e^S \rangle \\
&+ \langle \hat{\mathcal{P}}(e^{S^\dagger} \Omega^Y e^{-S^\dagger}) | e^{-S} e^{T^\dagger} X_0 e^{-T^\dagger} e^S \hat{\mathcal{P}}(e^{-S} e^{T^\dagger} \Omega^Z e^{-T^\dagger} e^S) \rangle \, .
\end{aligned} \tag{3.32}
$$

Gathering all the terms together gives

$$
\begin{aligned}
\langle\langle X; Y, Z \rangle\rangle^{(I)}_{\omega_Y, \omega_Z} &= P_{XYZ}(\mathcal{A}^{(I)} + \mathcal{B}^{(I)} + \mathcal{C}^{(I)} + \mathcal{D}^{(I)}) \\
&= P_{XYZ}\Big(\langle e^{-S} e^{T^\dagger} \Omega^Y e^{-T^\dagger} e^S | \Phi \rangle \, \langle e^{S^\dagger} \Omega^Z e^{-S^\dagger} \rangle \, \langle e^{S^\dagger} e^{-T} X_0 e^T e^{-S^\dagger} \rangle && (1) \\
&- \langle e^{-S} e^{T^\dagger} \Omega^Y e^{-T^\dagger} e^S | \Phi \rangle \, \langle e^{S^\dagger} \Omega^Z e^{-S^\dagger} \rangle \, \langle e^{S^\dagger} e^{-T} X_0 e^T e^{-S^\dagger} \rangle && (2) \\
&- \langle e^{-S} e^{T^\dagger} \Omega^Y e^{-T^\dagger} e^S | \Phi \rangle \, \langle e^{-S} e^{T^\dagger} X_0 e^{-T^\dagger} e^S | \hat{\mathcal{P}}(e^{S^\dagger} \Omega^Z e^{-S^\dagger}) \rangle && (3) \\
&- \langle e^{S^\dagger} \Omega^Z e^{-S^\dagger} \rangle \, \langle (e^{-S} e^{T^\dagger} \Omega^Y e^{-T^\dagger} e^S)^\dagger \rangle \, \langle e^{S^\dagger} e^{-T} X_0 e^T e^{-S^\dagger} \rangle && (4) \\
&- \langle e^{S^\dagger} \Omega^Z e^{-S^\dagger} \rangle \, \langle e^{-S} e^{T^\dagger} X_0 e^{-T^\dagger} e^S \hat{\mathcal{P}}(e^{-S} e^{T^\dagger} \Omega^Y e^{-T^\dagger} e^S) | \Phi \rangle && (5) \\
&+ \langle (e^{-S} e^{T^\dagger} \Omega^Y e^{-T^\dagger} e^S)^\dagger \rangle \, \langle e^{S^\dagger} e^{-T} X_0 e^T e^{-S^\dagger} \rangle \, \langle e^{S^\dagger} \Omega^Z e^{-S^\dagger} \rangle && (6) \\
&+ \langle (e^{-S} e^{T^\dagger} \Omega^Y e^{-T^\dagger} e^S)^\dagger \rangle \, \langle e^{-S} e^{T^\dagger} X_0 e^{-T^\dagger} e^S | \hat{\mathcal{P}}(e^{S^\dagger} \Omega^Z e^{-S^\dagger}) \rangle && (7) \\
&+ \langle e^{-S} e^{T^\dagger} X_0 e^{-T^\dagger} e^S \hat{\mathcal{P}}(e^{-S} e^{T^\dagger} \Omega^Y e^{-T^\dagger} e^S) | \Phi \rangle \, \langle e^{S^\dagger} \Omega^Z e^{-S^\dagger} \rangle && (8) \\
&+ \langle e^{-S} e^{T^\dagger} X_0 e^{-T^\dagger} e^S \hat{\mathcal{P}}(e^{-S} e^{T^\dagger} \Omega^Y e^{-T^\dagger} e^S) | \hat{\mathcal{P}}(e^{S^\dagger} \Omega^Z e^{-S^\dagger}) \rangle \Big) && (9)
\end{aligned} \tag{3.33}
$$

It is easy to notice that the following terms cancel: one with six, two with four, three with seven, and five with eight. The only remaining term is nine, and it constitutes the XCC quadratic response function. The same procedure is applied to the form

(II) of the quadratic response function

$$\begin{aligned}
\langle\langle X; Y, Z\rangle\rangle^{(II)}_{\omega_Y,\omega_Z} &= P_{XYZ}(\mathcal{A}^{(II)} + \mathcal{B}^{(II)} + \mathcal{C}^{(II)} + \mathcal{D}^{(II)}) \qquad (3.34)\\
&= P_{XYZ}\Big(\langle e^{-S}(\Omega^Y)^\dagger e^S\rangle \langle e^{-S} e^{T^\dagger}\Omega^Z e^{-T^\dagger} e^S\rangle \langle e^{S^\dagger} e^{-T} X_0 e^T e^{-S^\dagger}\rangle \\
&- \langle e^{-S}(\Omega^Y)^\dagger e^S\rangle \langle e^{-S} e^{T^\dagger}\Omega^Z e^{-T^\dagger} e^S\rangle \langle e^{-S} e^{T^\dagger} X_0 e^{-T^\dagger} e^S\rangle \\
&- \langle e^{-S}(\Omega^Y)^\dagger e^S\rangle \langle e^{S^\dagger} e^{-T} X_0 e^T e^{-S^\dagger} | \hat{\mathcal{P}}(e^{-S} e^{T^\dagger}\Omega^Z e^{-T^\dagger} e^S)\rangle \\
&- \langle e^{-S} e^{T^\dagger}\Omega^Z e^{-T^\dagger} e^S\rangle \langle (e^{S^\dagger}\Omega^Y e^{-S^\dagger})^\dagger\rangle \langle e^{-S} e^{T^\dagger} X_0 e^{-T^\dagger} e^S\rangle \\
&- \langle e^{-S} e^{T^\dagger}\Omega^Z e^{-T^\dagger} e^S\rangle \langle \hat{\mathcal{P}}(e^{S^\dagger}\Omega^Y e^{-S^\dagger}) | e^{-S} e^{T^\dagger} X_0 e^{-T^\dagger} e^S\rangle \\
&+ \langle (e^{S^\dagger}\Omega^Y e^{-S^\dagger})^\dagger\rangle \langle e^{-S} e^{T^\dagger}\Omega^Z e^{-T^\dagger} e^S\rangle \langle e^{-S} e^{T^\dagger} X_0 e^{-T^\dagger} e^S\rangle \\
&+ \langle (e^{S^\dagger}\Omega^Y e^{-S^\dagger})^\dagger\rangle \langle e^{-S} e^{T^\dagger} X_0 e^{-T^\dagger} e^S \hat{\mathcal{P}}(e^{-S} e^{T^\dagger}\Omega^Z e^{-T^\dagger} e^S)\rangle \\
&+ \langle e^{-S} e^{T^\dagger}\Omega^Z e^{-T^\dagger} e^S\rangle \langle \hat{\mathcal{P}}(e^{S^\dagger}\Omega^Y e^{-S^\dagger}) | e^{-S} e^{T^\dagger} X_0 e^{-T^\dagger} e^S\rangle \\
&+ \langle \hat{\mathcal{P}}(e^{S^\dagger}\Omega^Y e^{-S^\dagger}) | e^{-S} e^{T^\dagger} X_0 e^{-T^\dagger} e^S \hat{\mathcal{P}}(e^{-S} e^{T^\dagger}\Omega^Z e^{-T^\dagger} e^S)\rangle \Big)
\end{aligned}$$

The final expressions for $\langle\langle X; Y, Z\rangle\rangle^{(I)}_{\omega_Y,\omega_Z}$ and $\langle\langle X; Y, Z\rangle\rangle^{(II)}_{\omega_Y,\omega_Z}$ read

$$\begin{aligned}
&\langle\langle X; Y, Z\rangle\rangle^{(I)}_{\omega_Y,\omega_Z} = \\
&\qquad P_{XYZ}\left(\langle \hat{\mathcal{P}}(e^{S^\dagger}\Omega^Y e^{-S^\dagger}) | e^{-S} e^{T^\dagger} X_0 e^{-T^\dagger} e^S \hat{\mathcal{P}}(e^{-S} e^{T^\dagger}\Omega^Z e^{-T^\dagger} e^S)\rangle\right) \qquad (3.35)
\end{aligned}$$

$$\begin{aligned}
&\langle\langle X; Y, Z\rangle\rangle^{(II)}_{\omega_Y,\omega_Z} = \\
&\qquad P_{XYZ}\left(\langle \hat{\mathcal{P}}(e^{-S} e^{T^\dagger}\Omega^Y e^{-T^\dagger} e^S) | e^{S^\dagger} e^{-T} X_0 e^T e^{-S^\dagger} \hat{\mathcal{P}}(e^{-S^\dagger}\Omega^Z e^{S^\dagger})\rangle\right). \qquad (3.36)
\end{aligned}$$

Only $\langle\langle X; Y, Z\rangle\rangle^{(I)}_{\omega_Y,\omega_Z}$ is needed to compute XCC transition moments, but both forms are crucial for the discussion of the Hermiticity of the XCC quadratic response function in the next section.

3.4 Transition moments

The transition moment between the excited states is computed from the double residue of the quadratic response function in the same way as for the exact case, Eq. (3.6), Inserting the expression for Ω^Y and Ω^Z in the Jacobian basis set

$$\Omega^Y(\omega) = \sum_N O^Y_N(\omega) r_N \qquad (3.37)$$

we get

$$\begin{aligned}
\langle\langle X; Y, Z\rangle\rangle^{(I)}_{\omega_Y,\omega_Z} &= P_{XYZ} \sum_{K,N=1} \left(O^Y_K(\omega_Y)\right)^\star O^Z_N(-\omega_Z) \qquad (3.38)\\
&\times \langle \hat{\mathcal{P}}(e^{S^\dagger} r_K e^{-S^\dagger}) | e^{-S} e^{T^\dagger} X_0 e^{-T^\dagger} e^S \hat{\mathcal{P}}(e^{-S} e^{T^\dagger} r_N e^{-T^\dagger} e^S)\rangle .
\end{aligned}$$

We now introduce a shorthand notation for the projected parts of the above expression

$$\begin{aligned}\kappa(r_M, S, T) &= \hat{\mathcal{P}}\left(e^{-S} e^{T^\dagger} r_K e^{-T^\dagger} e^{S}\right)\\ \eta(r_N, S) &= \hat{\mathcal{P}}\left(e^{S^\dagger} r_N e^{-S^\dagger}\right),\end{aligned} \tag{3.39}$$

and arrive at our final form of the XCC quadratic response function

$$\begin{aligned}&\langle\langle X; Y, Z\rangle\rangle^{(I)}_{\omega_Y,\omega_Z} = \\ &P_{XYZ} \sum_{\substack{K=1\\N=1}} \left(O^Y_K(\omega_Y)\right)^\star O^Z_N(-\omega_Z) \left\langle \kappa(r_K, S, T)|e^{S^\dagger} e^{-T} X_0 e^{T} e^{-S^\dagger} \eta(r_N, S)\right\rangle \\ &= P_{XYZ} \sum_{\substack{K=1\\N=1}} \frac{\langle e^{-T} Y e^{T}|l_K\rangle}{\omega_K + \omega_Y} \frac{\langle l_N|e^{-T} Z e^{T}\rangle}{\omega_Z - \omega_N} \left\langle \kappa(r_K, S, T)|e^{S^\dagger} e^{-T} X_0 e^{T} e^{-S^\dagger}|\eta(r_N, S)\right\rangle .\end{aligned} \tag{3.40}$$

The double residue of the XCC quadratic response function reads

$$\begin{aligned}\mathcal{T}^Y_{0L}\mathcal{T}^{(I)}_{LM}\mathcal{T}^Z_{M0} &= \lim_{\omega_Y\to-\omega_L}(\omega_L+\omega_Y) \lim_{\omega_Z\to\omega_M}(\omega_M-\omega_Z) \langle\langle X; Y, Z\rangle\rangle^{(I)}_{\omega_Y,\omega_Z} \\ &= \langle e^{-T} Y e^{T}|l_L\rangle \left\langle \kappa(r_L, S, T)|e^{S^\dagger} e^{-T} X_0 e^{T} e^{-S^\dagger}|\eta(r_M, S)\right\rangle \langle l_M|e^{-T} Z e^{T}\rangle .\end{aligned} \tag{3.41}$$

The same procedure applied do $\langle\langle X; Y, Z\rangle\rangle^{(II)}_{\omega_Y,\omega_Z}$ leads to the following expression

$$\begin{aligned}\mathcal{T}^Y_{0L}\mathcal{T}^{(II)}_{LM}\mathcal{T}^Z_{M0} &= \lim_{\omega_Y\to-\omega_L}(\omega_L+\omega_Y) \lim_{\omega_Z\to\omega_M}(\omega_M-\omega_Z) \langle\langle X; Y, Z\rangle\rangle^{(II)}_{\omega_Y,\omega_Z} \\ &= \langle e^{-T} Y e^{T}|l_L\rangle \left\langle \eta(r_L, S)|e^{-S} e^{T^\dagger} X_0 e^{-T^\dagger} e^{S} \kappa(r_M, S, T)\right\rangle \langle l_M|e^{-T} Z e^{T}\rangle .\end{aligned} \tag{3.42}$$

It is important to notice that the separate transition moments cannot be identified from the r.h.s. of Eq. (3.41). The double residue of the quadratic response function needs to be treated as a whole and cannot arbitrarily be divided into the product of three transition moments. Our solution to this problem is to divide the whole quantity by the product of the left and right transition moments from the ground state. These are obtained from the double residue of $\langle\Psi^{(1)}(\omega_Y)|X|\Psi^{(1)}(-\omega_Z)\rangle$ with $L = M$ and $Y = Z$ and $X = 1$. For the exact quadratic response function this quantity is simply $|T^Y_{0L}|^2 = \langle\Psi_0|\, Y\, |\Psi_L\rangle \langle\Psi_L|\, Y\, |\Psi_0\rangle$, and thus can be used to extract the transition moment between the excited states. In the XCC theory, $|T^Y_{0L}|^2$ is a product of three integrals

$$|T^Y_{0L}|^2 = \langle e^{-T} Y e^{T}|l_L\rangle \langle\kappa(r_L, S, T)|\eta(r_L, S)\rangle \langle l_L|e^{-T} Y e^{T}\rangle . \tag{3.43}$$

As the final result, the double residue of the quadratic response function in the XCC theory divided by $|\mathcal{T}^Y_{0L}\mathcal{T}^Z_{M0}| = \sqrt{|T^Y_{0L}|^2|T^Z_{M0}|^2}$ is given by the expression

$$\begin{aligned}\mathcal{T}^{(I)}_{LM} &= \pm\frac{\lim_{\omega_Y\to-\omega_L}(\omega_L+\omega_Y) \lim_{\omega_z\to\omega_M}(\omega_M-\omega_Z) \langle\langle X; Y, Z\rangle\rangle_{\omega_Y,\omega_Z}}{\sqrt{|T^Y_{0L}|^2|T^Z_{M0}|^2}} \\ &= \pm\frac{\xi^Y_L \left\langle \kappa(r_L, S, T)|e^{S^\dagger} e^{-T} X_0 e^{T} e^{-S^\dagger} \eta(r_M, S)\right\rangle \xi^Z_M}{\sqrt{\xi^Y_L \langle\kappa(r_L, S, T)|\eta(r_L, S)\rangle (\xi^Y_L)^\star \xi^Z_M \langle\kappa(r_M, S, T)|\eta(r_M, S)\rangle (\xi^Z_M)^\star}},\end{aligned} \tag{3.44}$$

where

$$\xi_M^Z = \left\langle l_M \middle| e^{-T} Z e^{T} \right\rangle. \tag{3.45}$$

The $\pm$ sign of $\mathcal{T}_{LM}^X$ is a result of taking the square root of $|\mathcal{T}_{0L}^Y|^2$. This fact is of no concern because practical applications either require the transition strengths, i.e., the products $\mathcal{T}_{LM}^X \mathcal{T}_{ML}^X$, or it is possible to compute the necessary phases by setting up a system of equations (see chapter 4, where this problem is thoroughly discussed). From now on we abandon the $\pm$ sign for clarity.

The expression for $|T_{0L}^Y|^2$ derived above, Eq. (3.43), was also used in this thesis for the computation of the transition moments from the ground to an excited state, as an alternative to the theory described in Paper I.[18]

3.5 Hermiticity

The final expression for $T_{LM}^{(I)}$ in the XCC theory is given by

$$\mathcal{T}_{LM}^{(I)} = \frac{\langle \kappa(r_L, S, T) | e^{S^\dagger} e^{-T} X_0 e^{T} e^{-S^\dagger} \eta(r_M, S) \rangle}{\sqrt{\langle \kappa(r_L, S, T) | \eta(r_L, S) \rangle \, \langle \kappa(r_M, S, T) | \eta(r_M, S) \rangle}}. \tag{3.46}$$

Alternatively, from Eq. (3.42) we obtain

$$\mathcal{T}_{LM}^{(II)} = \frac{\langle \eta(r_L, S) | e^{-S} e^{T^\dagger} X_0 e^{-T^\dagger} e^{S} \kappa(r_M, S, T) \rangle}{\sqrt{\langle \kappa(r_L, S, T) | \eta(r_L, S) \rangle \, \langle \kappa(r_M, S, T) | \eta(r_M, S) \rangle}}. \tag{3.47}$$

To prove that $T_{LM}^{(I)}$ is Hermitian, i.e., $\mathcal{T}_{LM}^{(I)} = \left(\mathcal{T}_{ML}^{(I)}\right)^\star$, we compute

$$\begin{aligned}
\left(\mathcal{T}_{ML}^{(I)}\right)^\star &= \left(\frac{\langle \kappa(r_M, S, T) | e^{S^\dagger} e^{-T} X_0 e^{T} e^{-S^\dagger} \eta(r_L, S) \rangle}{\sqrt{\langle \kappa(r_M, S, T) | \eta(r_M, S) \rangle \, \langle \kappa(r_L, S, T) | \eta(r_L, S) \rangle}} \right)^\star \\
&= \frac{\langle \eta(r_L, S) | (e^{S^\dagger} e^{-T} X_0 e^{T} e^{-S^\dagger})^\star \kappa(r_M, S, T)^\star \rangle}{\sqrt{\langle \eta(r_M, S) | \kappa(r_M, S, T) \rangle \, \langle \eta(r_L, S) | \kappa(r_L, S, T) \rangle}} \\
&= \frac{\langle \eta(r_L, S) | e^{-S} e^{T^\dagger} X_0 e^{-T^\dagger} e^{S} \kappa(r_M, S, T) \rangle}{\sqrt{\langle \eta(r_M, S) | \kappa(r_M, S, T) \rangle \, \langle \eta(r_L, S) | \kappa(r_L, S, T) \rangle}} \\
&= \mathcal{T}_{LM}^{(II)},
\end{aligned} \tag{3.48}$$

The equality between forms (I) and (II) implies the Hermitian symmetry

$$\mathcal{T}_{LM}^{(I)} = \mathcal{T}_{LM}^{(II)} \quad \Rightarrow \quad \mathcal{T}_{LM}^{(I)} = \left(\mathcal{T}_{ML}^{(I)}\right)^\star. \tag{3.49}$$

It is clear from our derivation that Eq. (3.49) is true for the exact operators T and S. For the truncated operator T Eq. (3.49) still holds, but this is not the case for a truncated operator S. In the derivation of Eqs. (3.57) and (3.47) we have used the formal definition of the operator S, $e^S \Phi = \frac{e^{T^\dagger} e^{T}}{\langle e^T | e^T \rangle} \Phi$, which is true only for the exact operators S. Nonetheless, in section 5.4 we demonstrate that the deviations from the exact Hermitian symmetry are numerically negligible.

3.6 Size-extensivity and size-intensivity

Size-extensivity and size-intensivity are very desired features of any approximate electronic structure method. Size-extensive properties should properly scale with the system size and size-intensive properties should be independent of the system size. Our XCC formula for $\langle\langle X; Y, Z\rangle\rangle_{\omega_Y,\omega_Z}$, Eq. (3.35), is expressible solely in terms of commutators. Therefore, it is automatically size-extensive, regardless of the level of truncation of the operators T and S. The EOM-CC excitation energies for states localized at the monomer A with an infinitely distant monomer B, are size intensive.[58] We will prove that the XCC transition moment is also size-intensive.

The importance of the concept of size-intensivity was thoroughly investigated by Koch et al. in the work on the TD-CC transition moments.[58] The authors performed calculations of the dipole strength (which is directly related to transition moments) for a series of $n = 1$ to 15 noninteracting LiH molecules with the use of the size-intensive TD-CC and RPA, and not size-intensive EOM-CC methods. In Fig. 3.1 we present schematically the result of Ref. 58, which shows the dramatic fail of the approach that is not size-intensive approach.

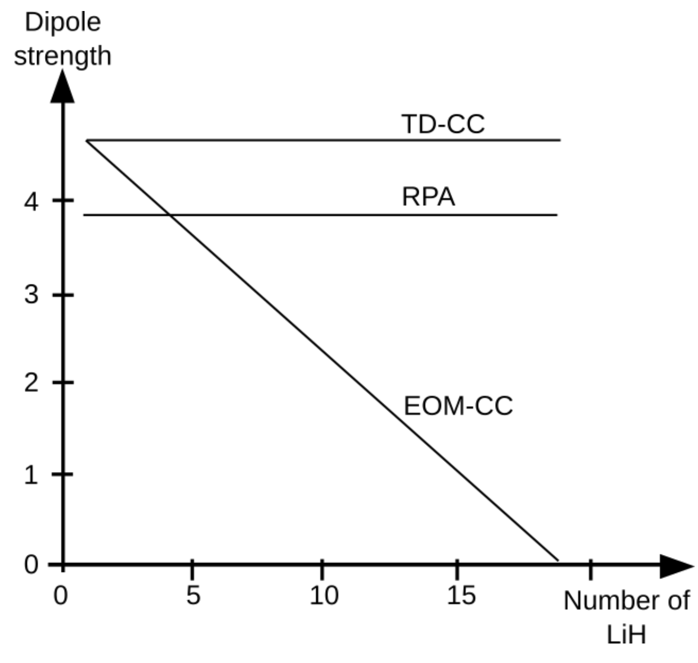

Figure 3.1: Dipole strength as a function of number of noninteracting LiH molecules. Figure generated using data from Ref. 58

To prove the size-intensivity of our expression (3.57) we consider two noninteracting subsystems A and B at the infinite separation. We can then write

$$H_{AB} = H_A + H_B \tag{3.50}$$

$$T_{AB} = T_A + T_B$$

$$S_{AB} = S_A + S_B.$$

Size-intensivity can easily be demonstrated for the exact transition moment

$$\begin{aligned}T_{LM}^{X_{AB}} &= \langle \Psi_{L_A}\Phi_B | \, X_A + X_B \, | \Psi_{M_A}\Phi_B \rangle = \\ &\langle \Psi_{L_A}\Phi_B | \, X_A \, | \Psi_{M_A}\Phi_B \rangle + \langle \Psi_{L_A}\Phi_B | \, X_B \, | \Psi_{M_A}\Phi_B \rangle = \\ &\langle \Psi_{L_A} | \, X_A \, | \Psi_{M_A} \rangle \underbrace{\langle \Phi_B | \Phi_B \rangle}_{=1} + \langle \Phi_B | \, X_B \, | \Phi_B \rangle \underbrace{\langle \Psi_{L_A} | \Psi_{M_A} \rangle}_{=0} \\ &= T_{LM}^{X_A}.\end{aligned} \tag{3.51}$$

Note that in some equations we write the reference state ϕ explicitly, in order to avoid any confusion. For the XCC transition moment the following commutation relations hold:

$$[X_0^A, T_B] = [X_0^B, T_A] = [X_0^A, S_B] = [X_0^B, S_A] = [L_A, T_B] = [L_A, S_B] = 0 \tag{3.52}$$

and

$$X_0^{AB} = X^{AB} - \langle \Psi_{AB} | X^{AB} | \Psi_{AB} \rangle \tag{3.53}$$

$$= X^A + X^B - \zeta(X^A, S_A, T_A) - \zeta(X^B, S_B, T_B) \tag{3.54}$$

where we used a shorthand notation

$$\zeta(X, S, T) = e^{S^\dagger} e^{-T} X e^{T} e^{-S^\dagger} \tag{3.55}$$

The transition moment for such a system in XCC can be presented as follows

$$\begin{aligned}\mathcal{T}_{LM}^{AB} &= \frac{\langle \kappa(r_{L_A}, S_{AB}, T_{AB}) | \zeta(X_0^{AB}, S_{AB}, T_{AB}) | \eta(r_{M_A}, S_{AB}) \rangle}{\sqrt{\langle \kappa(r_{L_A}, S_{AB}, T_{AB}) | \eta(r_{L_A}, S_{AB}) \rangle \, \langle \kappa(r_{M_A}, S_{AB}, T_{AB}) | \eta(r_{M_A}, S_{AB}) \rangle}} \\ &= \frac{\langle \kappa(r_{L_A}, S_A, T_A) | \zeta(X_0^{AB}, S_{AB}, T_{AB}) | \eta(r_{M_A}, S_A) \rangle}{\sqrt{\langle \kappa(r_{L_A}, S_A, T_A) | \eta(r_{L_A}, S_A) \rangle \, \langle \kappa(r_{M_A}, S_A, T_A) | \eta(r_{M_A}, S_A) \rangle}} \\ &= \Bigg(\frac{\langle \kappa(r_{L_A}, S_A, T_A) | \zeta(X_0^{A}, S_A, T_A) | \eta(r_{M_A}, S_A) \rangle \overbrace{\langle \Phi_B | \Phi_B \rangle}^{=1}}{\sqrt{\langle \kappa(r_{L_A}, S_A, T_A) | \eta(r_{L_A}, S_A) \rangle \, \langle \kappa(r_{M_A}, S_A, T_A) | \eta(r_{M_A}, S_A) \rangle}} \\ &+ \frac{\langle \kappa(r_{L_A}, S_A, T_A) | \eta(r_{M_A}, S_A) \rangle \, \langle \zeta(X_0^B, S_B, T_B) \rangle}{\sqrt{\langle \kappa(r_{L_A}, S_A, T_A) | \eta(r_{L_A}, S_A) \rangle \, \langle \kappa(r_{M_A}, S_A, T_A) | \eta(r_{M_A}, S_A) \rangle}} \Bigg) \\ &= \frac{\langle \kappa(r_{L_A}, S_A, T_A) | \zeta(X_0^{A}, S_A, T_A) | \eta(r_{M_A}, S_A) \rangle}{\sqrt{\langle \kappa(r_{L_A}, S_A, T_A) | \eta(r_{L_A}, S_A) \rangle \, \langle \kappa(r_{M_A}, S_A, T_A) | \eta(r_{M_A}, S_A) \rangle}} \\ &+ \frac{\langle \kappa(r_{L_A}, S_A, T_A) | \eta(r_{M_A}, S_A) \rangle \, \langle \zeta(X^B, S_B, T_B) \rangle}{\sqrt{\langle \kappa(r_{L_A}, S_A, T_A) | \eta(r_{L_A}, S_A) \rangle \, \langle \kappa(r_{M_A}, S_A, T_A) | \eta(r_{M_A}, S_A) \rangle}}\end{aligned} \tag{3.56}$$

$$
- \frac{\langle \kappa(r_{L_A}, S_A, T_A)|\eta(r_{M_A}, S_A)\rangle \langle \zeta(X^B, S_B, T_B)\rangle}{\sqrt{\langle \kappa(r_{L_A}, S_A, T_A)|\eta(r_{L_A}, S_A)\rangle \langle \kappa(r_{M_A}, S_A, T_A)|\eta(r_{M_A}, S_A)\rangle}}
$$

$$
= \mathcal{T}^{A}_{LM}
$$

The last two terms cancel out, therefore, the transition moment $\mathcal{T}^{X_{AB}}_{LM}$ for a transition between states L and M of molecule X_{AB} does not depend on the system size i.e., is size-intensive.

3.7 Workable formulas for the XCC transition moments

The final expression for $\mathcal{T}^{X}_{LM}$ in the XCC theory is given by

$$
\mathcal{T}^{X}_{LM} = \frac{\langle \kappa(r_L, S, T)|e^{S^\dagger} e^{-T} X_0 e^{T} e^{-S^\dagger} \eta(r_M, S)\rangle}{\sqrt{\langle \kappa(r_L, S, T)\rangle\, \eta(r_L, S)\, \langle \kappa(r_M, S, T)\rangle\, \eta(r_M, S)}}, \tag{3.57}
$$

where

$$
\begin{aligned}
\kappa(r_N) &= \hat{\mathcal{P}}\left(e^{-S} e^{T^\dagger} r_N e^{-T^\dagger} e^{S}\right), \\
\eta(r_N, S) &= \hat{\mathcal{P}}\left(e^{S^\dagger} r_N e^{-S^\dagger}\right).
\end{aligned} \tag{3.58}
$$

To compute properties, one needs to follow four independent steps: obtain the amplitudes t and s, then compute the excitation amplitudes r_N, and finally use Eq. (3.57) to compute $\mathcal{T}^{X}_{LM}$.

The calculation of the amplitudes t can be done by any standard CC method. In this work we used the coupled cluster method limited to single and double excitations (CCSD) and the coupled cluster method limited to single, double, and linear triple excitations (CC3).

The amplitudes s are computed from Eq. (2.38). It is a finite expansion, though it contains terms of high order in the fluctuation potential W.[68] To find the exact operator S one requires an iterative procedure. However, S can efficiently be approximated while retaining the size-consistency. In Paper I[18] we presented a hierarchy of approximations and assessed their accuracy. Let $S_n(m)$ denote the n-electron part of S, where all contributions up to and including the order m of MBPT are accounted for. In the computations based on the CC3 model (single, double, and linear triple excitations), we employ

$$
\begin{aligned}
S_1(3) &= T_1 + \hat{\mathcal{P}}_1\left([T_1^\dagger, T_2]\right), \\
&\quad + \hat{\mathcal{P}}_1\left([T_2^\dagger, T_3]\right), \\
S_2(3) &= T_2 + \frac{1}{2}\hat{\mathcal{P}}_2\left([[T_2^\dagger, T_2], T_2]\right), \\
S_3(2) &= T_3,
\end{aligned} \tag{3.59}
$$

where the CC3 equations for T_1, T_2 and T_3 are given by Koch et al.[66] It should be noted that we take $S_3 = T_3$ from the CC3 theory and no additional terms from Eq. (2.38), hence the operator S_3 is of the second-order in MBPT. In the instances where the underlying model of the wave function is CCSD (coupled cluster limited to single and double excitations), we employ $S = S_1(3) + S_2(3)$ neglecting the terms containing T_3.

The amplitudes r_N are obtained from the EOM-CCSD or EOM-CC3 model, depending on which approximation one uses for the ground state.

The most challenging part is a reasonable approximation of the transition moment formula. We expanded Eq. (3.57) in the orders of MBPT: zeroth, first, second, and third. The formulas were derived automatically by the program PALDUS (see section 4.5.2). Due to the computational or memory restrictions, not all of the terms in each order were possible to include. Therefore, we employed some additional approximations that are now described.

All of the terms in Eq. (3.57) are of the type:

$$\langle[[\mu_n, T^\dagger]_{k_1}, S]_{k_2}|[[X, T]_{k_3}, S^\dagger]_{k_4}|[\nu_m, S^\dagger]_{k_5}\rangle\,, \tag{3.60}$$

where $k_1 - k_5$ are integers and denote the order of nesting, m and n is the excitation levels, and for clarity we do not write the excitation levels at T and S. Generally, we include all of the terms with a few exceptions that are listed in the Table 3.1. One should interpret the description as:

- "*neglecting* $\langle\mu_n|\dots|\nu_m\rangle$" means that all the terms up to and including the kth order of MBPT are included with the exception of terms that have n-tuple excitations in the bra and m-tuple excitations in the ket.

- "*neglecting* $\langle\mu_n|\dots|\nu_m\rangle$ *unless* T_1 *or* S_1" means that all the terms up to the kth order of MBPT are included with the exception of terms that have n-tuple excitations in the bra and m-tuple excitations in the ket, unless the operator T_1 or S_1 appears at least once. E.g. $\langle X[\mu_3, T_2^\dagger]|[\nu_2, S_1^\dagger]\rangle$ is included, but $\langle X[S_2, [\mu_3, T_3^\dagger]]|\nu_2\rangle$ is not included

- "*include only terms with at least one* T_1 *or* S_1" means that only terms in which the operator T_1 or S_1 appears at least once are included.

This approximation was tested on a set of atoms (Ca, Sr, Ba) in different basis sets, and in the CCSD and CC3 approximations. The singlet-singlet, triplet-triplet and singlet-triplet transitions were investigated. Below (Figs. 3.2 to 3.7), we present a set of plots for all above mentioned cases that show how the XCC transition moment behaves with the increase of the order of MBPT. On the y axis, we show the ratio $\frac{T^X_{LM}(m)}{T^X_{LM}(3)}$, where m denotes the order of MBPT. It is clear that the results converge rapidly after the inclusion of the second order. In some cases we also computed

Table 3.1: Terms included in the XCC transition moments calculations.

MBPT order	CCSD	CC3
0	all	all
1	all	all
2	all	neglecting $\langle\mu_3\|\ldots\|\nu_3\rangle$
3	all	neglecting $\langle\mu_3\|\ldots\|\nu_3\rangle$ neglecting $\langle\mu_2\|\ldots\|\nu_3\rangle$ unless T_1 or S_1 neglecting $\langle\mu_1\|\ldots\|\nu_3\rangle$ unless T_1 or S_1
4	include only terms with at least one T_1 or S_1	include only terms with at least one T_1 or S_1

the fourth order, but the change compared to the third order was negligible, so we do not present these results here. Our conclusion is that the approximation to the third order of MBPT is sufficient, so all our results are computed at this level of theory.

CCSD

MBPT order 0

$$\begin{aligned}&+\langle X\mu_2|\nu_1\rangle+\langle X\mu_1|\nu_1\rangle+\langle X\mu_2|\nu_2\rangle\\&+\langle X\mu_1|\nu_2\rangle\end{aligned}\tag{3.61}$$

MBPT order 1

$$+\langle[S_2,X]\mu_1|\nu_2\rangle+\langle[X,T_2^\dagger]\mu_2|\nu_1\rangle\tag{3.62}$$

MBPT order 2

$$\begin{aligned}&+\langle X\mu_2|[\nu_2,S_1^\dagger]\rangle+\langle X[S_2,[\mu_2,T_2^\dagger]]|\nu_1\rangle+\langle X\mu_1|[\nu_2,S_1^\dagger]\rangle\\&+\langle X[\mu_2,T_1^\dagger]|\nu_1\rangle+\langle X[S_2,[\mu_1,T_2^\dagger]]|\nu_1\rangle+\langle X[S_2,[\mu_2,T_2^\dagger]]|\nu_2\rangle\\&+\langle X[\mu_2,T_1^\dagger]|\nu_2\rangle+\langle X[S_2,[\mu_1,T_2^\dagger]]|\nu_2\rangle+\langle[S_1,X]\mu_1|\nu_1\rangle\\&+\langle[S_1,X]\mu_2|\nu_2\rangle+\langle[S_1,X]\mu_1|\nu_2\rangle+\langle[X,T_1^\dagger]\mu_2|\nu_1\rangle\\&+\langle[X,T_1^\dagger]\mu_1|\nu_1\rangle+\langle[X,T_1^\dagger]\mu_2|\nu_2\rangle+\langle[S_2,[X,T_2^\dagger]]\mu_1|\nu_1\rangle\\&+\langle[S_2,[X,T_2^\dagger]]\mu_2|\nu_2\rangle+\langle[S_2,[X,T_2^\dagger]]\mu_1|\nu_2\rangle\end{aligned}\tag{3.63}$$

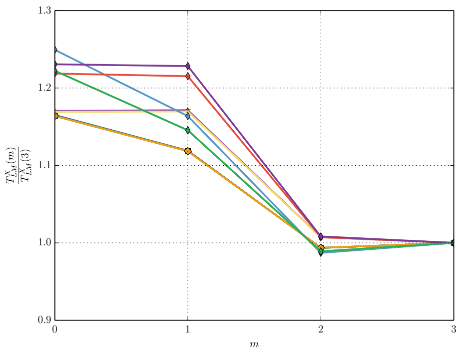

Figure 3.2: Singlet dipole transition in the CCSD approximation.

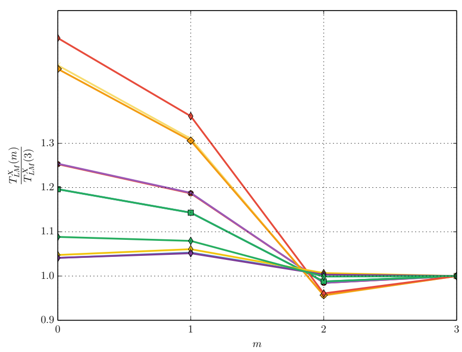

Figure 3.3: Singlet dipole transition in the CC3 approximation.

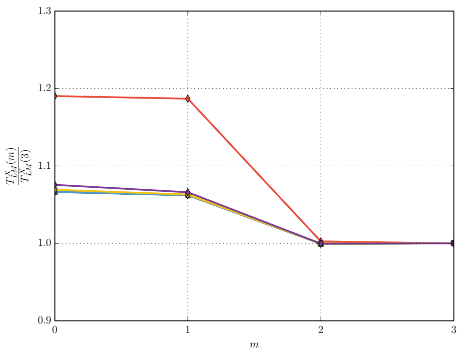

Figure 3.4: Triplet dipole transition in the CCSD approximation.

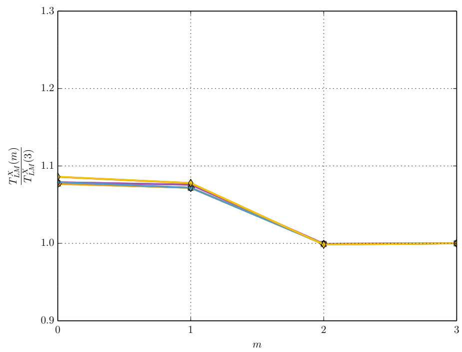

Figure 3.5: Triplet dipole transition in the CC3 approximation.

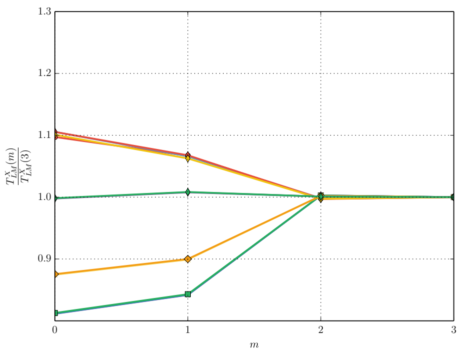

Figure 3.6: Spin-orbit matrix element in the CCSD approximation.

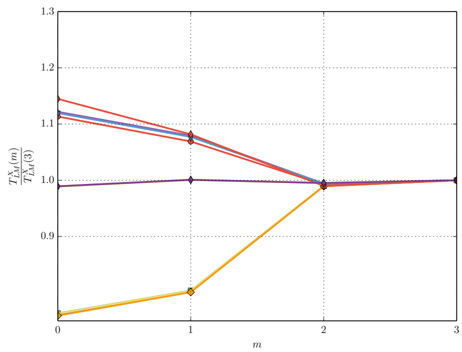

Figure 3.7: Spin-orbit matrix element in the CC3 approximation.

MBPT order 3

$$
\begin{aligned}
&+ \langle X[S_2,[\mu_1,T_1^\dagger]]|\nu_1\rangle + \langle X[S_2,[\mu_2,T_1^\dagger]]|\nu_2\rangle + \frac{1}{2}\langle X[S_2,[S_2,[\mu_1,T_2^\dagger]]]|\nu_2\rangle \\
&+ \langle X[S_2,[\mu_1,T_1^\dagger]]|\nu_2\rangle + \langle X[S_1,[\mu_2,T_2^\dagger]]|\nu_1\rangle + \langle X[S_1,[\mu_2,T_2^\dagger]]|\nu_2\rangle \\
&+ \langle [S_2,X][\mu_2,T_1^\dagger]|\nu_2\rangle + \langle [S_2,X][S_2,[\mu_1,T_2^\dagger]]|\nu_2\rangle + \langle [X,T_2^\dagger]\mu_2|[\nu_2,S_1^\dagger]\rangle \\
&+ \langle [X,T_2^\dagger][S_2,[\mu_2,T_2^\dagger]]|\nu_1\rangle + \langle [S_2,[X,T_1^\dagger]]\mu_1|\nu_2\rangle + \langle [S_1,[X,T_2^\dagger]]\mu_2|\nu_1\rangle \\
&+ \langle [S_1,[X,T_2^\dagger]]\mu_1|\nu_1\rangle + \langle [S_1,[X,T_2^\dagger]]\mu_2|\nu_2\rangle + \frac{1}{2}\langle [S_2,[[X,T_2^\dagger],T_2^\dagger]]\mu_2|\nu_1\rangle
\end{aligned} \tag{3.64}
$$

MBPT order 4 included

$$
\begin{aligned}
&+ \langle X[S_1,[\mu_2,T_1^\dagger]]|\nu_1\rangle + \langle X[S_2,[\mu_2,T_2^\dagger]]|[\nu_2,S_1^\dagger]\rangle + \frac{1}{2}\langle X[S_2,[S_1,[\mu_1,T_2^\dagger]]]|\nu_1\rangle \\
&+ \frac{1}{2}\langle X[S_2,[S_1,[\mu_2,T_2^\dagger]]]|\nu_2\rangle + \langle X[\mu_2,T_1^\dagger]|[\nu_2,S_1^\dagger]\rangle + \langle X[S_1,[\mu_1,T_1^\dagger]]|\nu_1\rangle \\
&+ \langle X[S_1,[\mu_2,T_1^\dagger]]|\nu_2\rangle + \langle X[S_2,[\mu_1,T_2^\dagger]]|[\nu_2,S_1^\dagger]\rangle + \frac{1}{2}\langle X[S_2,[S_1,[\mu_1,T_2^\dagger]]]|\nu_2\rangle \\
&+ \frac{1}{2}\langle X[S_2,[[\mu_2,T_1^\dagger],T_2^\dagger]]|\nu_1\rangle + \langle X[S_1,[\mu_1,T_1^\dagger]]|\nu_2\rangle + \frac{1}{2}\langle X[S_2,[[\mu_2,T_1^\dagger],T_2^\dagger]]|\nu_2\rangle \\
&+ \langle [S_1,X]\mu_1|[\nu_2,S_1^\dagger]\rangle + \langle [S_1,X][\mu_2,T_1^\dagger]|\nu_1\rangle + \langle [S_1,X][S_2,[\mu_1,T_2^\dagger]]|\nu_1\rangle \\
&+ \langle [S_1,X][S_2,[\mu_2,T_2^\dagger]]|\nu_2\rangle + \langle [S_1,X][\mu_2,T_1^\dagger]|\nu_2\rangle + \langle [S_1,X][S_2,[\mu_1,T_2^\dagger]]|\nu_2\rangle \\
&+ \langle [S_2,X][S_1,[\mu_2,T_2^\dagger]]|\nu_2\rangle + \frac{1}{2}\langle [S_1,[S_1,X]]\mu_1|\nu_2\rangle + \langle [X,T_1^\dagger]\mu_2|[\nu_2,S_1^\dagger]\rangle \\
&+ \langle [X,T_1^\dagger][S_2,[\mu_2,T_2^\dagger]]|\nu_1\rangle + \langle [X,T_1^\dagger]\mu_1|[\nu_2,S_1^\dagger]\rangle + \langle [X,T_1^\dagger][\mu_2,T_1^\dagger]|\nu_1\rangle \\
&+ \langle [X,T_1^\dagger][S_2,[\mu_1,T_2^\dagger]]|\nu_1\rangle + \langle [X,T_1^\dagger][S_2,[\mu_2,T_2^\dagger]]|\nu_2\rangle + \langle [X,T_2^\dagger][S_2,[\mu_2,T_1^\dagger]]|\nu_1\rangle \\
&+ \langle [X,T_2^\dagger][S_2,[\mu_1,T_1^\dagger]]|\nu_1\rangle + \langle [X,T_2^\dagger][S_2,[\mu_2,T_1^\dagger]]|\nu_2\rangle + \langle [S_1,[X,T_1^\dagger]]\mu_1|\nu_1\rangle \\
&+ \langle [S_1,[X,T_1^\dagger]]\mu_2|\nu_2\rangle + \langle [S_1,[X,T_1^\dagger]]\mu_1|\nu_2\rangle + \langle [S_2,[X,T_2^\dagger]]\mu_1|[\nu_2,S_1^\dagger]\rangle \\
&+ \langle [S_2,[X,T_2^\dagger]][\mu_2,T_1^\dagger]|\nu_1\rangle + \langle [S_2,[X,T_2^\dagger]][\mu_2,T_1^\dagger]|\nu_2\rangle + \frac{1}{2}\langle [S_2,[S_1,[X,T_2^\dagger]]]\mu_1|\nu_2\rangle \\
&+ \frac{1}{2}\langle [[X,T_1^\dagger],T_1^\dagger]\mu_2|\nu_1\rangle + \frac{1}{2}\langle [S_2,[[X,T_1^\dagger],T_2^\dagger]]\mu_1|\nu_1\rangle + \frac{1}{2}\langle [S_2,[[X,T_1^\dagger],T_2^\dagger]]\mu_2|\nu_2\rangle
\end{aligned} \tag{3.65}
$$

CC3 = CCSD + . . .

MBPT order 0

$$
+ \langle X\mu_3|\nu_2\rangle + \langle X\mu_3|\nu_3\rangle + \langle X\mu_2|\nu_3\rangle \tag{3.66}
$$

MBPT order 1

$$
\begin{aligned}
&+ \langle X\mu_2|[\nu_3,S_2^\dagger]\rangle + \langle X\mu_1|[\nu_3,S_2^\dagger]\rangle + \langle X[\mu_3,T_2^\dagger]|\nu_1\rangle \\
&+ \langle X[\mu_3,T_2^\dagger]|\nu_2\rangle + \langle [S_2,X]\mu_2|\nu_3\rangle + \langle [S_2,X]\mu_1|\nu_3\rangle
\end{aligned} \tag{3.67}
$$

$$+\langle [X, T_2^\dagger]\mu_3|\nu_1\rangle + \langle [X, T_2^\dagger]\mu_3|\nu_2\rangle$$

MBPT order 2

$$\begin{aligned}
&+\langle X[\mu_3, T_1^\dagger]|\nu_1\rangle + +\langle X[S_2, [\mu_3, T_2^\dagger]]|\nu_2\rangle + +\langle X\mu_2|[\nu_3, S_1^\dagger]\rangle \\
&+ + \langle X[\mu_3, T_1^\dagger]|\nu_2\rangle + +\langle X\mu_1|[\nu_3, S_1^\dagger]\rangle + +\langle X[S_2, [\mu_2, T_2^\dagger]]|\nu_3\rangle \\
&+ + \langle [S_1, X]\mu_2|\nu_3\rangle + +\langle [S_2, X][\mu_3, T_2^\dagger]|\nu_2\rangle + +\langle [X, T_1^\dagger]\mu_3|\nu_2\rangle \\
&+ + \langle [X, T_2^\dagger]\mu_2|[\nu_3, S_2^\dagger]\rangle + \langle [S_2, [X, T_2^\dagger]]\mu_2|\nu_3\rangle
\end{aligned} \tag{3.68}$$

not included

$$\begin{aligned}
&+\langle X\mu_3|[\nu_3, S_1^\dagger]\rangle + \langle X[\mu_3, T_2^\dagger]|[\nu_3, S_2^\dagger]\rangle + \langle X[S_2, [\mu_3, T_2^\dagger]]|\nu_3\rangle \\
&+\langle X[\mu_3, T_1^\dagger]|\nu_3\rangle + \langle [S_1, X]\mu_3|\nu_3\rangle + \langle [S_2, X][\mu_3, T_2^\dagger]|\nu_3\rangle \\
&+\langle [S_3, X]\mu_1|\nu_3\rangle + \langle [X, T_1^\dagger]\mu_3|\nu_3\rangle + \langle [X, T_2^\dagger]\mu_3|[\nu_3, S_2^\dagger]\rangle \\
&+\langle [X, T_3^\dagger]\mu_3|\nu_1\rangle + \langle [S_2, [X, T_2^\dagger]]\mu_3|\nu_3\rangle
\end{aligned} \tag{3.69}$$

MBPT order 3

$$\begin{aligned}
&+\langle X[S_1, [\mu_3, T_2^\dagger]]|\nu_1\rangle + \langle X[S_3, [\mu_1, T_2^\dagger]]|\nu_1\rangle + \langle X[S_3, [\mu_2, T_2^\dagger]]|\nu_2\rangle \\
&+\langle X[\mu_2, T_1^\dagger]|[\nu_3, S_2^\dagger]\rangle + \langle X[\mu_3, T_2^\dagger]|[\nu_2, S_1^\dagger]\rangle + \langle X[S_2, [\mu_2, T_1^\dagger]]|\nu_3\rangle \\
&+\langle X[S_1, [\mu_3, T_2^\dagger]]|\nu_2\rangle + \langle X[S_3, [\mu_1, T_2^\dagger]]|\nu_2\rangle + \langle X[S_2, [\mu_2, T_3^\dagger]]|\nu_1\rangle \\
&+\langle X[S_2, [\mu_1, T_1^\dagger]]|\nu_3\rangle + \langle X[S_2, [\mu_2, T_3^\dagger]]|\nu_2\rangle + \langle [S_1, X]\mu_1|[\nu_3, S_2^\dagger]\rangle \\
&+\langle [S_1, X][\mu_3, T_2^\dagger]|\nu_1\rangle + \langle [S_1, X][\mu_3, T_2^\dagger]|\nu_2\rangle + \langle [S_2, X]\mu_1|[\nu_3, S_1^\dagger]\rangle \\
&+\langle [S_2, X][\mu_2, T_1^\dagger]|\nu_3\rangle + \frac{1}{2}\langle [S_2, [S_1, X]]\mu_1|\nu_3\rangle + \langle [X, T_1^\dagger]\mu_2|[\nu_3, S_2^\dagger]\rangle \\
&+\langle [X, T_1^\dagger]\mu_1|[\nu_3, S_2^\dagger]\rangle + \langle [X, T_1^\dagger][\mu_3, T_2^\dagger]|\nu_1\rangle + \langle [X, T_2^\dagger]\mu_3|[\nu_2, S_1^\dagger]\rangle \\
&+\langle [X, T_2^\dagger][\mu_3, T_1^\dagger]|\nu_1\rangle + \langle [S_2, [X, T_1^\dagger]]\mu_2|\nu_3\rangle + \langle [S_2, [X, T_1^\dagger]]\mu_1|\nu_3\rangle \\
&+\langle [S_1, [X, T_2^\dagger]]\mu_3|\nu_2\rangle + \langle [S_3, [X, T_2^\dagger]]\mu_1|\nu_2\rangle + \langle [S_2, [X, T_3^\dagger]]\mu_2|\nu_1\rangle \\
&+\langle [S_2, [X, T_3^\dagger]]\mu_1|\nu_1\rangle + \langle [S_2, [X, T_3^\dagger]]\mu_2|\nu_2\rangle + \frac{1}{2}\langle [[X, T_1^\dagger], T_2^\dagger]\mu_3|\nu_1\rangle
\end{aligned} \tag{3.70}$$

not included

$$\begin{aligned}
&+\langle X[\mu_3, T_1^\dagger]|[\nu_3, S_2^\dagger]\rangle + \langle X[S_2, [\mu_3, T_1^\dagger]]|\nu_3\rangle + \langle X[S_2, [\mu_2, T_2^\dagger]]|[\nu_3, S_2^\dagger]\rangle \\
&+\langle X[S_3, [\mu_3, T_2^\dagger]]|\nu_3\rangle + \langle X[S_2, [\mu_3, T_3^\dagger]]|\nu_1\rangle + \frac{1}{2}\langle X[S_2, [S_2, [\mu_2, T_2^\dagger]]]|\nu_3\rangle \\
&+\langle X[S_2, [\mu_1, T_2^\dagger]]|[\nu_3, S_2^\dagger]\rangle + \langle X[S_3, [\mu_2, T_2^\dagger]]|\nu_3\rangle + \langle X[S_2, [\mu_3, T_3^\dagger]]|\nu_2\rangle \\
&+\frac{1}{2}\langle X[S_2, [S_2, [\mu_1, T_2^\dagger]]]|\nu_3\rangle + \frac{1}{2}\langle X[S_2, [[\mu_3, T_2^\dagger], T_2^\dagger]]|\nu_1\rangle + \langle X[\mu_3, T_2^\dagger]|[\nu_3, S_1^\dagger]\rangle \\
&+\langle X[S_1, [\mu_3, T_2^\dagger]]|\nu_3\rangle + \langle X[S_3, [\mu_1, T_2^\dagger]]|\nu_3\rangle + \langle X[S_2, [\mu_3, T_3^\dagger]]|\nu_3\rangle \\
&+\frac{1}{2}\langle X[S_2, [[\mu_3, T_2^\dagger], T_2^\dagger]]|\nu_2\rangle + \langle [S_2, X][\mu_3, T_1^\dagger]|\nu_3\rangle + \langle [S_2, X][S_2, [\mu_2, T_2^\dagger]]|\nu_3\rangle
\end{aligned} \tag{3.71}$$

$$
\begin{aligned}
&+\langle[S_2,X][S_2,[\mu_1,T_2^\dagger]]|\nu_3\rangle+\langle[S_3,X][\mu_3,T_2^\dagger]|\nu_3\rangle+\langle[X,T_2^\dagger][S_2,[\mu_3,T_2^\dagger]]|\nu_1\rangle\\
&+\langle[X,T_2^\dagger]\mu_3|[\nu_3,S_1^\dagger]\rangle+\langle[X,T_2^\dagger][S_2,[\mu_3,T_2^\dagger]]|\nu_2\rangle+\langle[X,T_3^\dagger]\mu_3|[\nu_3,S_2^\dagger]\rangle\\
&+\langle[S_1,[X,T_2^\dagger]]\mu_3|\nu_3\rangle+\langle[S_2,[X,T_2^\dagger]]\mu_1|[\nu_3,S_2^\dagger]\rangle+\langle[S_2,[X,T_2^\dagger]][\mu_3,T_2^\dagger]|\nu_1\rangle\\
&+\langle[S_2,[X,T_2^\dagger]][\mu_3,T_2^\dagger]|\nu_2\rangle+\langle[S_3,[X,T_2^\dagger]]\mu_2|\nu_3\rangle+\langle[S_3,[X,T_2^\dagger]]\mu_1|\nu_3\rangle\\
&+\langle[S_2,[X,T_3^\dagger]]\mu_3|\nu_2\rangle+\langle[S_2,[X,T_3^\dagger]]\mu_3|\nu_3\rangle+\frac{1}{2}\langle[S_2,[S_2,[X,T_2^\dagger]]]\mu_1|\nu_3\rangle\\
&+\frac{1}{2}\langle[S_2,[[X,T_2^\dagger],T_2^\dagger]]\mu_3|\nu_2\rangle
\end{aligned}
$$

MBPT order 4 included

$$
+\langle X[S_3,[\mu_1,T_1^\dagger]]|\nu_2\rangle+\langle[S_1,[X,T_3^\dagger]]\mu_2|\nu_1\rangle \tag{3.72}
$$

Chapter 4 Technical details

4.1 Radiative lifetimes

The transition probability from the initial state i to the final state f for the dipole (E1) and quadrupole (E2) transitions, respectively, is defined by the Einstein coefficients

$$\mathcal{A}_{if}(E1) = \frac{16\pi^3}{3h\epsilon_0\lambda^3(2J_i+1)}S_{if}(E1) \tag{4.1}$$

$$\mathcal{A}_{if}(E2) = \frac{16\pi^5}{15h\epsilon_0\lambda^5(2J_i+1)}S_{if}(E2), \tag{4.2}$$

where h is the Planck constant, ϵ_0 is the vacuum permittivity, λ is the energy in $[m]$, J is the total angular momentum for the initial state, $\mathcal{S}_{if}(E1)$ is the line strength of a dipole transition in $[m^2C^2]$, and $\mathcal{S}_{if}(E2)$ is the line strength of a quadrupole transition in $[m^4C^2]$. The line strength is defined as

$$\mathcal{S}_{if} = |\vec{T}_{if}^{\mathbf{R}}|^2 = |\langle\psi_i||\mathbf{R}||\psi_f\rangle|^2, \tag{4.3}$$

where $\langle\psi_i||\mathbf{R}||\psi_f\rangle$ is a reduced matrix element for the transition operator $\mathbf{R}$ from the state i to f. For an allowed transition, the procedure of computing the transition probability A_{if} is straightforward. One needs to compute transition moments from Eq. (3.44), and use Eq. (4.1) or Eq. (4.2). To derive the expression for the spin-forbidden transitions, we use the Rayleigh–Schrödinger perturbation theory (RSPT).[90] Assuming that we have an initial triplet state and final singlet state, the RSPT expansion is given by

$$\langle\Psi_i| = \langle\Psi_i^{(0)}| + \langle\Psi_i^{(1)}| + \dots \tag{4.4}$$

$$= \langle{}^3\psi_i^{(0)}| + \sum_{k,m}\frac{\langle{}^m\psi_k^{(0)}|H_{so}|{}^3\psi_i^{(0)}\rangle}{{}^mE_k^{(0)} - {}^3E_i^{(0)}}\langle{}^m\psi_k^{(0)}| + \dots \tag{4.5}$$

where Ψ and ψ are pure LS states coupled by the spin-orbit interaction. The index k runs over all of the states with a given multiplicity m. The final ground state is

$$|\Psi_f\rangle = |\Psi_f^{(0)}\rangle + |\Psi_f^{(1)}\rangle + \dots \tag{4.6}$$

$$= |{}^1\psi_f^{(0)}\rangle + \sum_k\frac{\langle{}^1\psi_f^{(0)}|H_{so}|{}^3\psi_f^{(0)}\rangle}{{}^1E_f^{(0)} - {}^3E_k^{(0)}}|{}^3\psi_k^{(0)}\rangle + \dots \tag{4.7}$$

Here k runs only over states with the triplet multiplicity, as other terms vanish due to the selection rules. Let us employ the electric dipole perturbation as an example to show how the perturbation theory is applied to compute the spin-forbidden transitions, i.e., $\mathbf{R} = \mathbf{D}$

$$\vec{\mathcal{T}}_{if}^{\mathbf{D}} = \langle \Psi_i^{(0)} + \Psi_i^{(1)} | \mathbf{D} | \Psi_f^{(0)} + \Psi_f^{(1)} \rangle \,. \tag{4.8}$$

The higher order terms are neglected in the following derivation, as these terms are usually small unless the difference in energies of the considered states is nearly degenerate.[53] We also take only $m = 1$ states in the expansion (4.4), as states of other multiplicities are not directly connected by the dipole transition with the ground state. The term $\langle \Psi_i^{(0)} | \mathbf{D} | \Psi_f^{(0)} \rangle$ vanishes due to the selection rules, so finally the expression for the transition dipole moment is given by

$$\vec{\mathcal{T}}_{if}^{\mathbf{D}} = \sum_k \frac{\langle {}^1\psi_f^{(0)} | H_{so} | {}^3\psi_f^{(0)} \rangle}{{}^1E_f^{(0)} - {}^3E_k^{(0)}} \langle {}^3\psi_i^{(0)} | \mathbf{D} | {}^3\psi_k^{(0)} \rangle + \sum_k \frac{\langle {}^1\psi_k^{(0)} | H_{so} | {}^3\psi_i^{(0)} \rangle}{{}^1E_k^{(0)} - {}^3E_i^{(0)}} \langle {}^1\psi_k^{(0)} | \mathbf{D} | {}^1\psi_f^{(0)} \rangle \tag{4.9}$$

The radiative lifetime[91] τ_k of an atomic level k is defined by Eqs. (4.1) and (4.2)

$$\tau_k = \frac{1}{\sum_i \mathcal{A}_{ki}} \tag{4.10}$$

where the sum over i runs over all states (channels) i to which the level k can decay.

4.2 Computation of the transition probabilities

The values of the transition moments are usually represented in the literature in the form of reduced matrix elements

$$\langle \alpha'^{2S'+1} L'_{J'} || T_q^{(k)} || \alpha^{2S+1} L_J \rangle \equiv \langle \alpha' L' S' J' || T_q^{(k)} || \alpha L S J \rangle \,, \tag{4.11}$$

where L, S, and J are quantum numbers of the orbital, spin, and total angular momentum, respectively, and $T_q^{(k)}$ is an irreducible tensor operator of rank k with $2k+1$ components $q \in (-k, \ldots, k)$ (e.g. dipole moment operator, quadrupole moment operator, spin-orbit coupling operator, etc.). The index α denotes other possible quantum numbers, not important in our considerations. In this notation it is clear that the bra and ket wave functions have L, S, and J specified, but m_J is not specified. The reduced and non-reduced matrix elements are connected by the Wigner-Eckart theorem with the use of the $3j$ coefficients, which we will denote as $C_{3j}(JJ'm_Jm_{J'}kq)$ or simply C_{3j}

$$\langle \alpha' J' m'_J | \; T_q^{(k)} \; | \alpha J m_J \rangle = \underbrace{(-1)^{(J'-m'_J)} \begin{pmatrix} J' & k & J \\ -m'_J & q & m_J \end{pmatrix}}_{C_{3j}(JJ'm_Jm_{J'}kq)} \langle \alpha' J' \left\| T^{(k)} \right\| \alpha J \rangle \tag{4.12}$$

The line strength from the state $i' = |\alpha' L' S' J'\rangle$ to the state $i = |\alpha LSJ\rangle$ is defined as[92]

$$\mathcal{S} = |\,\langle \alpha' L' S' J' ||\, T^{(k)}\, || \alpha LSJ\rangle\,|^2 = \sum_{m_J, m_{J'}} |\,\langle \alpha' L' S' J' m_{J'}|\, T^{(k)}_q\, |\alpha LSJm_J\rangle\,|^2. \quad (4.13)$$

Using the Wigner-Eckart theorem, $\mathcal{S}$ can be expressed without the summation over every m_J. In this way the computational cost is greatly reduced, as only one component has to be computed. It is important to note that the line strength $\mathcal{S}$ is constant and does not depend on the choice of m_J

$$\mathcal{S} = |C_{3j}(JJ'm_Jm_{J'}kq)^{-1}\,\langle \alpha' L' S' J' m_{J'}|\, T^{(k)}_q\, |\alpha LSJm_J\rangle\,|^2. \quad (4.14)$$

We now present a path to express a non-reduced matrix element in the $|\alpha LSJm_J\rangle$ basis in terms of the point group symmetry basis. The last one is always used in *ab initio* computations, and is used in the XCC program as well. The use of the point group symmetry allows to reduce the number of integrals, and simplifies the diagonalization of the Jacobian matrix.

The first step is to transform the $|\alpha LSJm_J\rangle$ basis to the $|\alpha Lm_LSm_S\rangle$ basis, and the second step is the express $|Lm_LSm_S\rangle$ in terms of the irreducible representations of the molecular point group.

4.3 Transformation from the $|\alpha LSJm_J\rangle$ basis to the $|\alpha Lm_LSm_S\rangle$ basis

As a consequence of the Wigner-Eckart theorem one can transform the $|\alpha LSJ\rangle$ basis to the $|\alpha Lm_LSm_S\rangle$ basis with the help of the Clebsh–Gordan coefficients

$$|\alpha LSJm_J\rangle = \sum_{m_L=-L}^{L}\sum_{m_S=-S}^{S} C^{Jm_J}_{Lm_LSm_S}|\alpha Lm_LSm_S\rangle. \quad (4.15)$$

The expression for the line strength becomes

$$\begin{aligned}\mathcal{S} &= |C_{3j}(JJ'm_Jm_{J'}kq)^{-1}\,\langle \alpha' L' S' J' m_{J'}|\, T^{(k)}_q\, |\alpha LSJm_J\rangle\,|^2 \quad (4.16)\\ &= |C_{3j}^{-1} \sum_{\substack{m_L=-L\\ m_{L'}=-L'}}^{L,L'} \sum_{\substack{m_S=-S\\ m_{S'}=-S'}}^{S,S'} C^{Jm_J}_{Lm_LSm_S} C^{J'm_{J'}}_{L'm_{L'}S'm_{S'}}\,\langle \alpha' L' m_{L'} S' m_{S'}|\, T^{(k)}_q\, |\alpha Lm_LSm_S\rangle\,|^2\end{aligned}$$

4.4 Transformation from the $|\alpha Lm_LSm_S\rangle$ basis to the point group symmetry basis

As the subject of the research in this thesis are atoms and homonuclear diatomic molecules, we use the D_{2h} point group symmetry in our calculations. This is a group of order eight with eight irreducible representations

$$\Gamma = \{\mathrm{A}_g, \mathrm{B}_{1g}, \mathrm{B}_{2g}, \mathrm{B}_{3g}, \mathrm{A}_u, \mathrm{B}_{1u}, \mathrm{B}_{2u}, \mathrm{B}_{3u}\}. \tag{4.17}$$

For each angular momentum L and quantum number m_L, there is a straightforward transformation between $|\alpha L m_L S m_S\rangle \to |\alpha^{2S+1}\Gamma^{m_S}\rangle$:

$L = 0$

$$\Gamma = \begin{cases} \mathrm{A}_g & \text{for} \quad L = 0, m_L = 0 \end{cases} \tag{4.18}$$

$L = 1$

$$\Gamma = \begin{cases} \mathrm{B}_{1u} & \text{for} \quad L = 1, m_L = 0 \\ -\frac{1}{\sqrt{2}}(\mathrm{B}_{3u} + i\mathrm{B}_{2u}) & \text{for} \quad L = 1, m_L = 1 \\ \frac{1}{\sqrt{2}}(\mathrm{B}_{3u} - i\mathrm{B}_{2u}) & \text{for} \quad L = 1, m_L = -1 \end{cases} \tag{4.19}$$

$L = 2$

$$\Gamma = \begin{cases} \frac{1}{\sqrt{2}}(2)\mathrm{A}_g + \frac{i}{\sqrt{2}}\mathrm{B}_{1g} & \text{for} \quad L = 2, m_L = 2 \\ -\frac{1}{\sqrt{2}}\mathrm{B}_{2g} - \frac{i}{\sqrt{2}}\mathrm{B}_{3g} & \text{for} \quad L = 2, m_L = 1 \\ (1)\mathrm{A}_g & \text{for} \quad L = 2, m_L = 0 \\ -\frac{i}{\sqrt{2}}\mathrm{B}_{3g} + \frac{1}{\sqrt{2}}\mathrm{B}_{2g} & \text{for} \quad L = 2, m_L = -1 \\ -\frac{i}{\sqrt{2}}\mathrm{B}_{1g} + \frac{1}{\sqrt{2}}(2)\mathrm{A}_g & \text{for} \quad L = 2, m_L = -2 \end{cases} \tag{4.20}$$

4.5 Programs

All of the new formulas developed in this thesis were implemented in the following programs: KOŁOS, a general purpose *ab initio* program for electronic structure calculations, the PALDUS program for symbolic manipulations and automatic generation of orbital-level expressions, and the WIGNER script for the angular momentum manipulations and the transformation of the transition moments from the point group symmetry basis to the $|\alpha LSJ\rangle$ basis. The one- and two-electron integrals in the Gaussian and Slater orbital basis sets were provided by Dr. M. Modrzejewski and Dr. M. Lesiuk, respectively. We will briefly discuss the technical details used in these programs.

4.5.1 KOŁOS

KOŁOS is a general purpose *ab initio* program for the electronic structure calculation. We implemented the CCSD, CC3, EOM-CCSD, and EOM-CC3 methods, as well as all the XCC formulas presented in this thesis. Our program uses efficient compiled-language representations of the symbolic formulae derived by PALDUS. All computations employ Gaussian and Slater basis sets. A unique feature of the developed code, not available in any software, e.g., the Dalton and Molpro programs, is an interface to the Slater integral subprograms of Lesiuk et al.[93–95] The code is parallel on two levels: at a thread level (OpenMP) and at the vector instructions level. Support for the vector instructions, i.e., simultaneous identical arithmetic operations performed on vectors of numbers.

Memory saving

Due to the size of the EOM-CC3 Jacobian matrix,[29] we have used the generalized form of the Davidson[96] method for solving the eigenvalue problem, or in this case its generalized form.[97] The Davidson scheme, combined with the root homing,[98] allowed us to obtain approximate solutions for a number of selected states without the necessity of storing the full $N \times N$ matrix in memory. It does require, however, storing a few tens of vectors of size N at a time. In the case of the EOM-CC3 method $N \sim (v^3 o^3)/6$, where v and o denote the number of virtual and occupied orbitals, respectively. For a large basis this could be problematic. For example, storing of a single vector for the Sr_2 system with 250 virtual orbitals and 10 active occupied orbitals requires 20 GB of memory.

For the purpose of memory saving we modified the Davidson algorithm. We reduced the size of the single vector to $N \sim (n^2 o^2)/2$, with only a slight increase of the computational cost. The EOM-CC3 Jacobian

$$\begin{pmatrix} A_{\mu_1\nu_1} & A_{\mu_1\nu_2} & A_{\mu_1\nu_3} \\ A_{\mu_2\nu_1} & A_{\mu_2\nu_2} & A_{\mu_2\nu_3} \\ A_{\mu_3\nu_1} & A_{\mu_3\nu_2} & \delta_{\mu_3\nu_3}\epsilon_{\mu_3\nu_3} \end{pmatrix} \begin{pmatrix} R_1 \\ R_2 \\ R_3 \end{pmatrix} = \lambda \begin{pmatrix} R_1 \\ R_2 \\ R_3 \end{pmatrix} \tag{4.21}$$

is cast in a 2×2 form using the fact that $A_{\mu_3\nu_3}$ is diagonal:[99]

$$\begin{pmatrix} A_{\mu_1\nu_1} - \frac{A_{\mu_1\nu_3}A_{\nu_3\kappa_1}}{\epsilon_{\mu_3\mu_3}-\lambda} & A_{\mu_1\nu_2} - \frac{A_{\mu_1\nu_3}A_{\nu_3\kappa_2}}{\epsilon_{\mu_3\mu_3}-\lambda} \\ A_{\mu_2\nu_1} - \frac{A_{\mu_2\nu_3}A_{\nu_3\kappa_1}}{\epsilon_{\mu_3\mu_3}-\lambda} & A_{\mu_2\nu_2} - \frac{A_{\mu_2\nu_3}A_{\nu_3\kappa_2}}{\epsilon_{\mu_3\mu_3}-\lambda} \end{pmatrix} \begin{pmatrix} R_1 \\ R_2 \end{pmatrix} = \lambda \begin{pmatrix} R_1 \\ R_2 \end{pmatrix} \tag{4.22}$$

The R_3 vector is computed after the Davidson step, directly from the vectors R_1 and R_2. The formula relevant for the triplet EOM-CC3 is

$$\begin{pmatrix} A_{\mu_1\nu_1} & A_{\mu_1\nu_{2+}} & A_{\mu_1\nu_{2-}} & A_{\mu_1\nu_3} \\ A_{\mu_{2+}\nu_1} & A_{\mu_{2+}\nu_{2+}} & A_{\mu_{2+}\nu_{2-}} & A_{\mu_{2+}\nu_3} \\ A_{\mu_{2-}\nu_1} & A_{\mu_{2-}\nu_{2+}} & A_{\mu_{2-}\nu_{2-}} & A_{\mu_{2-}\nu_3} \\ A_{\mu_3\nu_1} & A_{\mu_3\nu_{2+}} & A_{\mu_3\nu_{2-}} & \delta_{\mu_3\nu_3}\epsilon_{\mu_3\nu_3} \end{pmatrix} \begin{pmatrix} R_1 \\ R_{2+} \\ R_{2-} \\ R_3 \end{pmatrix} = \lambda \begin{pmatrix} R_1 \\ R_{2+} \\ R_{2-} \\ R_3 \end{pmatrix} \tag{4.23}$$

Similarly to the singlet case, R_3 can be expressed in terms of R_1, R_{2+} i R_{2-}, and computed in one step after a Davidson iteration.

4.5.2 PALDUS

The derivation of the orbital-level coupled-cluster expressions relevant for this thesis is extremely error-prone. We automated this process with the PALDUS code, which is designed to derive, simplify, and automatically implement expressions of the type

$$\langle [V_1, \mu_n]_{k_1} | [V_2, V_3]_{k_2} | [V_4, \nu_m]_{k_3} \rangle \,, \tag{4.24}$$

where k_1, k_2, k_3 denote k-tuply nested commutators. The operators $V_1 - V_4$ could be any excitation, de-excitation, or general operators that are represented by the products of the E_{pq} and/or T_{pq} operators. Each of the integrals is approximated within the requested level of theory and integrated using the Wick's theorem.[100]

The integration is carried out into a parallel mode. The result of the integration can contain tens of thousands of terms that need to be compared efficiently. This is done by the standardization of each term to an unambiguous form according to index names and their permutations. Subsequently, each term is translated to a compiled-language representation and the simplification is carried out in this form. Finally, the result is translated back and a parallel Fortran ready to attach module is produced.

The implementation is optimized in the sense that PALDUS automatically computes and selects the best intermediates for each term, considering memory usage to computational time ratio.

4.5.3 WIGNER

WIGNER is a Mathematica script designed to transform transition moments

$$\langle {}^{2S+1}\mathrm{L}_J || T^{(k)} || \, {}^{2S+1}\mathrm{L}'_J \rangle \tag{4.25}$$

to the basis of the point group symmetry

$$|LSJm_J\rangle \rightarrow |{}^{2S+1}\Gamma^{m_S}\rangle. \tag{4.26}$$

The user gives as an input an initial and final state in the case of transition probability computation, or only the initial state in the case of the lifetime computation. In the second case the program checks all possible transitions from the initial state, and using the selection rules discards the vanishing transitions. In the case of spin-forbidden transitions, the script uses perturbation expansion and incorporates the spin-orbit correction.

The main challenge for this script was to establish consistent signs of the transition moments obtained in the XCC theory. As it was noted in section 3.3, the transition moments in the XCC theory do not have a definite sign. To deal with this problem we introduce the following procedure.

For the given transition $\langle {}^{2S+1}\mathrm{L}_J || T^{(k)} || \, {}^{2S+1}\mathrm{L}'_J \rangle$ we generate a set of equations $\mathtt{eq_i}$ for each m_J, $m_{J'}$, and all of the $2k+1$ components for the tensor operator $T^{(k)}$, where $i = 1, \ldots m_J \cdot (2k+1) \cdot m_{J'}$:

for $\mathtt{m_J}$ in range -J, J

  for $\mathtt{m_{J'}}$ in range -J', J'

    $\mathtt{LHS} = \dfrac{\mathtt{R}}{\mathtt{C_{3j}}}$

    $\mathtt{RHS} = \langle L'S'J'm_{J'}|T^{(k)}|LSJm_J\rangle \rightarrow \langle {}^{2S'+1}(\Gamma^{m_{S'}})'|T^{(k)}|{}^{2S+1}\Gamma^{m_S}\rangle$

    $\mathtt{eq_i} : \mathtt{LHS} = \mathtt{RHS}$

Each of the RHS in the set of equations $\mathtt{eq_i}$ is a sum of integrals in the point group symmetry basis, with indefinite signs I. We put the unknown sign $I_l, \in \{1, -1\}$ in front of each integral.

Here we present a sample of such set for the ${}^3\mathrm{D} - {}^3\mathrm{P}$ transition, for the D_{2h} group with eight irreducible representations $\Gamma \in \{\mathrm{A}_g, \mathrm{B}_{1g}, \mathrm{B}_{2g}, \mathrm{B}_{3g}, \mathrm{A}_u, \mathrm{B}_{1u}, \mathrm{B}_{2u}, \mathrm{B}_{3u}\}$. Note that since ${}^3\mathrm{D}$ is quintuply degenerate state, it appears in five irreducible representations $(1)\,{}^3\mathrm{A}_g, (2)\,{}^3\mathrm{A}_g, {}^3\mathrm{B}_{1g}, {}^3\mathrm{B}_{2g}, {}^3\mathrm{B}_{3g}$, where we use $(1)\,{}^3\mathrm{A}_g$ and $(2)\,{}^3\mathrm{A}_g$ to distinguish between the two strictly degenerate states in the same irrep ${}^3\mathrm{A}_g$. Details of this transformation are described in section 4.4.

$$
\begin{aligned}
\frac{R}{\sqrt{5}} = {} & I_1 \frac{\langle {}^3\mathrm{B}_{1u}|x|{}^3\mathrm{B}_{2g}\rangle}{2\sqrt{6}} + I_2 \frac{\langle {}^3\mathrm{B}_{2u}|x|{}^3\mathrm{B}_{1g}\rangle}{2\sqrt{6}} + I_3 \frac{\langle (2)\,{}^3\mathrm{A}_g|x|{}^3\mathrm{B}_{3u}\rangle}{2\sqrt{6}} \\
& - I_4 \frac{\langle (2)\,{}^3\mathrm{A}_g|y|{}^3\mathrm{B}_{2u}\rangle}{2\sqrt{6}} + I_5 \frac{\langle {}^3\mathrm{B}_{1u}|y|{}^3\mathrm{B}_{3g}\rangle}{2\sqrt{6}} + I_6 \frac{\langle {}^3\mathrm{B}_{1g}|y|{}^3\mathrm{B}_{3u}\rangle}{2\sqrt{6}}
\end{aligned} \tag{4.27}
$$

$$
\begin{aligned}
0 = {} & -I_2 \frac{\langle {}^3\mathrm{B}_{1g}|x|{}^3\mathrm{B}_{2u}\rangle}{4\sqrt{3}} + I_7 \frac{\langle (1)\,{}^3\mathrm{A}_g|x|{}^3\mathrm{B}_{3u}\rangle}{4} - I_3 \frac{\langle (2)\,{}^3\mathrm{A}_g|x|{}^3\mathrm{B}_{3u}\rangle}{4\sqrt{3}} \\
& - I_8 \frac{\langle (1)\,{}^3\mathrm{A}_g|y|{}^3\mathrm{B}_{2u}\rangle}{4} - I_4 \frac{\langle (2)\,{}^3\mathrm{A}_g|y|{}^3\mathrm{B}_{2u}\rangle}{4\sqrt{3}} + I_6 \frac{\langle {}^3\mathrm{B}_{1g}|y|{}^3\mathrm{B}_{3u}\rangle}{4\sqrt{3}}
\end{aligned} \tag{4.28}
$$

$$\vdots$$

R is the value of a requested, reduced transition moments. Next, we solve the set of equations for all possible sign configurations, and find the set which gives the consistent R value.

Chapter 5 Numerical results

5.1 Operators used in this work and their representation

5.1.1 Dipole moment operator

The transition dipole moment is defined as

$$\vec{\mathcal{T}}^{\mathbf{D}}_{LM} = \langle \Psi_L | \mathbf{D} | \Psi_M \rangle \tag{5.1}$$

where the dipole moment operator in the spherical and Cartesian forms is defined as

$$\mathbf{D} = (d^1_{-1}, d^1_0, d^1_1) = (x, y, z) \tag{5.2}$$

and the components are connected one to the other by the transformation

$$d^1_0 = z, \quad d^1_1 = -\sqrt{\frac{1}{2}}(x + iy), \quad d^1_{-1} = \sqrt{\frac{1}{2}}(x - iy) \tag{5.3}$$

This operator is simply represented as

$$d = \sum_{pq} d_{pq} E_{pq} \tag{5.4}$$

where $d_{pq} = \int \phi^\star_p(\mathbf{r}) d \phi_q(\mathbf{r}) d\mathbf{r}$.

5.1.2 Quadrupole moment operator

The transition quadrupole moment is defined as

$$\overleftrightarrow{\mathcal{T}}^{\mathbf{Q}}_{LM} = \langle \Psi_L | \mathbf{Q} | \Psi_M \rangle \,, \tag{5.5}$$

where the quadrupole moment operator in the spherical form is defined by

$$\mathbf{Q} = (Q^2_{-2}, Q^1_{-1}, Q^2_0, Q^2_1, Q^2_2) \tag{5.6}$$

and in the Cartesian form

$$\mathbf{Q} = -\frac{3}{2} \begin{pmatrix} xx - \frac{r^2}{3} & xy & xz \\ yx & yy - \frac{r^2}{3} & yz \\ zx & zy & zz - \frac{r^2}{3} \end{pmatrix}. \tag{5.7}$$

The spherical and Cartesian components are connected by the transformation

$$Q^2_0 = \sqrt{\frac{3}{2}} Q_{zz} \tag{5.8}$$

$$Q^2_1 = (Q_{xz} - iQ_{yz}) \tag{5.9}$$

$$Q^2_{\text{-}1} = (-Q_{xz} - iQ_{yz}) \tag{5.10}$$

$$Q^2_{22} = \frac{1}{2}(Q_{xx} + 2iQ_{xy} - Q_{yy}) \tag{5.11}$$

$$Q^2_{\text{-}2} = \frac{1}{2}(Q_{xx} - 2iQ_{xy} - Q_{yy}) \tag{5.12}$$

This operator is represented simply as

$$Q = \sum_{pq} Q_{pq} E_{pq} \tag{5.13}$$

5.1.3 Spin-orbit coupling matrix elements

The effective spin-orbit operator is defined in the Cartesian form as[51]

$$H_{\text{SO}} = \sum_{k=1}^{N_{el}} \sum_l P_l \xi_l(r_k) \mathbf{l} \cdot \mathbf{S} P_l = \sum_{k=1}^{N_{el}} \sum_l P_l \xi_l(r_k)(l_x S_x + l_y S_y + l_z S_z) P_l \tag{5.14}$$

where $P_l = \sum_{m_l} |lm_l\rangle \langle lm_l|$, $\xi_l(r_k)$ is a radial function, and $\mathbf{l}$ and $\mathbf{S}$ are the angular momentum and spin operators respectively. We skipped the index k in the operators $\mathbf{l}$ and $\mathbf{S}$ for clarity. With use of the shift operators $S_\pm$,

$$S_x = \frac{1}{2}(S_+ + S_-), \qquad S_y = \frac{1}{2i}(S_+ - S_-), \tag{5.15}$$

the expression for H_{SO} can be reformulated as

$$H_{\text{SO}} = \sum_{k=1}^{N_{el}} \sum_l P_l \xi_l(r_k) \left\{ \frac{1}{2} l_x (S_+ + S_-) + \frac{1}{2i} l_y (S_+ - S_-) + l_z S_z \right\} P_l, \tag{5.16}$$

and, subsequently, using the second-quantized form of the operators S_+, S_-, and S_z transformed to

$$H_{\text{SO}} = \sum_{pq} (\frac{i}{2} V^x_{pq} (a^\dagger_{p\alpha} a_{q\beta} + a^\dagger_{p\beta} a_{q\alpha}) + \frac{1}{2} V^y_{pq} (a^\dagger_{p\alpha} a_{q\beta} - a^\dagger_{p\beta} a_{q\alpha}) + \frac{i}{2} V^z_{pq} (a^\dagger_{p\alpha} a_{q\alpha} - a^\dagger_{p\beta} a_{q\beta})). \tag{5.17}$$

In the last expression we use the following definition of V^μ_{pq}:

$$V^\mu_{pq} = \frac{1}{i} \sum_l \int \phi^\star_p(\mathbf{r}) P_l \xi_l(r) l_\mu P_l \phi_q(\mathbf{r}) d\mathbf{r} \qquad \mu \in (x, y, z). \tag{5.18}$$

Our goal is to express the spin-orbit coupling matrix element in the spin-free formulation. We start by defining the triplet excitation operators in a the spherical form

$$T^{11}_{pq} = -a^\dagger_{p\alpha} a_{q\beta} \tag{5.19}$$

$$
\begin{aligned}
T^{1-1}_{pq} &= a^{\dagger}_{p\beta} a_{q\alpha} \\
T^{10}_{pq} &= \frac{1}{\sqrt{2}} (a^{\dagger}_{p\alpha} a_{q\alpha} - a^{\dagger}_{p\beta} a_{q\beta}),
\end{aligned}
$$

and rearranging H_{SO} to group terms standing with the same operator T^{kl}_{pq}

$$
H_{\mathrm{SO}} = \sum_{pq} ((-\frac{i}{2} V^x_{pq} - \frac{1}{2} V^y_{pq}) T^{11}_{pq} + (\frac{i}{2} V^x_{pq} - \frac{1}{2} V^y_{pq}) T^{1-1}_{pq} + \frac{i}{2\sqrt{2}} V^z_{pq} T^{10}_{pq}). \tag{5.20}
$$

The transition moment of thus formulated operator is (we skip α from now on)

$$
\begin{aligned}
&\langle L' m_{L'} S' m_{S'} | H_{\mathrm{SO}} | L m_L S m_S \rangle = && (5.21)\\
&= -\frac{1}{2} \sum_{pq} \langle L' m_{L'} S' m_{S'} | (i V^x_{pq} + V^y_{pq}) T^{11}_{pq} | L m_L S m_S \rangle && (5.22)\\
&+ \frac{1}{2} \sum_{pq} \langle L' m_{L'} S' m_{S'} | (i V^x_{pq} - V^y_{pq}) T^{1-1}_{pq} | L m_L S m_S \rangle && (5.23)\\
&+ \frac{i}{2\sqrt{2}} \sum_{pq} \langle L' m_{L'} S' m_{S'} | V^z_{pq} T^{10}_{pq} | L m_L S m_S \rangle && (5.24)\\
&= -\frac{1}{2} \sum_{pq} \langle L' m_{L'} | (V^x_{pq} + V^y_{pq}) | L m_L \rangle \langle S' m_{S'} | T^{11}_{pq} | S m_S \rangle && (5.25)\\
&+ \frac{1}{2} \sum_{pq} \langle L' m_{L'} | (i V^x_{pq} - V^y_{pq}) | L m_L \rangle \langle S' m_{S'} | T^{1-1}_{pq} | S m_S \rangle && (5.26)\\
&+ \frac{i}{2\sqrt{2}} \sum_{pq} \langle L' m_{L'} | V^z_{pq} | L m_L \rangle \langle S' m_{S'} | T^{10}_{pq} | S m_S \rangle , && (5.27)
\end{aligned}
$$

where in the last equation we separated the spin and angular parts. To use the spin-free formalism, we express the m_S-changing spin-tensor operators T^{11}_{pq} and T^{1-1}_{pq} in terms of T^{10}_{pq}, as the last one does not change m_S. This is easily done by virtue of the Wigner-Eckart theorem

$$
\langle S' m'_s | T^{(k)}_q | S m_s \rangle = (-1)^{(S' - m'_s)} \begin{pmatrix} S' & k & S \\ -m'_s & q & m_s \end{pmatrix} \langle S' || T^{(k)} || S \rangle \tag{5.28}
$$

and leads to the following equalities

$$
\begin{aligned}
\langle 00 | T^{(1\text{-}1)} | 11 \rangle &= \frac{1}{\sqrt{3}} \langle 0 || T^{(1)} || 1 \rangle && (5.29)\\
\langle 00 | T^{(10)} | 10 \rangle &= -\frac{1}{\sqrt{3}} \langle 0 || T^{(1)} || 1 \rangle \\
\langle 00 | T^{(11)} | 1\text{-}1 \rangle &= \frac{1}{\sqrt{3}} \langle 0 || T^{(1)} || 1 \rangle
\end{aligned}
$$

The transition moment for H_{SO} can now be represented in the spin-free formalism

$$
\begin{aligned}
&\langle L' m_{L'} S' m_{S'} | \; H_{\mathrm{SO}} \; | L m_L S m_S \rangle = && (5.30)\\
&= \frac{1}{2} \sum_{pq} \langle L' m_{L'} | \; (i V^x_{pq} + V^y_{pq}) \; | L m_L \rangle \langle S' m_{S'} | \; T^{10}_{pq} \; | S m_S \rangle && (5.31)
\end{aligned}
$$

$$+\frac{1}{2}\sum_{pq}\langle L'm_{L'}|\left(-iV^x_{pq}+V^y_{pq}\right)|Lm_L\rangle\langle S'm_{S'}|\,T^{10}_{pq}\,|Sm_S\rangle \tag{5.32}$$

$$+\frac{i}{2\sqrt{2}}\sum_{pq}\langle L'm_{L'}|\,V^z_{pq}\,|Lm_L\rangle\langle S'm_{S'}|\,T^{10}_{pq}\,|Sm_S\rangle \tag{5.33}$$

5.2 Basis sets

All of the results reported in this work were obtained with two types of basis sets (where possible): Gaussian-type orbitals (GTO)[101,102] and Slater-type orbitals (STO).[103,104] STO basis sets are usually significantly smaller when compared with Gaussian-type basis sets of a comparable quality. Therefore, there is a strong reason to use them in the computationally demanding coupled cluster theory. STOs used in this work were constructed according to the correlation-consistency principle.[105] For the Mg atom the STOs were constructed analogously to the beryllium basis set in Ref. 95. This basis is referred to as mg-dawtcc5d. For the Ca, Sr, and Ba atoms we used the STO basis sets specifically designed for the calculations with the effective core potentials.[106] They are referred to as ca-dawtcc5ex, sr-dawtcc5ex, and ba-dawtcc5ex, respectively. For the Mg atom we also used the Gaussian basis set d-aug-cc-pVQZ.[107,108] For Sr the following Gaussian basis set was used: $[8s8p5d4f1g]$ augmented with a set of $[1s1p1d1f3g]$ diffuse functions[43] and the ECP28MDF pseudopotential.[107–109] For Ba we used the ECP46MDF pseudopotential[109] together with the $[9s9p6d4f2g]$ Gaussian basis set.[109]

To assess the quality of the basis sets, we present in Tables 5.1 - 5.3 the excitation energies obtained with the EOM-CCSD and EOM-CC3 codes and compare them with the experimental results. In the case of the triplet states we used the nonrelativistic values deduced from the Landé rule.

Table 5.1: Excitation energies of the calcium atom in cm^{-1}.

State	EXP[110,111]	XCCSD(G)	XCCSD(S)	XCC3(G)	XCC3(S)
$^3\mathrm{P}^\circ$	15263.1	15098.7	15173.2	15063.5	15195.3
$^3\mathrm{D}$	20356.6	27638.4	20856.1	27581.2	21299.6
$^1\mathrm{D}$	21849.6	28554.2	22878.6	27962.4	22859.0
$^1\mathrm{P}^\circ$	23652.3	24724.4	24845.8	24080.5	23879.6
$^3\mathrm{S}$	31539.5	31518.3	31828.7	31157.3	31545.5
$^1\mathrm{S}$	33317.3	33566.5	33890.9	32983.0	33336.9

Apart from the results for a few states of the Ca atom in the Gaussian basis set (^{1}D and ^{3}D), it can be seen from Tables 5.1 - 5.3 that our results are generally in

Table 5.2: Excitation energies of the strontium atom in cm^{-1}.

State	EXP[112]	XCCSD(G)	XCCSD(S)	XCC3(G)	XCC3(S)
$^3P^\circ$	14702.9	14575.6	14546.3	14570.8	14597.2
^3D	18253.8	18414.5	18155.0	18668.8	18393.7
^1D	20149.7	20814.1	20584.7	20650.3	20411.1
$^1P^\circ$	21698.5	22632.7	22701.9	21764.3	21797.5
^3S	29038.8	29137.0	29189.7	28885.3	28939.3
^1S	30591.8	31014.0	31063.1	30464.4	30508.6

Table 5.3: Excitation energies of the barium atom in cm^{-1}.

State	EXP[113]	XCCSD(G)	XCCSD(S)	XCC3(G)	XCC3(S)
^3D	9357.8	9270.9	8923.7	9581.6	9178.1
^1D	11395.4	12063.6	11653.5	11869.7	11391.4
$^3P^\circ$	13085.5	12970.5	12823.6	13069.8	12925.9
$^1P^\circ$	18060.3	19569.0	19527.3	18372.2	18284.6
^3S	26160.3	26136.6	26269.3	24275.7	26141.9
^1S	26757.3	27760.6	27971.9	25826.2	25213.0

a very good agreement with the experimental data. For the Sr atom we observe the best performance in the case of the Slater basis set and EOM-CC3 method, where the average deviation from the experiment is only 0.6%. For the Ba atom, the disagreement is slightly worse than in the Sr case, with the average error of 0.9%. For the Ca atom, most of the states are in a perfect agreement with the experiment (average error 0.3% for Slater/EOM-CC3 case), but there were some significant problems with the ^1D and ^3D states. For the Gaussian basis set the EOM iterations did not converge to the desired state, and for the Slater basis set the errors were around 5%. The analysis of this problem was done by Lesiuk et al.[106] and the important conclusion was that this is an inherent problem with the pseudopotentials used in the calculations. The authors of Ref. 106 noted that this artifact was also observed in the original paper of Lim.[109]

The lifetimes computed in this work employ EOM coupled cluster energies and eigenvectors. Whenever an energy level for a specific J was required, we used the experimental energies.

5.3 Lifetimes of the alkali earth atoms

5.3.1 Notation

Symbol	Meaning
$\mathcal{T}(N-M)$	reduced transition moment from state N to M
$A(N-M)$	transition probability from state N to M
$S(N-M)$	line strength between states N and M
XCCSD(G)	This work, CCSD approximation, Gaussian basis set
XCC3(G)	This work, CC3 approximation, Gaussian basis set
XCCSD(S)	This work, CCSD approximation, Slater basis set
XCC3(S)	This work, CC3 approximation, Slater basis set

5.3.2 Lifetimes of the singlet states of the Mg atom

In Table 5.4 we present a comparison of our computed transition strengths with other theoretical approaches, the relativistic multiconfigurational Hartree Fock approximation (Fischer[114]), the CI approximation with the B-spline basis (Chang and Tang[115]), and the semi-empirical weakest bound electron potential model (Zheng et al.[116]). The $\mathcal{S}_{LM}^{X}$ values of Chang and Tang were derived from A_{LM}^{X} with the experimental excitation energies.

Table 5.4: Transition strengths $\mathcal{S}_{LM}^{X}$ (a.u.) for the Mg atom.

Transition			XCC3(G)	XCC3(S)	Chang[115]	Fischer[114]	Zheng[116]
$3s4s\,^1\mathrm{S}$	–	$3s3p\,^1\mathrm{P}^\circ$	16.0	15.8	17.9	18.1	18.8
$3s4p\,^1\mathrm{P}^\circ$	–	$3s4s\,^1\mathrm{S}$	69.9	70.8	69.9	65.4	77.2
$3s5s\,^1\mathrm{S}$	–	$3s4p\,^1\mathrm{P}^\circ$	101.8	98.2	91.7	92.3	87.4
$3s5s\,^1\mathrm{S}$	–	$3s3p\,^1\mathrm{P}^\circ$	0.3	0.3	0.4	0.3	0.9
$3s3d\,^1\mathrm{D}$	–	$3s3p\,^1\mathrm{P}^\circ$	12.2	20.3	21.5	21.4	61.5
$3s4p\,^1\mathrm{P}^\circ$	–	$3s3d\,^1\mathrm{D}$	42.4	79.6	76.6	81.9	83.7

The XCC3(S) results are in a much better agreement with the results calculated with other theoretical methods than the results obtained with the XCC3(G). The most dramatic improvement is observed for the $3d\,^1\mathrm{D}$ - $3p\,^1\mathrm{P}^\circ$ and $4p\,^1\mathrm{P}^\circ$ - $3d\,^1\mathrm{D}$ transitions.

The combination of the XCC3 method and the STOs basis set results in lifetimes of the excited states of the Mg atom in a very good agreement with the available experimental and theoretical data (Tables 5.5 and 5.6). For the singlet states, we find an excellent agreement with the most recent experimental data of Gratton et al.,[117] but not with the older experiment of Schaefer.[118] The mean absolute percentage error of our results for the singlet states is about 8% relative to the data of Gratton et al.[117] The largest error, slightly above 10%, is found for the $3s4s\,^1$S state. Our results are also consistent with the lifetimes computed by Froese[114] and Chang[119] and in a significant disagreement with the semi-empirical values of Zheng.[116]

Table 5.5: Lifetimes τ in ns of the singlet excited states of the Mg atom.

Year	Reference	$3s3p\,^1$P°	$3s4s\,^1$S	$3s3d\,^1$D	$3s4p\,^1$P°	$3s5s\,^1$S
			Experiment			
(2003)	Ref. 117	–	46.2 ± 2.6	74.8 ± 3	14.3	101.0 ± 3.5
(1989)	Ref. 120	2.3	44.0 ± 5	72.0 ± 4	13.4 ± 0.5	102.0 ± 5
(1984)	Ref. 121	–	47.0 ± 3	81.0 ± 6	–	100.0 ± 5
(1971)	Ref. 118	–	–	57.0 ± 4	–	163.0 ± 8
			Theory			
(1975)	Ref. 114	2.1	44.8	77.2	13.8	102.0
(1990)	Ref. 119	2.1	45.8	79.5	14.3	100.0
(2001)	Ref. 116	–	42.3	27.4	–	65.3
(2016)	TDCC3(G)	2.1	47.0	200.0	–	99.8
(2016)	XCC3(G)	2.1	53.8	163.9	14.6	91.9
(2016)	XCC3(S)	2.1	51.7	79.7	14.1	111.9

All the computed lifetimes for the triplet states of Mg agree well with the existing experimental and theoretical results (Table 5.6). Remarkably, the XCCSD(S) results are close to the most recent experimental data of Aldenius[122] for all states where the data are available. The mean absolute percentage deviation from this data is about 8% and the largest error is found for the $3s4s\,^3$S state. For the $3s5s\,^3$S state other theoretical results support the older values of Schaefer[118] and Gratton.[117] Similarly, in the case of the $3s4s\,^3$S state, the lifetimes calculated at the XCCSD(S) level are slightly larger than the other theoretical results, yet in an excellent agreement with the Aldenius experiment.[122] For the $3s4p\,^3$P state there are no experimental results available, but all the theoretical lifetimes, including the XCCSD(S) one, are consistent within 10% at worst. The triplet-triplet transition dipole moments which are necessary to compute the lifetimes of the triplet states are not available in the TD-CC implementation. Therefore, no comparison with the TD-CC method is possible.

Table 5.6: Lifetimes τ in ns of the triplet excited states of the Mg atom.

Year	Reference	$3s4s\,^3$S	$3s5s\,^3$S	$3s4p\,^3$P	$3s3d\,^3$D
		Experiment			
(2007)	Ref. 122	11.5 $\pm$ 1.0	29.0 $\pm$ 0.3	–	5.9 $\pm$ 0.4
(1980)	Ref. 123	9.7 $\pm$ 0.6	–	–	5.9 $\pm$ 0.4
(1972)	Ref. 124	10.1 $\pm$ 0.8	–	–	6.6 $\pm$ 0.5
(1971)	Ref. 118	14.8 $\pm$ 0.7	25.6 $\pm$ 2.1	–	11.3 $\pm$ 0.8
(1982)	Ref. 125	9.9 $\pm$ 1.25	–	–	5.93
(1977)	Ref. 126	9.7 $\pm$ 0.5	–	–	–
(2003)	Ref. 117	9.8 $\pm$ 0.3	25.6 $\pm$ 2.1	–	–
		Theory			
(1975)	Ref. 114	9.86	26.8	74.5	6.18
(1988)	Ref. 127	9.7	26.5	81.0	5.8
(1976)	Ref. 128	9.07	–	–	6.25
(1990)	Ref. 119	9.98	27.5	77.0	5.89
(1981)	Ref. 129	9.79	–	–	–
(2001)	Ref. 116	–	–	78.49	–
(2016)	XCCSD(S)	12.7	29.9	70.44	5.33

5.3.3 The $4s4p\,^1\mathrm{P}_1^\circ$ of the Ca atom and the $5s5p\,^1\mathrm{P}_1^\circ$ state of the Sr atom

The $4s4p\,^1\mathrm{P}_1^\circ$ state of the Ca atom and the $5s5p\,^1\mathrm{P}_1^\circ$ state of the Sr atom, can undergo radiative dipole transitions to the ground states $4s^2\,^1\mathrm{S}_0$ and $5s^2\,^1\mathrm{S}_0$, respectively. The reduced dipole transition moment is expressed by the formula

$$\mathcal{T}(^1\mathrm{P}_1^\circ - {}^1\mathrm{S}_0) = \langle {}^1\mathrm{P}_1 || \mathbf{D}^1 || \, {}^1\mathrm{S}_0 \rangle = \sqrt{3}\,\langle {}^1\mathrm{P}_1^0 | z | \, {}^1\mathrm{S}_0^0 \rangle = \sqrt{3}\,\langle {}^1\mathrm{B}_{1u} | z | \, {}^1\mathrm{A}_g \rangle \,. \quad (5.34)$$

We used Eq. (4.1) and Eq. (4.10) to compute the lifetime of the $^1\mathrm{P}_1^\circ$ state for both atoms (Tables 5.7 and 5.8). One should note that $4s4p\,^1\mathrm{P}_1^\circ$ can also undergo transitions to the $3d4s\,^1\mathrm{D}_2$, $3d4s\,^3\mathrm{D}_1$ and $3d4s\,^3\mathrm{D}_2$ states, but the transition probabilities to these states are a few orders of magnitude smaller than the transition to the ground state, therefore their influence on the lifetime is negligible.

In both cases we observe that the lifetimes computed with the XCC3 method are about 15% longer than those computed with the XCCSD method, regardless of the basis used. Since the energies computed with the EOM-CC3 method (Tables 5.1 and 5.2) are in a much better agreement with the experimental values than those computed with EOM-CCSD, we believe that the vectors used for the transition moments computations are also of a better quality.

Table 5.7: Lifetime τ in ns of $4s4p\,^1\mathrm{P}_1^\circ$ state of the Ca atom.

Year	Reference	τ [ns]
	Theory	
(2018)	This work XCCSD(S)	3.90
(2018)	This work XCC3(S)	4.49
(2018)	Yu and Derevianko[130]	4.61
(1991)	Vaeck et al.[131]	4.52
(1981)	Diffenderfer et al.[132]	4.17
	Experiment	
(2000)	Zinner et al.[133]	4.535 ± 0.028
(1977)	Havey et al.[126]	4.7 ± 0.5

Table 5.8: Lifetime τ in ns of the $5s5p\,^1\mathrm{P}_1^\circ$ state of the Sr atom.

Year	Reference	τ [ns]
	Theory	
(2018)	This work XCCSD(G)	4.50
(2018)	This work XCC3(G)	5.15
(2018)	This work XCCSD(S)	4.47
(2018)	This work XCC3(S)	5.16
(2012)	Skomorowski et al.[43]	5.09
(2010)	Mitroy et al.[134]	5.35
(2008)	Porsev et al.[135]	5.38
	Experiment	
(2006)	Yasuda et al.[136]	5.263 ± 0.004
(2005)	Nagel et al.[137]	5.22 ± 0.03

For the Ca atom our computed value of 4.49 ns is in perfect agreement with the newest experimental result of Zinner et al.[133] We also observe a very good agreement with the computed lifetime $\tau = 4.61$ ns of Yu and Derevianko[130] where the authors used CI+MBPT method, and $\tau = 4.52$ of Vaeck et al.[131] who used multiconfigurational Hartree-Fock method.

Our theoretical result, $\tau = 5.16$ ns, lays between the results of Skomorowski et al. who used the TD-CC method using the Dalton code,[138] Porsev et al,[135] who used the MBPT+CI method and Mitroy et al.[134] who used the large basis, CI computations. Our computed lifetime is in a good agreement with both available experimental results.

5.3.4 The $3d4s\,{}^1\mathrm{D}_2$ state of the Ca atom and $5s4d\,{}^1\mathrm{D}_2$ of the Sr atom

The $6s5d\,{}^1\mathrm{D}_2$ state of calcium and strontium is of special importance to this work as three different transitions give contributions to the lifetime

$$\tau_{[{}^1\mathrm{D}_2]} = \frac{1}{\mathcal{A}({}^1\mathrm{D}_2, {}^1\mathrm{S}_0) + \mathcal{A}({}^1\mathrm{D}_2, {}^3\mathrm{P}_2) + \mathcal{A}({}^1\mathrm{D}_2, {}^3\mathrm{P}_1)}. \tag{5.35}$$

The following equations, derived by the WIGNER code, were employed to compute the quadrupole $\mathcal{T}({}^1\mathrm{D}_2, {}^1\mathrm{S}_0)$, and two spin-forbidden transitions, $\mathcal{T}({}^1\mathrm{D}_2, {}^3\mathrm{P}_2)$ and $\mathcal{T}({}^1\mathrm{D}_2, {}^3\mathrm{P}_1)$,

$$\begin{aligned}
\mathcal{T}({}^1\mathrm{D}_2, {}^1\mathrm{S}_0) &= \langle {}^1\mathrm{D}_2 || \mathbf{Q}^2 || \,{}^1\mathrm{S}_0 \rangle = \sqrt{5}\sqrt{\frac{3}{2}}\,\langle {}^1\mathrm{D}_2^0 | Q_{zz} | \,{}^1\mathrm{S}_0^0 \rangle && (5.36)\\
&= \sqrt{5}\sqrt{\frac{3}{2}}\,\langle {}^1\mathrm{A}_g | Q_{zz} | (1)\,{}^1\mathrm{A}_g \rangle \,, \\
\mathcal{T}({}^1\mathrm{D}_2, {}^3\mathrm{P}_2) &= -\sqrt{10}\frac{\langle {}^1\mathrm{D}_2^{\text{-}1} | H_{\mathrm{SO}} | \,{}^3\mathrm{D}_2^{\text{-}1} \rangle}{E_{{}^1\mathrm{D}_2} - E_{{}^3\mathrm{D}_2}}\,\langle {}^3\mathrm{D}_2^{\text{-}1} | d^1_{\text{-}1} | \,{}^3\mathrm{P}_2^0 \rangle && (5.37)\\
&= -\sqrt{10}\frac{\left(-\frac{1}{2}\,\langle (1)\,{}^1\mathrm{A}_g | V^x | \,{}^3\mathrm{B}_{3g} \rangle + \frac{1}{2}\,\langle (1)\,{}^1\mathrm{A}_g | V^y | \,{}^3\mathrm{B}_{2g} \rangle\right)}{E_{{}^1\mathrm{D}_2} - E_{{}^3\mathrm{D}_2}} \\
&\times \left(\frac{1}{4}\,\langle {}^3\mathrm{B}_{1u} | x | \,{}^3\mathrm{B}_{2g} \rangle - \frac{1}{4}\,\langle {}^3\mathrm{B}_{1u} | y | \,{}^3\mathrm{B}_{3g} \rangle\right), \\
\mathcal{T}({}^1\mathrm{D}_2, {}^3\mathrm{P}_1) &= -\sqrt{\frac{15}{2}}\frac{\langle {}^1\mathrm{D}_2^{\text{-}1} | H_{\mathrm{SO}} | \,{}^3\mathrm{D}_2^{\text{-}1} \rangle}{E_{{}^1\mathrm{D}_2} - E_{{}^3\mathrm{D}_2}}\,\langle {}^3\mathrm{D}_2^{\text{-}1} | d^1_{\text{-}1} | \,{}^3\mathrm{P}_1^0 \rangle && (5.38)\\
&- \sqrt{\frac{15}{2}}\frac{\langle {}^3\mathrm{P}_1^0 | H_{\mathrm{SO}} | \,{}^1\mathrm{P}_1^0 \rangle}{E_{{}^1\mathrm{P}_1} - E_{{}^3\mathrm{P}_1}}\,\langle {}^1\mathrm{P}_1^0 | d^1_0 | \,{}^1\mathrm{D}_2^0 \rangle \\
&= -\sqrt{\frac{15}{2}}\frac{\left(-\frac{1}{2}\,\langle (1)\,{}^1\mathrm{A}_g | V^x | \,{}^3\mathrm{B}_{3g} \rangle + \frac{1}{2}\,\langle (1)\,{}^1\mathrm{A}_g | V^y | \,{}^3\mathrm{B}_{2g} \rangle\right)}{E_{{}^1\mathrm{D}_2} - E_{{}^3\mathrm{D}_2}} \\
&\times \left(\frac{1}{2}\,\langle {}^3\mathrm{B}_{2u} | z | \,{}^3\mathrm{B}_{3g} \rangle + \frac{1}{2}\,\langle {}^3\mathrm{B}_{2g} | z | \,{}^3\mathrm{B}_{3u} \rangle\right) \\
&- \sqrt{\frac{15}{2}}\frac{\left(-\frac{1}{2}\,\langle {}^3\mathrm{B}_{1u} | V^x | \,{}^3\mathrm{B}_{2u} \rangle + \frac{1}{2}\,\langle {}^3\mathrm{B}_{1u} | V^y | \,{}^3\mathrm{B}_{3u} \rangle\right)}{E_{{}^1\mathrm{P}_1} - E_{{}^3\mathrm{P}_1}}\,\langle (1)\,{}^1\mathrm{A}_g | z | \,{}^3\mathrm{B}_{1u} \rangle \,.
\end{aligned}$$

Our computed lifetime for the Ca atom lies above both the experimental and theoretical results. This is probably due to the fact that the quality of the obtained excited states is not satisfactory (see the discussion in section 5.2).

For the Sr atom the situation is more interesting. We see that in the Gaussian basis set the XCC3 lifetime Table 5.10 is larger than the XCCSD value. In the Slater basis set, the trend is opposite. As the EOM-CC3(S) states are of the best quality (see section 5.2), we compare the XCC3(S) value with the experiment. As shown in Table 5.10, the existing experimental and theoretical results are scattered on the interval from 0.30 to 0.49 ms. Our computed lifetime 0.34 ms is in the middle of that range, which is close to the most recent (2005) experimental result $\tau = 0.30$ ms of Courtillot et al.[143]

Table 5.9: Lifetime τ in ms of $3d4s\,^1\mathrm{D}_2$ state of the Ca atom.

Year	Reference	τ [ms]		
	Theory			
(2018)	This work XCC3(S)	3.5		
(1985)	Bauschlicher et al.[139]	3.05		
(1985)	Bauschlicher et al.[139]	2.76		
	Experiment			
(2003)	Beverini et al.[140]	2.3	$\pm$	0.5
(1993)	Drozdowski et al.[141]	1.5	$\pm$	0.4
(1980)	Pasternack et al.[142]	2.3	$\pm$	0.5

Table 5.10: Lifetime τ in ms of $5s5p\,^1\mathrm{D}_2$ state of the Sr atom.

Year	Reference	τ [ms]		
	Theory			
(2018)	This work XCCSD(G)	0.43		
(2018)	This work XCC3(G)	0.52		
(2018)	This work XCCSD(S)	0.36		
(2018)	This work XCC3(S)	0.34		
(2012)	Skomorowski et al.[43]	0.23		
(1985)	Bauschlicher et al.[139]	0.49		
	Experiment			
(2005)	Courtillot et al.[143]	0.30		
(1988)	Husain and Roberts[144]	0.41	$\pm$	0.01

5.3.5 The $5s5p\,^3\mathrm{P}^\circ_1$ state of the Sr atom

The transition from the $^3\mathrm{P}^\circ_1$ state to the ground state is a spin-forbidden transition, therefore we compute it using Eq. (4.9). The WIGNER code was used to obtain formulas in the point group symmetry basis

$$\begin{aligned}\mathcal{T}(^3\mathrm{P}^\circ_1 - {}^1\mathrm{S}_0) &= \sqrt{3}\,\langle {}^1\mathrm{S}^0_0|z|\,{}^1\mathrm{P}^1_1\rangle\,\frac{\langle {}^1\mathrm{P}^1_1|H_{\mathrm{SO}}|\,{}^3\mathrm{P}^1_1\rangle}{E_{^3\mathrm{P}_1} - E_{^1\mathrm{P}_1}} = \\ &= \sqrt{3}\,\langle {}^1\mathrm{A}_g|z|\,{}^1\mathrm{B}_{1u}\rangle\,\frac{1}{2}\frac{(\langle {}^1\mathrm{B}_{1u}|V^x|\,{}^3\mathrm{B}_{2u}\rangle + \langle {}^1\mathrm{B}_{1u}|V^y|\,{}^3\mathrm{B}_{3u}\rangle)}{E_{^3\mathrm{P}_1} - E_{^1\mathrm{P}_1}} \end{aligned} \tag{5.39}$$

Comparison of our results with the existing numerical and experimental data are presented in Table 5.11. Skomorowski et al.[43] obtained $\tau = 21.40\ \mu$s using TD-CC3 method together with the multireference CI for the spin-orbit coupling matrix elements. Porsev et al.[145] obtained $\tau = 19\ \mu$s with the use of the CI+MBPT method. Our computed lifetime $\tau = 24.6\ \mu$s is in a perfect agreement with the value obtained by Santra et al.[146] $\tau = 24.4\ \mu$s using an accurate effective core potential.

The experimental result from 2006 of Zelevinsky et al.[147] suggest a lower value of $\tau = 21.5$ μs.

Table 5.11: Lifetime τ in μs of $5s5p\,{}^3\mathrm{P}_1^\circ$ state of the Sr atom.

Year	Reference	τ [μs]		
	Theory			
(2018)	This work XCCSD(G)	23.67		
(2018)	This work XCC3(G)	25.00		
(2018)	This work XCCSD(S)	23.24		
(2018)	This work XCC3(S)	24.60		
(2012)	Skomorowski et al.[43]	21.40		
(2004)	Santra et al.[146]	24.4		
(2001)	Porsev et al.[145]	19.0		
	Experiment			
(2006)	Zelevinsky et al.[147]	21.5	$\pm$	0.2

5.3.6 The $5s4d\,{}^3\mathrm{D}_1$ state of the Sr atom

We start by a comparison of the electric dipole reduced matrix elements for the $5s4d\,{}^3\mathrm{D}_1 \to 5s5p\,{}^3\mathrm{P}_0$ transition. Using the WIGNER code we derived the following formula for this transition

$$\begin{aligned}\mathcal{T}({}^3\mathrm{D}_1, {}^3\mathrm{P}_0) &= \langle {}^3\mathrm{D}_1 || \mathbf{D}^1 || \, {}^3\mathrm{P}_0\rangle = \sqrt{3}\,\langle {}^3\mathrm{D}_1^0 | d_0^1 | \, {}^3\mathrm{P}_0^0\rangle = \sqrt{3}\Big(\sqrt{\frac{2}{15}}\,\langle (1)\,{}^3\mathrm{A}_g | z | \, {}^3\mathrm{B}_{1u}\rangle \\ &+ \sqrt{\frac{1}{10}}\,\langle {}^3\mathrm{B}_{3g} | z | \, {}^3\mathrm{B}_{2u}\rangle + \sqrt{\frac{1}{10}}\,\langle {}^3\mathrm{B}_{2g} | z | \, {}^3\mathrm{B}_{3u}\rangle\Big). \end{aligned} \tag{5.40}$$

Our result $\mathcal{T}({}^3\mathrm{D}_1, {}^3\mathrm{P}_0) = 3.06$ is slightly above error bars of the experimental and theoretical estimates (Table 5.12). The total lifetime of the $5s4d\,{}^3\mathrm{D}_1$ state gets contributions from three decay channels

$$\tau_{[{}^3\mathrm{D}_1]} = \frac{1}{\mathcal{A}({}^3\mathrm{D}_2, {}^3\mathrm{P}_0) + \mathcal{A}({}^3\mathrm{D}_2, {}^3\mathrm{P}_1) + \mathcal{A}({}^3\mathrm{D}_2, {}^3\mathrm{P}_2)}. \tag{5.41}$$

Our result is $\tau_{[{}^3\mathrm{D}_1]} = 1679$ ns to be compared with the result of Porsev et al.[135], where the value of $\tau_{[{}^3\mathrm{D}_1]} = 2040$ ns was obtained. Other results are not available in the literature so the present agreement between the two theoretical results should be considered as fair.

The only available measurements are for the whole multiplet $\overline{{}^3\mathrm{D}}$, where the transition probability is defined as[135]

$$\mathcal{A}_{\overline{{}^3\mathrm{D}}} = \frac{1}{15}\sum_{JJ'}(2J'+1)A({}^3\mathrm{D}_{J'}, {}^3\mathrm{P}_J), \tag{5.42}$$

Table 5.12: Comparison of the electric dipole reduced matrix elements in [a.u.] for the $\mathcal{T}(^3\mathrm{D}_1, ^3\mathrm{P}_0)$ transition in the Sr atom.

Year	Reference	$\mathcal{T}(^3\mathrm{D}_1, ^3\mathrm{P}_0)$
	Theory	
(2018)	This work XCCSD(G)	3.07
(2018)	This work XCC3(G)	3.09
(2018)	This work XCCSD(S)	3.04
(2018)	This work XCC3(S)	3.06
(2008)	Porsev et al.[135]	2.74
(2010)	Guo[148]	2.53
	Experiment	
(2013)	Safranova et al.[149]	2.675 ± 0.013
(1992)	Miller et al.[150]	2.5 ± 0.1

therefore we computed all the components from the above sum. Below, we present the formulas derived by WIGNER for all of the allowed transitions in this multiplet

$$\begin{aligned}
\mathcal{T}(^3\mathrm{D}_1, ^3\mathrm{P}_1) &= \langle ^3\mathrm{D}_1 || \mathbf{D}^1 || ^3\mathrm{P}_1 \rangle = \sqrt{6}\, \langle ^3\mathrm{D}^1_1 | d^1_0 | ^3\mathrm{P}^1_0 \rangle = \sqrt{3}\Big(\frac{1}{2\sqrt{5}} \langle (1)\, ^3\mathrm{A}_g | z | ^3\mathrm{B}_{1u} \rangle \\
&+ \frac{1}{4}\sqrt{\frac{3}{5}} \langle ^3\mathrm{B}_{3g} | z | ^3\mathrm{B}_{2u} \rangle + \frac{1}{4}\sqrt{\frac{3}{5}} \langle ^3\mathrm{B}_{2g} | z | ^3\mathrm{B}_{3u} \rangle \Big), && (5.43) \\
\mathcal{T}(^3\mathrm{D}_1, ^3\mathrm{P}_2) &= \langle ^3\mathrm{D}_1 || \mathbf{D}^1 || ^3\mathrm{P}_2 \rangle = && (5.44) \\
&= \sqrt{5}\Big(\frac{1}{2\sqrt{10}} \langle (1)\, ^3\mathrm{A}_g | x | ^3\mathrm{B}_{3u} \rangle + \frac{1}{2\sqrt{10}} \langle (1)\, ^3\mathrm{A}_g | y | ^3\mathrm{B}_{2u} \rangle \Big), \\
\mathcal{T}(^3\mathrm{D}_2, ^3\mathrm{P}_1) &= \langle ^3\mathrm{D}_2 || \mathbf{D}^1 || ^3\mathrm{P}_1 \rangle = && (5.45) \\
&= \sqrt{30}\Big(\frac{1}{4} \langle ^3\mathrm{B}_{2g} | x | ^3\mathrm{B}_{1u} \rangle + \frac{1}{4} \langle ^3\mathrm{B}_{3g} | y | ^3\mathrm{B}_{2u} \rangle \Big), \\
\mathcal{T}(^3\mathrm{D}_2, ^3\mathrm{P}_2) &= \langle ^3\mathrm{D}_2 || \mathbf{D}^1 || ^3\mathrm{P}_2 \rangle = && (5.46) \\
&= \sqrt{10}\Big(\frac{1}{4} \langle ^3\mathrm{B}_{2g} | x | ^3\mathrm{B}_{1u} \rangle + \frac{1}{4} \langle ^3\mathrm{B}_{3g} | y | ^3\mathrm{B}_{2u} \rangle \Big), \\
\mathcal{T}(^3\mathrm{D}_3, ^3\mathrm{P}_2) &= \langle ^3\textsc{d} || \mathbf{D}^1 || ^3\mathrm{P}_2 \rangle = && (5.47) \\
&= \sqrt{21}\Big(\frac{1}{\sqrt{6}} \langle ^3\mathrm{B}_{3g} | z | ^3\mathrm{B}_{2u} \rangle + \frac{1}{\sqrt{6}} \langle ^3\mathrm{B}_{2g} | z | ^3\mathrm{B}_{3u} \rangle \Big).
\end{aligned}$$

From Table 5.13 it can be seen that there is no clear agreement between any theoretical and experimental results.

5.3.7 The $6s6p\,^3\mathrm{P}^\circ_1$ state of the Ba atom

The $6s6p\,^3\mathrm{P}^\circ_1$ state of the Ba atom can undergo radiative dipole transition to the $^3\mathrm{D}_1$ and $^3\mathrm{D}_2$ states, as well as undergo a spin-induced dipole transition to the ground

Table 5.13: Lifetime τ in ns of $3d4s\,\overline{^3\mathrm{D}}$ state of the Sr atom.

Year	Reference	τ ns
Theory		
(2018)	This work XCC3(S)	1813
(2008)	Porsev et al.[135]	2400
Experiment		
(1987)	Borisov[151]	4100
(1992)	Miller et al.[150]	2900

state $^1\mathrm{S}_0$. The total lifetime of the $6s6p\,^3\mathrm{P}^\circ_1$ state is thus computed from

$$\tau_{^3\mathrm{P}_1} = \frac{1}{\mathcal{A}(^3\mathrm{P}_1, {}^3\mathrm{D}_1) + \mathcal{A}(^3\mathrm{P}_1, {}^3\mathrm{D}_2) + \mathcal{A}(^3\mathrm{P}_1, {}^1\mathrm{S}_0)}. \tag{5.48}$$

The expressions for these transitions derived by WIGNER code are

$$\begin{aligned}
\mathcal{T}(^3\mathrm{P}^\circ_1 - {}^3\mathrm{D}_1) &= \langle ^3\mathrm{P}_1||\mathbf{D}^1||\,^3\mathrm{D}_1\rangle = \sqrt{6}\,\langle ^3\mathrm{P}^{\text{-}1}_1||d^1_1||\,^3\mathrm{D}^{\text{-}1}_1\rangle & (5.49)\\
&= \sqrt{6}\left(\frac{\langle (1)\,^3\mathrm{A}_g|z|\,^3\mathrm{B}_{1u}\rangle}{2\sqrt{5}} + \frac{\sqrt{3}\,\langle ^3\mathrm{B}_{3g}|z|\,^3\mathrm{B}_{2u}\rangle}{4\sqrt{5}} + \frac{\sqrt{3}\,\langle ^3\mathrm{B}_{2g}|z|\,^3\mathrm{B}_{3u}\rangle}{4\sqrt{5}}\right)\\
\mathcal{T}(^3\mathrm{P}^\circ_1 - {}^3\mathrm{D}_2) &= \langle ^3\mathrm{P}_1||\mathbf{D}^1||\,^3\mathrm{D}_2\rangle = \sqrt{30}\,\langle ^3\mathrm{P}^{\text{-}1}_1||d^1_{\text{-}1}||\,^3\mathrm{D}^0_2\rangle & (5.50)\\
&= \sqrt{30}\left(\frac{\langle ^3\mathrm{B}_{2g}|x|\,^3\mathrm{B}_{1u}\rangle}{4} + \frac{\langle ^3\mathrm{B}_{3g}|y|\,^3\mathrm{B}_{1u}\rangle}{4}\right)\\
\mathcal{T}(^3\mathrm{P}^\circ_1 - {}^1\mathrm{S}_0) &= \sqrt{3}\,\langle ^1\mathrm{S}^0_0|z|\,^1\mathrm{P}^1_1\rangle\,\frac{\langle ^1\mathrm{P}^1_1|H_{\mathrm{SO}}|\,^3\mathrm{P}^1_1\rangle}{E_{^3\mathrm{P}_1} - E_{^1\mathrm{P}_1}} = & (5.51)\\
&= \sqrt{3}\,\langle ^1\mathrm{A}_g|z|\,^1\mathrm{B}_{1u}\rangle\,\frac{1}{2}\frac{(\langle ^1\mathrm{B}_{1u}|V^x|\,^3\mathrm{B}_{2u}\rangle + \langle ^1\mathrm{B}_{1u}|V^y|\,^3\mathrm{B}_{3u}\rangle)}{E_{^3\mathrm{P}_1} - E_{^1\mathrm{P}_1}}
\end{aligned}$$

Kulaga et al.[154] used Hartree-Fock with relativistic corrections with the inclusion of the core-valence electron correlation. Within slight modifications of their approach they obtained τ in the range of $0.994 - 1.120$ μs. Hafner et al.[152] used the relativistic pseudo potential approach and obtained $\tau = 1.25$. Our computed value of 1.33 μs is in a very good agreement with the result $\tau = 1.37$ μs of Dzuba et al.[153] obtained with the relativistic Hartree-Fock method together with the CI method.

We also observe very good agreement with the experimental results, especially with the newer experiments. One should note that the computation of the lifetime of the $6s6p\,^3\mathrm{P}^\circ_1$ state is very subtle and sensitive to the value of the $\langle ^1\mathrm{P}^1_1|H_{\mathrm{SO}}|\,^3\mathrm{P}^1_1\rangle$ transition. Therefore, the agreement of our result with the measured values of τ is a considerable achievement.

Table 5.14: Lifetime τ in μs of the $6s6p\,^3\mathrm{P}^\circ_1$ state of the Ba atom.

Year	Reference	τ [μs]		
	Theory			
2018	This work XCCSD(G)	1.16		
2018	This work XCC3(G)	1.33		
2018	This work XCCSD(S)	1.24		
2018	This work XCC3(S)	1.33		
1978	Hafner et al.[152]	1.25		
2000	Dzuba et al.[153]	1.37		
2001	Kulaga et al.[154]	0.994	−	1.120
	Experiment			
2006	Scielzo et al.[155]	1.345	±	0.014
1995	Brustand Gallagher[156]	1.351	±	0.055
1968	Swagel and Lurio[157]	1.2	±	1
1961	Bucka[158]	1.200	±	0.100

5.3.8 The $6s6p\,^1\mathrm{P}_1$ state of the Ba atom

The $6s6p\,^1\mathrm{P}_1$ state of the Ba atom, undergo radiative dipole transition to the $6s^2\,^1\mathrm{S}_0$ state, and the transition moment is given by

$$\mathcal{T}(^1\mathrm{P}^\circ_1 - {}^1\mathrm{S}_0) = \sqrt{3}\,\langle ^1\mathrm{A}_g|z|\,^1\mathrm{B}_{1u}\rangle\,. \tag{5.52}$$

The total lifetime of the $6s6p\,^1\mathrm{P}_1$ state gets contributions from four decay channels

$$\tau_{^1\mathrm{P}_1} = \frac{1}{\mathcal{A}(^1\mathrm{P}_1, {}^1\mathrm{S}_0) + \mathcal{A}(^1\mathrm{P}_1, {}^3\mathrm{D}_2) + \mathcal{A}(^1\mathrm{P}_1, {}^3\mathrm{D}_1) + \mathcal{A}(^1\mathrm{P}_1, {}^1\mathrm{D}_2)}. \tag{5.53}$$

While the $\mathcal{A}(^1\mathrm{P}_1, {}^1\mathrm{S}_0)$ transition probability is of order 10^8 s^{-1}, the remaining transition probabilities are of order 10^5 s^{-1} and less. Therefore their influence on the radiative lifetime (within the presented accuracy) is negligible. In Table 5.15 we present the result for the transition probability $\mathcal{A}(^1\mathrm{P}_1, {}^1\mathrm{S}_0)$

While our result is well within the error bars of the older experiments of Hulpke et al.[165] and Bernhardt et al.,[164] it is slightly higher than the newer experiment of Niggli and Huber.[162] Our computed value of $\mathcal{A} = 1.28$ is placed in the middle of the other theoretical results. Unfortunately the lifetime is very sensitive to change in $\mathcal{A}$, therefore our lifetime is about 8% shorter than the theoretical and experimental results from Table 5.16.

Table 5.15: Transition probability A [10^8 s^{-1}] of the $6s6p\,^1\mathrm{P}_1 - 6s^2\,^1\mathrm{S}_0$ transition in the Ba atom.

Year	Reference	A [10^8 s^{-1}]		
	Theory			
(2018)	This work XCCSD(G)	1.67		
(2018)	This work XCC3(S)	1.30		
(2018)	This work XCCSD(S)	1.66		
(2018)	This work XCC3(S)	1.28		
(1987)	Migdalek et al.[159]	1.06[a]		
(1985)	Bauschlicher et al.[160]	1.23		
(1969)	Friedrich et al.[161]	1.33		
	Experiment			
(1987)	Niggli and Huber[162]	1.19	$\pm$	0.01
(1985)	Jahreiss and Huber[163]	1.19	$\pm$	0.60
(1976)	Bernhardt et al.[164]	1.18[a]	$\pm$	0.12
(1964)	Hulpke et al.[165]	1.15[a]	$\pm$	0.12

[a] Values computed from oscillator strengths given in Ref. 159

Table 5.16: Lifetime τ in ns of the $6s6p\,^1\mathrm{P}_1^\circ$ state of the Ba atom.

Year	Reference	τ ns		
	Theory			
(2018)	This work XCCSD(G)	5.98		
(2018)	This work XCC3(G)	7.68		
(2018)	This work XCCSD(S)	6.00		
(2018)	This work XCC3(S)	7.82		
(2000)	Dzuba et al.[153]	9.1		
	Experiment			
(1977)	Kelly and Mathur[166]	8.37	$\pm$	0.08
(1964)	Hulpke et al.[165]	8.36	$\pm$	0.25

5.3.9 The $6s5d\,^3\mathrm{D}_2$ state of the Ba atom

We performed computation of the spin-induced quadrupole transition for the $6s5d\,^3\mathrm{D}_2$ state. The following expression was derived by the WIGNER code

$$\begin{aligned}\mathcal{T}(^3\mathrm{D}_2, {}^1\mathrm{S}_0) &= \langle 6s5d\,^3\mathrm{D}_2||\mathbf{Q}||6s^2\,^1\mathrm{S}_0\rangle = \sqrt{5}\,\langle 6s5d\,^3\mathrm{D}_2^0|Q_0^2|6s^2\,^1\mathrm{S}_0^0\rangle \\ &= \sqrt{5}\frac{\langle 6s5d\,^3\mathrm{D}_2^0|H_{\mathrm{SO}}|6s5d\,^1\mathrm{D}_2^0\rangle}{E_{^3\mathrm{D}_2^0} - E_{^1\mathrm{D}_2^0}}\,\langle 6s5d\,^1\mathrm{D}_2^0|Q_0^2|6s^2\,^1\mathrm{S}_0^0\rangle\end{aligned} \tag{5.54}$$

$$= \sqrt{5}\frac{\left(-\frac{1}{2}\left\langle(1)\,^1\mathrm{A}_g|V^x|\,^3\mathrm{B}_{3g}\right\rangle + \frac{1}{2}\left\langle(1)\,^1\mathrm{A}_g|V^y|\,^3\mathrm{B}_{2g}\right\rangle\right)}{E_{^3\mathrm{D}_2^0} - E_{^1\mathrm{D}_2^0}}$$
$$\times \sqrt{\frac{3}{2}}\left\langle^1\mathrm{A}_g|Q_{zz}|(1)\,^1\mathrm{A}_g\right\rangle .$$

$$Q_0^2 = \sqrt{\frac{3}{2}}Q_{zz} \tag{5.55}$$

In Table 5.17 we present the comparison of our results with the available theoretical data, as no experimental results could be obtained thus far. Unfortunately, there

Table 5.17: Lifetimes for $5s6d\,^3\mathrm{D}_2$ $[s]$ for barium atom. (T/E, L/V) denote Theoretical/Experimental energy and Length/Velocity representation.

Ref.	Method	τ[s]
This work	XCC3(G)	20.0
Ref. 167	MCDF-I (T, L)	418.3
Ref. 167	MCDF-I (T, V)	3404.2
Ref. 167	MCDF-I (E, L)	582.6
Ref. 167	MCDF-I (E, V)	4153.0
Ref. 167	MCDF-II (T, L)	43.6
Ref. 167	MCDF-II (T, V)	50.6
Ref. 167	MCDF-II (E, L)	59.4
Ref. 167	MCDF-II (E, V)	60.9
Ref. 168	MCHF	20.0

are very few theoretical data available for this state in the literature. Migdalek et al.[167] employed a relativistic multiconfigurational Dirac-Fock method (MCDF), and performed two types of calculations. In MCDF-I the relativistic counterparts of only $6s5d$ and $5d^2$ configurations are included, and in MCDF-II the $6p^2$ configuration is also included. The authors presented their results for the $5s6d\,^3\mathrm{D}_2$ Ba lifetime both in the length and velocity representations, and it is clear from Table 5.17 that a huge scatter in the results was observed for MCDF-I. As the difference between length-velocity could be used to verify the quality of a method, the authors suggest that the MCDF-II method worked better in this case. We also compare our results with the computations of Trefftz,[168] where multi-configurational Hartree-Fock (MCHF) wave functions were used with the configuration interaction method including the spin-orbit coupling. The authors obtained $\tau = 20$ [s] which is in a perfect agreement with our computed value of $\tau = 20.0$ [s].

5.4 Numerical demonstration of the Hermiticity

The exact transition moment $\mathcal{T}^X_{LM}$ is Hermitian, i.e., it satisfies the relation given by

$$\mathcal{T}^X_{LM} = (\mathcal{T}^X_{ML})^\star. \tag{5.56}$$

This implies that the transition strength $\mathcal{S}^X_{LM}$,

$$\mathcal{S}_{LM} = |\mathcal{T}_{LM}|^2 \tag{5.57}$$

cannot be negative.

For illustration we investigated some problematic transitions in the Mg atom and Mg_2 molecule which have been encountered beforehand.[40] We found that the transitions strengths for the $3s3d\,^1\mathrm{D} - 3s3p\,^1\mathrm{P}^\circ$, $3s3d\,^1\mathrm{D} - 3s4p\,^1\mathrm{P}$ and $3s3d\,^1\mathrm{D} - 3s5p\,^1\mathrm{P}$ transitions computed with the TD-CC code exhibited a non-physical behavior, i.e., some of the contributions were negative. No such artifacts were found in any transition strengths contributions with the XCC theory. In Table 5.18 we present the differences between $\mathcal{T}^X_{LM}$ and $(\mathcal{T}^X_{ML})^\star$ computed with the TD-CC and XCC theories. In TD-CC these differences are significant, especially in situations where one is positive and the other is negative. In the XCC method the Hermiticity is numerically insignificant, and the errors are usually an order of magnitude smaller compared to TD-CC.

Table 5.18: $\mathcal{T}^X_{LM}$ and $(\mathcal{T}^X_{ML})^\star$ computed with the TD-CC and XCC methods for the Mg atom.

Transition	$\mathcal{T}^X_{LM}$(TDCC)	$(\mathcal{T}^X_{ML})^\star$(TDCC)	$\mathcal{T}^X_{LM}$(XCC)	$(\mathcal{T}^X_{ML})^\star$(XCC)
aug-cc-pVQZ				
$3s4s\,^1\mathrm{S} - 3s3p\,^1\mathrm{P}^\circ$	4.30	4.26	4.00	4.01
$3s4p\,^1\mathrm{P}^\circ - 3s4s\,^1\mathrm{S}$	8.39	8.30	8.36	8.36
d-aug-cc-pVQZ				
$3s5s\,^1\mathrm{S} - 3s4p\,^1\mathrm{P}^\circ$	10.12	10.04	10.08	10.09
$3s5s\,^1\mathrm{S} - 3s3p\,^1\mathrm{P}^\circ$	0.60	0.60	0.51	0.51
$3s3d\,^1\mathrm{D} - 3s3p\,^1\mathrm{P}^\circ$	0.67	−0.40	1.40	1.43
$3s4p\,^1\mathrm{P} - 3s3d\,^1\mathrm{D}$	−1.18	0.72	2.64	2.63

Chapter 6 Summary and Conclusions

In the present thesis, the extension of the expectation value coupled cluster method (XCC) for the computation of transition matrix elements between a ground state and an excited state and between a pair of excited states, for the singlet-singlet, triplet-triplet and singlet-triplet transitions is reported. The XCC theory for the singlet-singlet and triplet-triplet transitions was originally published by Tucholska et al. in Paper I[18] and Paper II.[19] We demonstrate that our approach can easily be applied to any one-electron operator, including the spin-orbit operator. The work on the computation of the spin-orbit matrix elements is published in this thesis for the first time and is the basis for an upcoming publication.[77]

Using the XCC formalism we were able to propose a methodology alternative to the conventional TD-CC response theory. The latter is less straightforward and computationally more demanding. The difference between these approaches lays in the steps that follow the computation of conventional ground-state amplitudes of the operator T. The TD-CC method requires the computation of both the left and right CC Jacobian eigenvectors and, in addition to that, an iterative procedure to solve the equations for the Lagrange multipliers. In contrast, the XCC theory for the excited states requires only the right (or left) Jacobian eigenvectors, and only a single-step computation of the amplitudes of the auxiliary operator S. In addition to that, while in both approaches the formulas are size-intensive, the XCC is the only method that yields the proper Hermitian symmetry. Apart from this, our formalism is conceptually simple and easily extendable to general operators.

We have shown that the violation of the Hermiticity in the TD-CC theory leads to unphysical results in some cases. In Table 5.18, we presented specific examples where the left and right transition moments have different signs and as a result the transition strength, which should be a positive value, is negative. Although XCC is strictly Hermitian only if one uses the exact operator S, in practice, for truncated S, the deviations from the Hermitian symmetry of the transition moments are numerically negligible.

In this dissertation we have also presented an approach for the computation of transition moments between a ground and an excited state which is an alternative to the approach of our previous work.[18] We have derived the expression for the transition strength between the ground and exited states, from the quadratic response function $\langle\langle X, Y, Z\rangle\rangle_{\omega_Y,\omega_Z}$. This is our preferred approach because it treats the ground state-excited state and excited state-excited state transition moments using consistent approximations.

The methodology presented here can easily be extended to the CC models other that CCSD and CC3 provided that the set of commutators/contributions retained in the working formulas for the transition moment matrix elements properly corresponds to the choice of the ground state amplitudes. Our final result, Eq. (3.57), is presented in a commutator form, and can be approximated at any level.

To apply the main equation for the transition matrix element, Eq. (3.57), we expand it in MBPT orders, taking into account that the amplitudes t are from the CCSD or CC3 calculations and the Jacobian eigenvectors are computed with the EOM-CCSD or EOM-CC3 methods. Our conclusion is that the third order of MBPT is sufficient to obtain converged results, see Figs. 3.2 to 3.7

The results for the radiative lifetimes, and transition probabilities are presented in the literature in a rich variety of conventions. Therefore, we wrote a simple Mathematica code to deal with the arduous task of obtaining the results that are comparable to the experimental and theoretical works.

The performance of our method was tested on selected systems, the Mg, Ca, Sr and Ba atoms. Several aspects were investigated. Mainly, our interest was to compute lifetimes for systems where very few or none experimental results are available. Next, we analyzed the existing computations from other theoretical works. We discussed the possible origins of differences. Within our own theory we compared the CCSD vs CC3 results. Also the use of the Slater basis set and it is influence on the excited states energies and transition moments was discussed. One of the most striking advantages of the Slater basis was much better convergence to desired states, even in CCSD case, where the Gaussian basis performed poorly.

The spin-orbit interaction in this work was included perturbatively by computing the matrix element of the SO part of the pseudopotential. This approach allowed us to test the performance of our method for medium and heavy atoms where the SO interaction is most important. There is yet still a necessity to adapt our theory for light atoms were pseudopotentials are not that common, and usually all-electron computations are performed.

There is room to extend the XCC theory for magnetic moments, nonadiabatic coupling, open-shell systems. The features presented in this thesis form a strong basis for a complete theory for the computation of the transition properties.

Bibliography

[1] H. Werner, P. Knowles, R. Lindh, F. Manby, M. Schütz, *et al.*, "Molpro, version 2015.1, a package of ab initio programs, see www.molpro.net," (2015).

[2] K. Aidas, C. Angeli, K. L. Bak, V. Bakken, R. Bast, L. Boman, O. Christiansen, R. Cimiraglia, S. Coriani, P. Dahle, *et al.*, "The Dalton quantum chemistry program system," WIREs Comput. Mol. Sci. **4**, 269 (2014).

[3] D. Zubarev, Usp. Fiz. Nauk **3**, 320 (1960).

[4] J. Linderberg and Y. Öhrn, *Propagators in quantum chemistry* (John Wiley & Sons, 2004).

[5] P. Jørgensen, *Second quantization-based methods in quantum chemistry* (Elsevier, 2012).

[6] J. Oddershede, "Propagator methods," Adv. Chem. Phys. **69**, 201 (1987).

[7] P. Jorgensen, "Molecular and atomic applications of time-dependent Hartree-Fock theory," Annu. Rev. Phys. Chem **26**, 359 (1975).

[8] J. Oddershede, "Polarization propagator calculations," in *Adv. Quantum Chem.*, Vol. 11 (Elsevier, 1978) pp. 275–352.

[9] J. Oddershede, P. Jørgensen, and D. L. Yeager, "Polarization propagator methods in atomic and molecular calculations," Comp. Phys. Rep. **2**, 33 (1984).

[10] W. Rijks and P. Wormer, "Correlated van der waals coefficients for dimers consisting of He, Ne, H_2, and N_2," J. Chem. Phys. **88**, 5704 (1988).

[11] J. E. Rice and N. C. Handy, "The calculation of frequency-dependent polarizabilities as pseudo-energy derivatives," J. Chem. Phys. **94**, 4959 (1991).

[12] H. J. Monkhorst, "Calculation of properties with the coupled-cluster method," Int. J. Quant. Chem. **12**, 421 (1977).

[13] E. Dalgaard and H. J. Monkhorst, "Some aspects of the time-dependent coupled-cluster approach to dynamic response functions," Phys. Rev. A **28**, 1217 (1983).

[14] H. Sekino and R. J. Bartlett, "A linear response, coupled-cluster theory for excitation energy," Int. J. Quant. Chem. **26**, 255 (1984).

[15] M. Takahashi and J. Paldus, "Time-dependent coupled cluster approach: Excitation energy calculation using an orthogonally spin-adapted formalism," J. Chem. Phys. **85**, 1486 (1986).

[16] H. Koch and P. Jørgensen, "Coupled cluster response functions," J. Chem. Phys. **93**, 3333 (1990).

[17] R. Moszynski, P. S. Żuchowski, and B. Jeziorski, "Time-Independent Coupled-Cluster Theory of the Polarization Propagator," Coll. Czech. Chem. Commun **70**, 1109 (2005).

[18] A. M. Tucholska, M. Modrzejewski, and R. Moszynski, "Transition properties from the hermitian formulation of the coupled cluster polarization propagator," J. Chem. Phys. **141**, 124109 (2014).

[19] A. M. Tucholska, M. Lesiuk, and R. Moszynski, "Transition moments between excited electronic states from the hermitian formulation of the coupled cluster quadratic response function," J. Chem. Phys. **146**, 034108 (2017).

[20] J. Čížek, "On the correlation problem in atomic and molecular systems. calculation of wavefunction components in ursell-type expansion using quantum-field theoretical methods," J. Chem. Phys. **45**, 4256 (1966).

[21] J. Čížek, "On the use of the cluster expansion and the technique of diagrams in calculations of correlation effects in atoms and molecules," Adv. Chem. Phys. **14**, 35 (1969).

[22] C. Dykstra, G. Frenking, K. Kim, and G. Scuseria, *Theory and Applications of Computational Chemistry: the first forty years* (Elsevier, 2011).

[23] K. Brueckner and C. Levinson, "Approximate reduction of the many-body problem for strongly interacting particles to a problem of self-consistent fields," Phys. Rev. **97**, 1344 (1955).

[24] J. Goldstone, "Derivation of the Brueckner many-body theory," Proc. R. Soc. Lond. A **239**, 267 (1957).

[25] J. Paldus, J. Čížek, and I. Shavitt, "Correlation problems in atomic and molecular systems. IV. Extended coupled-pair many-electron theory and its application to the BH_3 molecule," Phys. Rev. A **5**, 50 (1972).

[26] J. Pople, R. Krishnan, H. Schlegel, and J. Binkley, "Electron correlation theories and their application to the study of simple reaction potential surfaces," Int. J. Quant. Chem. **14**, 545 (1978).

[27] G. D. Purvis III and R. J. Bartlett, "A full coupled-cluster singles and doubles model: The inclusion of disconnected triples," J. Chem. Phys. **76**, 1910 (1982).

[28] R. J. Bartlett and M. Musiał, "Coupled-cluster theory in quantum chemistry," Rev. Mod. Phys. **79**, 291 (2007).

[29] T. B. Pedersen and H. Koch, "Coupled cluster response functions revisited," J. Chem. Phys. **106**, 8059 (1997).

[30] T. Korona, M. Przybytek, and B. Jeziorski, "Time-Independent Coupled-Cluster Theory of the Polarization Propagator. Implementation and application of the singles and doubles model to dynamic polarizabilities and van der Waals constants," Mol. Phys. **104**, 2303 (2006).

[31] T. Korona and B. Jeziorski, "One-electron properties and electrostatic interaction energies from the expectation value expression and wave function of singles and doubles coupled cluster theory," J. Chem. Phys. **125**, 184109 (2006).

[32] A. I. Krylov, “Equation-of-motion coupled-cluster methods for open-shell and electronically excited species: The hitchhiker’s guide to Fock space,” Annu. Rev. Phys. Chem **59** (2008).

[33] L. Adamowicz, W. Laidig, and R. Bartlett, “Analytical gradients for the coupled-cluster method,” Int. J. Quant. Chem. **26**, 245 (1984).

[34] S. Hirata, I. Grabowski, M. Tobita, and R. J. Bartlett, “Highly accurate treatment of electron correlation in polymers: coupled-cluster and many-body perturbation theories,” Chem. Phys. Lett. **345**, 475 (2001).

[35] S. Hirata, R. Podeszwa, M. Tobita, and R. J. Bartlett, “Coupled-cluster singles and doubles for extended systems,” J. Chem. Phys. **120**, 2581 (2004).

[36] B. Mihaila and J. H. Heisenberg, “Ground state correlations and mean field in ^{16}O. II. Effects of a three-nucleon interaction,” Phys. Rev. C **61**, 054309 (2000).

[37] K. Kowalski, D. Dean, M. Hjorth-Jensen, T. Papenbrock, and P. Piecuch, “Coupled cluster calculations of ground and excited states of nuclei,” Phys. Rev. Lett. **92**, 132501 (2004).

[38] L. Rybak, Z. Amitay, S. Amaran, R. Kosloff, M. Tomza, R. Moszynski, and C. P. Koch, “Femtosecond coherent control of thermal photoassociation of magnesium atoms,” Faraday Discuss. **153**, 383 (2011).

[39] L. Rybak, S. Amaran, L. Levin, M. Tomza, R. Moszynski, R. Kosloff, C. P. Koch, and Z. Amitay, “Generating molecular rovibrational coherence by two-photon femtosecond photoassociation of thermally hot atoms,” Phys. Rev. Lett. **107**, 273001 (2011).

[40] S. Amaran, R. Kosloff, M. Tomza, W. Skomorowski, F. Pawłowski, R. Moszynski, L. Rybak, L. Levin, Z. Amitay, J. M. Berglund, D. M. Reich, and C. P. Koch, “Femtosecond two-photon photoassociation of hot magnesium atoms: A quantum dynamical study using thermal random phase wavefunctions,” J. Chem. Phys. **139**, 164124 (2013).

[41] L. Levin, W. Skomorowski, L. Rybak, R. Kosloff, C. P. Koch, and Z. Amitay, “Coherent control of bond making,” Phys. Rev. Lett. **114**, 233003 (2015).

[42] R. M. Wilson, “A femtosecond laser pulse makes molecular bonds,” Phys. Today **68**, 19 (2015).

[43] W. Skomorowski, F. Pawłowski, C. P. Koch, and R. Moszynski, “Rovibrational dynamics of the strontium molecule in the $\mathrm{A}^1\Sigma_u^{+1}$, $\mathrm{c}^3\Pi_u$, and $\mathrm{a}^3\Sigma_u^{+3}$ manifold from state-of-the-art ab initio calculations,” J. Chem. Phys. **136**, 194306 (2012).

[44] B. McGuyer, M. McDonald, G. Iwata, M. Tarallo, W. Skomorowski, R. Moszynski, and T. Zelevinsky, “Precise study of asymptotic physics with subradiant ultracold molecules,” Nature Phys. **11**, 32 (2015).

[45] M. McDonald, B. McGuyer, F. Apfelbeck, C.-H. Lee, I. Majewska, R. Moszynski, and T. Zelevinsky, “Photodissociation of ultracold diatomic strontium molecules with quantum state control,” Nature **534**, 122 (2016).

[46] B. McGuyer, C. Osborn, M. McDonald, G. Reinaudi, W. Skomorowski, R. Moszynski, and T. Zelevinsky, “Nonadiabatic effects in ultracold molecules via anomalous linear and quadratic zeeman shifts,” Phys. Rev. Lett. **111**, 243003 (2013).

[47] B. McGuyer, M. McDonald, G. Iwata, W. Skomorowski, R. Moszynski, and T. Zelevinsky, "Control of optical transitions with magnetic fields in weakly bound molecules," Phys. Rev. Lett. **115**, 053001 (2015).

[48] M. Tomza, M. H. Goerz, M. Musiał, R. Moszynski, and C. P. Koch, "Optimized production of ultracold ground-state molecules: Stabilization employing potentials with ion-pair character and strong spin-orbit coupling," Phys. Rev. A **86**, 043424 (2012).

[49] W. Skomorowski and R. Moszynski, "Long-range interactions between an atom in its ground s state and an open-shell linear molecule," J. Chem. Phys. **134**, 124117 (2011).

[50] M. Tomza, W. Skomorowski, M. Musiał, R. González-Férez, C. P. Koch, and R. Moszynski, "Interatomic potentials, electric properties and spectroscopy of the ground and excited states of the Rb_2 molecule: ab initio calculations and effect of a non-resonant field*," Mol. Phys. **111**, 1781 (2013).

[51] C. M. Marian, "Spin-orbit coupling in molecules," Rev. Comp. Chem. **17**, 99 (2001).

[52] W. Pauli, "Zur quantenmechanik des magnetischen elektrons," in *Wolfgang Pauli* (Springer, 1988) pp. 282–305.

[53] C. M. Marian, "Spin–orbit coupling and intersystem crossing in molecules," Wiley Interdisciplinary Reviews: Computational Molecular Science **2**, 187 (2012).

[54] M. Dolg and X. Cao, "Relativistic pseudopotentials: their development and scope of applications," Chem. Rev. **112**, 403 (2011).

[55] Y. S. Lee, W. C. Ermler, and K. S. Pitzer, "Ab initio effective core potentials including relativistic effects. I. Formalism and applications to the Xe and Au atoms." J. Chem. Phys. **61**, 5861 (1977).

[56] P. Hafner and W. Schwarz, "Pseudo-potential approach including relativistic effects," J. Phys. B **11**, 2975 (1978).

[57] R. M. Pitzer and N. W. Winter, "Electronic-structure methods for heavy-atom molecules," J. Phys. Chem. **92** (1988).

[58] H. Koch, R. Kobayashi, A. S. de Meras, and P. Jørgensen, "Calculation of size-intensive transition moments from the coupled cluster singles and doubles linear response function," J. Chem. Phys. **100**, 4393 (1994).

[59] O. Christiansen, P. Jørgensen, and C. Hättig, "Response functions from Fourier component variational perturbation theory applied to a time-averaged quasienergy," Int. J. Quant. Chem. **68**, 1 (1998).

[60] O. Christiansen, A. Halkier, H. Koch, P. Jo/rgensen, and T. Helgaker, "Integral-direct coupled cluster calculations of frequency-dependent polarizabilities, transition probabilities and excited-state properties," J. Chem. Phys. **108**, 2801 (1998).

[61] O. Christiansen and J. Gauss, "Radiative singlet–triplet transition properties from coupled-cluster response theory: The importance of the $S_0 \rightarrow T_1$ transition for the photodissociation of water at 193 nm," J. Chem. Phys. **116**, 6674 (2002).

[62] B. Helmich-Paris, C. Hättig, and C. van Wüllen, "Spin-free CC2 implementation of induced transitions between singlet ground and triplet excited states," J. Chem. Theory Comput. **12**, 1892 (2016).

[63] T. Helgaker, S. Coriani, P. Jørgensen, K. Kristensen, J. Olsen, and K. Ruud, "Recent advances in wave function-based methods of molecular-property calculations," Chem. Rev. **112**, 543 (2012).

[64] O. Christiansen, H. Koch, and P. Jørgensen, "The second-order approximate coupled cluster singles and doubles model CC2," Chem. Phys. Lett. **243**, 409 (1995).

[65] K. Hald, C. Hättig, D. L. Yeager, and P. Jørgensen, "Linear response CC2 triplet excitation energies," Chem. Phys. Lett. **328**, 291 (2000).

[66] H. Koch, O. Christiansen, P. Jørgensen, A. M. Sanchez De Merás, and T. Helgaker, "The CC3 model: An iterative coupled cluster approach including connected triples," J. Chem. Phys. **106**, 1808 (1997).

[67] K. Hald and P. Jørgensen, "Calculation of first-order one-electron properties using the coupled-cluster approximate triples model CC3," Phys. Chem. Chem. Phys. **4**, 5221 (2002).

[68] B. Jeziorski and R. Moszynski, "Explicitly connected expansion for the average value of an observable in the coupled-cluster theory," Int. J. Quant. Chem. **48**, 161 (1993).

[69] T. Korona and B. Jeziorski, "Dispersion energy from density-fitted density susceptibilities of singles and doubles coupled cluster theory," J. Chem. Phys. **128**, 144107 (2008).

[70] T. Korona, "Exchange-dispersion energy: A formulation in terms of monomer properties and coupled cluster treatment of intramonomer correlation," J. Chem. Theory Comput. **5**, 2663 (2009).

[71] T. Korona, "Coupled cluster treatment of intramonomer correlation effects in intermolecular interactions," in *Recent Progress in Coupled Cluster Methods* (Springer, 2010) pp. 267–298.

[72] T. Korona, "A coupled cluster treatment of intramonomer electron correlation within symmetry-adapted perturbation theory: Benchmark calculations and a comparison with a density-functional theory description," Mol. Phys. **111**, 3705 (2013).

[73] T. Korona, "Second-order exchange-induction energy of intermolecular interactions from coupled cluster density matrices and their cumulants," Phys. Chem. Chem. Phys. **10**, 6509 (2008).

[74] T. B. Pedersen and H. Koch, "Coupled cluster response functions revisited," J. Chem. Phys. **106**, 8059 (1997).

[75] R. Moszynski and A. Ratkiewicz, "Many-body perturbation theory of electrostatic interactions between molecules: Comparison with full configuration interaction for four-electron dimers," J. Chem. Phys. **99**, 8856 (1993).

[76] R. Moszynski, B. Jeziorski, S. Rybak, K. Szalewicz, and H. L. Williams, "Many-body theory of exchange effects in intermolecular interactions. density matrix approach and applications to He–F-, He–HF, H_2–HF, and Ar–H_2 dimers," J. Chem. Phys. **100**, 5080 (1994).

[77] A. M. Tucholska, M. Lesiuk, and R. Moszynski, "Spin-orbit coupling matrix elements from the hermitian formulation of the coupled cluster quadratic response function," In preparation (2018).

[78] J. Paldus and B. Jeziorski, "Clifford algebra and unitary group formulations of the many-electron problem," Theor. Chim. Acta **73**, 81 (1988).

[79] B. Jeziorski, J. Paldus, and P. Jankowski, "Unitary group approach to spin-adapted open-shell coupled cluster theory," Int. J. Quant. Chem. **56**, 129 (1995).

[80] T. Helgaker, P. Jorgensen, and J. Olsen, *Molecular electronic-structure theory* (Wiley, New York, 2013).

[81] J. Noga and R. J. Bartlett, "The full CCSDT model for molecular electronic structure," J. Chem. Phys. **86**, 7041 (1987).

[82] J. Noga and R. Bartlett, "Erratum: The full CCSDT model for molecular electronic structure," J. Chem. Phys. **89**, 3401 (1988).

[83] G. E. Scuseria and H. F. Schaefer III, "A new implementation of the full CCSDT model for molecular electronic structure," Chem. Phys. Lett. **152**, 382 (1988).

[84] Y. S. Lee, S. A. Kucharski, and R. J. Bartlett, "A coupled cluster approach with triple excitations," J. Chem. Phys. **81**, 5906 (1984).

[85] M. Urban, J. Noga, S. J. Cole, and R. J. Bartlett, "Towards a full CCSDT model for electron correlation," J. Chem. Phys. **83**, 4041 (1985).

[86] K. Raghavachari, G. W. Trucks, J. A. Pople, and M. Head-Gordon, "A fifth-order perturbation comparison of electron correlation theories," Chem. Phys. Lett. **157**, 479 (1989).

[87] T. H. Dunning, "A road map for the calculation of molecular binding energies," J. Phys. Chem. A **104**, 9062 (2000).

[88] R. J. Bartlett, J. Watts, S. Kucharski, and J. Noga, "Non-iterative fifth-order triple and quadruple excitation energy corrections in correlated methods," Chem. Phys. Lett. **165**, 513 (1990).

[89] J. F. Stanton and R. J. Bartlett, "The equation of motion coupled-cluster method. a systematic biorthogonal approach to molecular excitation energies, transition probabilities, and excited state properties," J. Chem. Phys. **98**, 7029 (1993).

[90] J. Oddershede, "Calculation of radiative lifetimes of allowed and forbidden transitions," in *Mol. Astrophys.* (Springer, 1985) pp. 533–549.

[91] G. W. Drake, *Springer Handbook of Atomic, Molecular, and Optical Physics* (Springer, New York, 2006).

[92] G. H. Shortley, "The computation of quadrupole and magnetic-dipole transition probabilities," Phys. Rev. **57**, 225 (1940).

[93] M. Lesiuk and R. Moszynski, "Reexamination of the calculation of two-center, two-electron integrals over Slater-type orbitals. I. Coulomb and hybrid integrals," Phys. Rev. E **90**, 063318 (2014).

[94] M. Lesiuk and R. Moszynski, "Reexamination of the calculation of two-center, two-electron integrals over Slater-type orbitals. II. Neumann expansion of the exchange integrals," Phys. Rev. E **90**, 063319 (2014).

[95] M. Lesiuk, M. Przybytek, M. Musiał, B. Jeziorski, and R. Moszynski, "Reexamination of the calculation of two-center, two-electron integrals over Slater-type orbitals. III. Case study of the beryllium dimer," Phys. Rev. A **91**, 012510 (2015).

[96] J. H. Wilkinson, *The algebraic eigenvalue problem*, Vol. 87 (Clarendon Press Oxford, 1965).

[97] K. Hirao and H. Nakatsuji, "A generalization of the Davidson's method to large nonsymmetric eigenvalue problems," J. Chem. Phys. **45**, 246 (1982).

[98] W. Butscher and W. Kammer, "Modification of Davidson's method for the calculation of eigenvalues and eigenvectors of large real-symmetric matrices:"root homing procedure"," J. Comp. Phys. **20**, 313 (1976).

[99] K. Hald, P. Jørgensen, O. Christiansen, and H. Koch, "Implementation of electronic ground states and singlet and triplet excitation energies in coupled cluster theory with approximate triples corrections," J. Chem. Phys. **116**, 5963 (2002).

[100] G.-C. Wick, "The evaluation of the collision matrix," Phys. Rev. **80**, 268 (1950).

[101] S. F. Boys, "Electronic wave functions-I. A general method of calculation for the stationary states of any molecular system," Proc. R. Soc. Lond. A **200**, 542 (1950).

[102] S. Boys, G. Cook, C. Reeves, and I. Shavitt, "Automatic fundamental calculations of molecular structure," Nature **178**, 1207 (1956).

[103] J. C. Slater, "Atomic shielding constants," Phys. Rev. **36**, 57 (1930).

[104] C. Zener, "Analytic atomic wave functions," Phys. Rev. **36**, 51 (1930).

[105] T. H. Dunning Jr, "Gaussian basis sets for use in correlated molecular calculations. I. The atoms boron through neon and hydrogen," J. Chem. Phys. **90**, 1007 (1989).

[106] M. Lesiuk, A. M. Tucholska, and R. Moszynski, "Combining Slater-type orbitals and effective core potentials," Phys. Rev. A **95**, 052504 (2017).

[107] D. Feller, "The role of databases in support of computational chemistry calculations," J. Comp. Chem. **17**, 1571 (1996).

[108] K. L. Schuchardt, B. T. Didier, T. Elsethagen, L. Sun, V. Gurumoorthi, J. Chase, J. Li, and T. L. Windus, "Basis set exchange: A community database for computational sciences," J. Chem. Inf. Model. **47**, 1045 (2007).

[109] I. S. Lim, H. Stoll, and P. Schwerdtfeger, "Relativistic small-core energy-consistent pseudopotentials for the alkaline-earth elements from Ca to Ra," J. Chem. Phys. **124**, 034107 (2006).

[110] J. Sugar and C. Corliss, "Energy levels of calcium, Ca I through Ca XX," **8**, 865 (1979).

[111] M. Miyabe, C. Geppert, M. Kato, M. Oba, I. Wakaida, K. Watanabe, and K. D. Wendt, "Determination of ionization potential of calcium by high-resolution resonance ionization spectroscopy," J. Phys. Soc. Jap. **75**, 034302 (2006).

[112] J. Sansonetti and G. Nave, "Wavelengths, transition probabilities, and energy levels for the spectrum of neutral strontium (SrI)," **39**, 033103 (2010).

[113] B. Post, W. Vassen, W. Hogervorst, M. Aymar, and O. Robaux, "Odd-parity rydberg levels in neutral barium: term values and multichannel quantum defect theory analysis," Journal of Physics B: Atomic and Molecular Physics **18**, 187 (1985).

[114] C. F. Fischer, "Theoretical Oscillator Strengths for nS-mP Transitions in Mg," Can. J. Phys. **53**, 338 (1975).

[115] T. Chang, "Effect of the configuration interaction on the $(3snl)$ ^1L bound states of the magnesium atom," Phys. Rev. A **34**, 4550 (1986).

[116] N. W. Zheng, T. Wang, R. Y. Yang, T. Zhou, D. X. Ma, Y. G. Wu, and H. T. Xu, "Transition probabilities for Be I, Be II, Mg I, and Mg II," At. Data Nucl. Data Tables **79**, 109 (2001).

[117] R. G. Gratton, E. Carretta, R. Claudi, S. Lucatello, and M. Barbieri, "Abundances for metal-poor stars with accurate parallaxes-I. basic data," A & A **404**, 187 (2003).

[118] A. Schaefer, "Measured lifetimes of excited states of magnesium," Astrophys. J. **163**, 411 (1971).

[119] T. Chang and X. Tang, "Oscillator strengths for the bound-bound transitions in beryllium and magnesium," J. Quant. Spectrosc. Radiat. Transfer **43**, 207 (1990).

[120] M. Chantepie, B. Cheron, J. Cojan, J. Landais, B. Laniepce, A. Moudden, and M. Aymar, "Time-resolved fluorescence of the $^1S_0$ and $^1D_2$ series of Mg I," J. Phys. B **22**, 2377 (1989).

[121] G. Jönsson, C. Levinson, A. Persson, and C.-G. Wahlström, "Natural radiative lifetimes in the $^1P_1$ and $^1F_3$ sequences of Sr I," Z. Phys. A **316**, 255 (1984).

[122] M. Aldenius, J. D. Tanner, S. Johansson, H. Lundberg, and S. G. Ryan, "Experimental Mg I oscillator strengths and radiative lifetimes for astrophysical applications on metal-poor stars," A & A **461**, 767 (2007).

[123] M. Kwiatkowski, U. Teppner, and P. Zimmermann, "Lifetime measurements in the triplet system of Mg I," Z. Phys. A **294**, 109 (1980).

[124] T. Andersen, L. Molhave, and G. Sorensen, "Lifetimes of excited states in Mg I, Cd I, and Mg II," Astrophys. J. **178**, 577 (1972).

[125] K. Ueda, M. Karasawa, and K. Fukuda, "Measurements of oscillator strengths for the transitions from the metastable ^3P levels of alkaline-earth atoms. II. Magnesium," J. Phys. Soc. Jpn **51**, 2267 (1982).

[126] M. Havey, L. Balling, and J. Wright, "Direct measurements of excited-state lifetimes in Mg, Ca, and Sr," J. Opt. Soc. Am. **67**, 488 (1977).

[127] R. Moccia and P. Spizzo, "Atomic magnesium: II. One-photon transition probabilities and ionisation cross sections. A valence-shell L_2 CI calculation," J. Phys. B **21**, 1133 (1988).

[128] G. Victor, R. Stewart, and C. Laughlin, "Oscillator strengths in the Mg isoelectronic sequence," Astrophys. J. Suppl. Ser. **31**, 237 (1976).

[129] C. Mendoza, "Term structure of Mg I calculated in a frozen-cores approximation," J. Phys. B **14**, 397 (1981).

[130] Y. Yu and A. Derevianko, "Transition rates and radiative lifetimes of Ca I," Atomic Data and Nuclear Data Tables **119**, 263 (2018).

[131] N. Vaeck, M. Godefroid, and J. Hansen, "MCHF oscillator strength and lifetime calculations in neutral calcium," J. Phys. B **24**, 361 (1991).

[132] R. Diffenderfer, P. Dagdigian, and D. Yarkony, "Spin-forbidden radiative transitions in atomic calcium," J. Phys. B **14**, 21 (1981).

[133] G. Zinner, T. Binnewies, F. Riehle, and E. Tiemann, "Photoassociation of cold Ca atoms," Physical review letters **85**, 2292 (2000).

[134] J. Mitroy and J. Zhang, "Dispersion and polarization interactions of the strontium atom," Mol. Phys. **108**, 1999 (2010).

[135] S. Porsev, A. D. Ludlow, M. M. Boyd, and J. Ye, "Determination of Sr properties for a high-accuracy optical clock," Phys. Rev. A **78**, 032508 (2008).

[136] M. Yasuda, T. Kishimoto, M. Takamoto, and H. Katori, "Photoassociation spectroscopy of Sr 88: Reconstruction of the wave function near the last node," Phys. Rev. A **73**, 011403 (2006).

[137] S. B. Nagel, P. G. Mickelson, A. Saenz, Y. Martinez, Y. Chen, T. C. Killian, P. Pellegrini, and R. Côté, "Photoassociative spectroscopy at long range in ultracold strontium," Phys. Rev. Lett. **94**, 083004 (2005).

[138] K. Aidas, C. Angeli, K. L. Bak, V. Bakken, R. Bast, L. Boman, O. Christiansen, R. Cimiraglia, S. Coriani, P. Dahle, *et al.*, "The dalton quantum chemistry program system," WIREs: Comp. Mol. Sci. **4**, 269 (2014).

[139] C. W. Bauschlicher Jr, S. R. Langhoff, and H. Partridge, "The radiative life- of the $^1\mathrm{D}_2$ state of Ca and Sr: a core-valence treatment," J. Phys. B **18**, 1523 (1985).

[140] N. Beverini, E. Maccioni, F. Sorrentino, V. Baraulia, and M. Coca, "Measurementof the transition probability in calcium," Eur. Phys. J. D **23**, 223 (2003).

[141] R. Drozdowski, J. Kwela, and M. Walkiewicz, "Lifetimes of the $4s4p^3\mathrm{P}_1$ and $4s3d^1\mathrm{D}_2$ states of Ca I," Z. Phys. D **27**, 321 (1993).

[142] L. Pasternack, D. Yarkony, P. Dagdigian, and D. Silver, "Experimental and theoretical study of the Ca I $4s3d^1\mathrm{D} - 4s2^1\mathrm{S}$ and $4s4p^3\mathrm{P}_1 - 4s2^1\mathrm{S}$ forbidden transitions," J. Phys. B **13**, 2231 (1980).

[143] I. Courtillot, A. Quessada-Vial, A. Brusch, D. Kolker, G. D. Rovera, and P. Lemonde, "Accurate spectroscopy of Sr atoms," Eur. Phys. J. D **33**, 161 (2005).

[144] D. Husain and G. Roberts, "Radiative lifetimes, diffusion and energy pooling of Sr $(5s5p(^3\mathrm{P}_1))$ and Sr $(5s4d(^3\mathrm{D}_2))$ studied by time-resolved atomic emission following pulsed dye-laser excitation," Chem. Phys. **127**, 203 (1988).

[145] S. Porsev, M. Kozlov, Y. G. Rakhlina, and A. Derevianko, "Many-body calculations of electric-dipole amplitudes for transitions between low-lying levels of Mg, Ca, and Sr," Phys. Rev. A **64**, 012508 (2001).

[146] R. Santra, K. V. Christ, and C. H. Greene, "Properties of metastable alkaline-earth-metal atoms calculated using an accurate effective core potential," Phys. Rev. A **69**, 042510 (2004).

[147] T. Zelevinsky, M. M. Boyd, A. D. Ludlow, T. Ido, J. Ye, R. Ciuryło, P. Naidon, and P. S. Julienne, "Narrow line photoassociation in an optical lattice," Phys. Rev. Lett. **96**, 203201 (2006).

[148] K. Guo, G. Wang, and A. Ye, "Dipole polarizabilities and magic wavelengths for a Sr and Yb atomic optical lattice clock," Journal of Physics B: Atomic, Molecular and Optical Physics **43**, 135004 (2010).

[149] M. Safronova, S. Porsev, U. Safronova, M. Kozlov, and C. W. Clark, "Blackbody-radiation shift in the Sr optical atomic clock," Phys. Rev. A **87**, 012509 (2013).

[150] D. Miller, L. You, J. Cooper, and A. Gallagher, "Collisional energy transfer between excited-state strontium and noble-gas atoms," Phys. Rev. A **46**, 1303 (1992).

[151] E. N. Borisov, P. N. P., and T. P. Redko, Opt. Spectrosc. **63**, 475 (1987).

[152] P. Hafner and W. Schwarz, "Atomic transition probabilities from the relativistic pseudopotential approach," J. Phys. B **11**, 2975 (1978).

[153] V. Dzuba, V. Flambaum, and J. Ginges, "Calculation of parity and time invariance violation in the radium atom," Phys. Rev. A **61**, 062509 (2000).

[154] D. Kulaga, J. Migdalek, and O. Bar, "Transition probabilities and lifetimes in neutral barium," J. Phys. B **34**, 4775 (2001).

[155] N. Scielzo, J. Guest, E. Schulte, I. Ahmad, K. Bailey, D. Bowers, R. Holt, Z.-T. Lu, T. O'Connor, and D. Potterveld, "Measurement of the lifetimes of the lowest $^3\mathrm{P}_1$ state of neutral Ba and Ra," Phys. Rev. A **73**, 010501 (2006).

[156] J. Brust and A. Gallagher, "Excitation transfer in barium by collisions with noble gases," Phys. Rev. A **52**, 2120 (1995).

[157] M. W. Swagel and A. Lurio, "g_J factor of the lowest $^1\mathrm{P}_1$ and $^3\mathrm{P}_1$ states of Ba; level-crossing determination of $\frac{\mathcal{A}^1\mathrm{P}_1}{\mu_0 g_j(^1\mathrm{P}_1)}$ $\mathrm{Hg}^1 99$," Phys. Rev. **169**, 114 (1968).

[158] H. Bucka and H. Nagel, Ann. Phys. **8**, 329 (1961).

[159] J. Migdalek and W. Baylis, "Correlation effects in a relativistic calculation of the $6s^{21}\mathrm{S}_0 - -6s6p^3\mathrm{P}_1, {}^1\mathrm{P}_1$ transitions in barium," Phys. Rev. A **35**, 3227 (1987).

[160] C. J. Bauschlicher, R. Jaffe, S. Langhoff, F. Mascarello, and H. Partridge, "Theoretical electric quadrupole transition probabilities for Ca, Sr and Ba," J. Phys. B **18**, 2147 (1985).

[161] H. Friedrich and E. Trefftz, J. Quant. Spectrosc. Radiat. Transfer **9**, 333 (1969).

[162] S. Niggli and M. Huber, "Transition probabilities in neutral barium," Physical Review A **35**, 2908 (1987).

[163] L. Jahreiss and M. Huber, "Ba oscillator strengths from a laser-excited vapor," Physical Review A **31**, 692 (1985).

[164] A. Bernhardt, D. Duerre, J. Simpson, and L. Wood, "Oscillator strength of the barium $6s6p^1\mathrm{P}_1 - -6s5d^1\mathrm{D}_2$ transition inferred from photodeflection efficiency," J. Opt. Soc. America **66**, 416 (1976).

[165] E. Hulpke, E. Paul, and W. Paul, "Bestimmung von oszillatorenstärken durch lebensdauermessungen der ersten angeregten niveaus für die elemente Ba, Sr, Ca, In und Na," Z. Phys. **177**, 257 (1964).

[166] F. Kelly and M. Mathur, "The density dependence of the hanle effect in the resonance line of atomic barium," Canadian Journal of Physics **55**, 83 (1977).

[167] J. Migdalek and W. Baylis, "Multiconfiguration Dirac-Fock calculations of two electric quadrupole transitions in neutral barium," Phys. Rev. A **42**, 6897 (1990).

[168] E. Trefftz, "On the mutual influence of configuration interaction and spin-orbit coupling in heavy atoms," J. Phys. B **7**, L342 (1974).

Appendices

Appendix A Paper I: J. Chem. Phys. 141, 124109 (2014)

THE JOURNAL OF CHEMICAL PHYSICS **141**, 124109 (2014)

Transition properties from the Hermitian formulation of the coupled cluster polarization propagator

Aleksandra M. Tucholska,[a)] Marcin Modrzejewski, and Robert Moszynski
Faculty of Chemistry, University of Warsaw, Pasteura 1, 02-093 Warsaw, Poland

(Received 3 July 2014; accepted 8 September 2014; published online 24 September 2014)

Theory of one-electron transition density matrices has been formulated within the time-independent coupled cluster method for the polarization propagator [R. Moszynski, P. S. Żuchowski, and B. Jeziorski, Coll. Czech. Chem. Commun. **70**, 1109 (2005)]. Working expressions have been obtained and implemented with the coupled cluster method limited to single, double, and linear triple excitations (CC3). Selected dipole and quadrupole transition probabilities of the alkali earth atoms, computed with the new transition density matrices are compared to the experimental data. Good agreement between theory and experiment is found. The results obtained with the new approach are of the same quality as the results obtained with the linear response coupled cluster theory. The one-electron density matrices for the ground state in the CC3 approximation have also been implemented. The dipole moments for a few representative diatomic molecules have been computed with several variants of the new approach, and the results are discussed to choose the approximation with the best balance between the accuracy and computational efficiency. © *2014 AIP Publishing LLC*. [http://dx.doi.org/10.1063/1.4896056]

I. INTRODUCTION

One of the most challenging problems of modern quantum chemistry is an accurate and fast computation of molecular properties. Coupled cluster theory (CC), which is the gold standard of quantum chemical methods, combines an accurate description of the electronic structure with an affordable computational cost for medium sized molecules. The coupled cluster Ansatz is presented as[1–9]

$$\Psi = e^{T}\Phi, \tag{1}$$

where the cluster operator T for an N electron system is the sum of single, double, and higher excitations, $T = T_1 + T_2 + \cdots + T_N$, and Φ is the reference function. Due to the exponential form of the Ansatz, the CC theory is size-extensive for any truncation of T. The possibility of restricting T to a particular excitation level introduces a hierarchy of approximations: coupled cluster singles and doubles (CCSD), coupled cluster singles, doubles, and triples (CCSDT), etc. Also, the methods CC2[10] and CC3,[11] approximating CCSD and CCSDT, respectively, were developed. The CC3 equations for T_1 and T_2 have the same form as in CCSDT. The equation for T_3, however, includes only terms up to the second order in the fluctuation potential. The CC3 approximation ensures that the triple amplitudes are correct through the second order, while there is no need for storing T_3 in memory: they are readily computable on the fly with expressions including single and double excitations. The ground state CC3 model scales as $\mathcal{N}^7$, whereas CCSDT scales as $\mathcal{N}^8$, with the size of the basis $\mathcal{N}$.

Currently, molecular properties of the ground state within the CC framework are computed as the derivative of the first-order Lagrangian with respect to the field strength.[12,13] An alternative method, referred to as XCC, was proposed by Jeziorski and Moszynski[14] and further investigated by Moszynski *et al.*,[15,16] Korona and Jeziorski,[17] and Korona, Przybytek, and Jeziorski.[18] In the XCC approach, the first-order properties are computed directly from the definition of the quantum-mechanical expectation value. This formalism is conceptually simple and its computational cost is lower than in the case of the Lagrangian technique as it does not require finding the expensive left-hand solution of the CC equations, the so-called Λ or Z vector.[12,13]

The main object of interest in this study is the linear response function $\langle\langle X; Y\rangle\rangle_\omega$, often referred to in the literature as the polarization propagator. The linear response function describes the response of an observable X to the perturbation Y oscillating with the frequency ω. The residues of the polarization propagator are connected to many physical observables, e.g., transition probabilities, lifetimes, and line strengths. For real ω and for purely real or purely imaginary perturbations Y, the polarization propagator satisfies the following relation:

$$\langle\langle X; Y\rangle\rangle_\omega = \langle\langle X; Y\rangle\rangle_{-\omega}, \tag{2}$$

which reflects the time-reversal symmetry.

The linear response function within CC theory can be computed either from the response theory (LRCC)[19–21] or from the time-independent XCC theory.[22] Both theories give the polarization propagator satisfying Eq. (2). In the LRCC approach, the time-reversal symmetry of the linear response function follows from the restriction of the time-dependent expectation value to the real part, which is otherwise not guaranteed to be real if an approximate coupled cluster wave function is employed. In XCC, one starts from the exact expression for the polarization propagator. Thus, the correct symmetry is present in the XCC theory from the start. The final form of the polarization propagator in this theory is

[a)]Electronic mail: tuchol@tiger.chem.uw.edu.pl

Hermitian in the sense that any truncation of the cluster operators does not violate the correct time-reversal symmetry.

During the 20 years since the initial formulation of the XCC method,[14] numerous studies restricted to the CCSD level were reported: electrostatic[15] and exchange[16] contributions to the interaction energies of closed-shell systems, first-order molecular properties,[17] static and dynamic dipole polarizabilites,[18] frequency-dependent density susceptibilities employed in SAPT(CC).[23] In this paper, we present the derivation and implementation of the transition density matrices obtained from the XCC linear response function[22] at the CC3 level. Also, the results for the first-order one-electron properties at the CC3 level are presented in order to test various approximations to the XCC theory.

This paper is organized as follows. In Sec. II, we derive the formula for the first-order properties within the XCC3 theory. We also report the derivation of the transition density matrices from the XCC linear response function. Next, in Sec. III we present the numerical results for the ground-state dipole moments of some representative diatomic molecules. We discuss various approximations to the XCC3 theory that offer the best balance between the accuracy and computational efficiency. We continue the discussion of the results with the atomic dipole and quadrupole transition probabilities computed within the XCC3 theory. Whenever possible, extensive comparison with the experimental data as well as with the data obtained from the LRCC3 calculations is reported. Finally in Sec. IV we conclude our paper.

II. THEORY

A. Basic definitions

All the operators in this work are expressed through the singlet orbital replacement operators[24]

$$E_{pq} = a^\dagger_{p\alpha}a_{q\alpha} + a^\dagger_{p\beta}a_{q\beta}, \tag{3}$$

which satisfy the commutation relation $[E_{pq}, E_{rs}] = E_{ps}\delta_{rq} - E_{rq}\delta_{ps}$. From now on, $a, b, c\ldots$ and $i, j, k\ldots$ denote virtual and occupied orbital indices, respectively, and $p, q, r\ldots$ general indices. The cluster operator T is represented in a compact form as a sum of n-tuple excitation operators T_n,

$$T_n = \frac{1}{n!}\sum_{\mu_n} t_{\mu_n}\mu_n, \tag{4}$$

where μ_n stands for the product of the n singlet excitation operators $E_{ai}E_{bj}\cdots E_{fm}$. The CC amplitudes satisfy the following permutation symmetry relations:

$$\begin{aligned} t^{ab}_{ij} &= t^{ba}_{ji} \\ t^{abc}_{ijk} &= t^{acb}_{ikj} = t^{bac}_{jik} = t^{bca}_{jki} = t^{cab}_{kij} = t^{cba}_{kji}. \end{aligned} \tag{5}$$

The excitation energies in this work are obtained from the diagonalization of the CC Jacobian matrix,[19,25,26]

$$A_{\mu_n\mu_m} = \langle \widetilde{\mu}_n | [e^{-T}He^{T}, \mu_m] \rangle, \tag{6}$$

where we introduce the shorthand notation $\langle X|Y\rangle = \langle X\Phi|Y\Phi\rangle$, $\langle X\rangle = \langle\Phi|X\Phi\rangle$. The elements of the Jacobian are defined in the biorthonormal basis

$$\langle\widetilde{\mu}_n|\nu_n\rangle = \delta_{\mu_n\nu_n}. \tag{7}$$

For the single and double excitation manifolds we used the basis proposed by Helgaker, Jorgensen, and Olsen.[26] A biorthonormal and nonredundant basis for the triply excited manifold is derived in the Appendix.

The expectation value of an observable in the XCC theory is given by the explicitly connected, size-consistent expression introduced by Jeziorski and Moszynski[14]

$$\bar{X} = \langle e^{S^\dagger}e^{-T}Xe^{T}e^{-S^\dagger}\rangle. \tag{8}$$

The auxiliary operator $S = S_1 + S_2 + \cdots + S_N$ is the solution of the following equation:

$$\begin{aligned} S_n = T_n &- \frac{1}{n}\hat{\mathcal{P}}_n\left(\sum_{k=1}\frac{1}{k!}[\widetilde{T}^\dagger, T]_k\right) \\ &- \frac{1}{n}\hat{\mathcal{P}}_n\left(\sum_{k=1}\sum_{m=0}\frac{1}{k!}\frac{1}{m!}[[\widetilde{S}, T^\dagger]_k, T]_m\right), \end{aligned} \tag{9}$$

where

$$\widetilde{T} = \sum_{n=1}^{N} nT_n, \qquad \widetilde{S} = \sum_{n=1}^{N} nS_n \tag{10}$$

and

$$[A, B]_k = \underbrace{[[\cdots[[A, B], B]\cdots]}_{\text{nested } k \text{ times}}. \tag{11}$$

The superoperator $\hat{\mathcal{P}}_n(X)$ projects the n-tuple excitation part of an arbitrary operator X,

$$\hat{\mathcal{P}}_n(X) = \frac{1}{n!}\sum_{\mu_n}\langle\widetilde{\mu}_n|X\rangle\mu_n. \tag{12}$$

The expanded expression for S_n, Eq. (9), is finite, though it contains cumbersome terms with multiply-nested commutators. These terms are of high order in the fluctuation potential.[14] Also, the r.h.s. of Eq. (9) depends on S, therefore solving this equation requires an iterative procedure. However, S can efficiently be approximated while retaining the size consistency of the expectation value expression. Below, we present the expressions for $S_n(m)$ for $n \in \{1, 2, 3\}$ and $m \in \{2, 3, 4\}$, with m denoting the highest many-body perturbation theory (MBPT) order fully included,

$$S_1(2) = T_1$$

$$S_1(3) = S_1(2) + \hat{\mathcal{P}}_1\left([T_1^\dagger, T_2]\right) + \hat{\mathcal{P}}_1\left([T_2^\dagger, T_3]\right)$$

$$S_1(4) = S_1(3) + \hat{\mathcal{P}}_1\left([[T_2^\dagger, T_1], T_2]\right) + \frac{1}{2}\hat{\mathcal{P}}_1\left([[T_3^\dagger, T_2], T_2]\right)$$

$$
\begin{aligned}
S_2(2) &= T_2 \\
S_2(3) &= S_2(2) + \frac{1}{2}\hat{\mathcal{P}}_2\left([[T_2^\dagger, T_2], T_2]\right) \\
S_2(4) &= S_2(3) + \hat{\mathcal{P}}_2\left([T_1^\dagger, T_3]\right) \\
S_3(2) &= T_3 \\
S_3(4) &= S_3(3) + \frac{1}{2}\hat{\mathcal{P}}_3\left([[T_1^\dagger, T_2], T_2]\right) \\
&\quad + \hat{\mathcal{P}}_3\left([[T_2^\dagger, T_2], T_3]\right).
\end{aligned}
\tag{13}
$$

We test the accuracy of three approximations denoted as XCC3S(m), with $m = 2, 3, 4$,

$$
\begin{aligned}
&\mathrm{XCC3S}(2): S_1(2) + S_2(2) + S_3(2) \\
&\mathrm{XCC3S}(3): S_1(3) + S_2(3) + S_3(2) \\
&\mathrm{XCC3S}(4): S_1(4) + S_2(4) + S_3(2).
\end{aligned}
\tag{14}
$$

One should note that in all three approximations $S_3 = T_3$.

The accuracy of S depends on the underlying wave function model. The CC3 method includes T_1 and T_2 correct through the third order and T_3 correct through the second order. The accuracy of S_1, S_2, and S_3 is of the same order of MBPT as the accuracy of the corresponding T_1, T_2, and T_3 amplitudes. The lowest order contributions to S_4 are of the third order, but this quantity appears only in the fourth order contributions to the transition density matrices, and is not required.

Using the commutator expansion in Eq. (8) we obtain the following formula for the expectation value of an operator at the CC3 level of theory:

$$
\begin{aligned}
\bar{X} = \sum_{\mathcal{M}=0}^{8} \bar{X}^{(\mathcal{M})} &= \langle X\rangle^{(0)} \\
&+ \langle S_1 | X\rangle^{(2)} + \langle [X, T_1]\rangle^{(2)} + \langle S_2 | [X, T_2]\rangle^{(2)} \\
&+ \langle S_1 | [X, T_2]\rangle^{(3)} + \langle S_2 | [X, T_3]\rangle^{(3)} \\
&+ \langle S_1 | [X, T_1]\rangle^{(4)} + \langle S_2 | [[X, T_1], T_2]\rangle^{(4)} \\
&+ \langle S_3 | [X, T_3]\rangle^{(4)} + \frac{1}{2}\langle S_3 | [[X, T_2], T_2]\rangle^{(4)} \\
&+ \frac{1}{2}\langle S_1^2 | [X, T_2]\rangle^{(5)} + \frac{1}{2}\langle S_1 S_2 | [[X, T_2], T_2]\rangle^{(5)} \\
&+ \frac{1}{2}\langle S_1 S_2 | [X, T_3]\rangle^{(5)} \\
&+ \frac{1}{2}\langle S_1 | [[X, T_1], T_1]\rangle^{(6)} + \frac{1}{2}\langle S_1^2 | [X, T_3]\rangle^{(6)} \\
&+ \frac{1}{2}\langle S_1^2 | [[X, T_1], T_2]\rangle^{(7)} \\
&+ \frac{1}{12}\langle S_1^3 | [[X, T_2], T_2]\rangle^{(8)} + \frac{1}{6}\langle S_1^3 | [X, T_3]\rangle^{(8)}.
\end{aligned}
\tag{15}
$$

The upper index of $\bar{X}^{(\mathcal{M})}$ indicates an $\mathcal{M}$th order contribution. Apart from T_n and S_n for $n > 3$, no other approximations have been introduced in Eq. (15).

B. XCC3 transition density matrices

In the exact theory, the polarization propagator is defined by the following expression:[27]

$$
\begin{aligned}
\langle\langle X; Y\rangle\rangle_\omega = &-\left\langle \Psi_0 | Y \frac{Q}{H - E_0 + \omega} X \Psi_0 \right\rangle \\
&-\left\langle \Psi_0 | X \frac{Q}{H - E_0 - \omega} Y \Psi_0 \right\rangle,
\end{aligned}
\tag{16}
$$

where H denotes the Hamiltonian, Ψ_0 is the normalized ground-state wave function, E_0 is the ground state energy, and Q is the projection operator on the space spanned by all excited states. The line strength S_{XY}^{0K} of the transition to the Kth excited state is obtained as the residue of the linear response function

$$
\begin{aligned}
&\lim_{\omega\to\omega_K} (\omega - \omega_K)\langle\langle X; Y\rangle\rangle_\omega \\
&\quad = \sum_{K'} \langle \Psi_0 | X \Psi_{K'}\rangle \langle \Psi_{K'} | Y \Psi_0\rangle = S_{XY}^{0K}
\end{aligned}
\tag{17}
$$

$$
\begin{aligned}
&\lim_{\omega\to-\omega_K} (\omega + \omega_K)\langle\langle X; Y\rangle\rangle_\omega \\
&\quad = -\sum_{K'} \langle \Psi_0 | Y \Psi_{K'}\rangle \langle \Psi_{K'} | X \Psi_0\rangle = S_{XY}^{K0},
\end{aligned}
\tag{18}
$$

where K' runs over all degenerate states corresponding to the excitation energy ω_K. The time-reversal symmetry, Eq. (2), is transferred from the polarization propagator to the line strength S_{XY} through the relation

$$
S_{XY}^{0K} = -\left(S_{XY}^{K0}\right)^\star. \tag{19}
$$

Moszynski, Zuchowski, and Jeziorski[22] have expressed the polarization propagator within the framework of the XCC theory

$$
\begin{aligned}
&\langle\langle X; Y\rangle\rangle_\omega \\
&\quad = \langle e^{-S} e^{T^\dagger} Y e^{-T^\dagger} e^{S} | \hat{\mathcal{P}}(e^{S^\dagger} \Omega^X(\omega) e^{-S^\dagger})\rangle + \text{g.c.c.},
\end{aligned}
\tag{20}
$$

where g.c.c. (generalized complex conjugate) denotes the complex conjugation of the r.h.s. and substitution of ω for $-\omega$. Not only this expression satisfies the time reversal symmetry, but is also size-consistent because it can solely be represented in terms of commutators.

The operator $\Omega^X(\omega)$ appearing in Eq. (20) is solution of the linear response equation,[22]

$$
\left\langle \widetilde{\mu} | [e^{-T} H e^{T}, \Omega^X(\omega)] + \omega \Omega^X(\omega) + e^{-T} X e^{T} \right\rangle = 0, \tag{21}
$$

where $\Omega^X(\omega) = \Omega_1^X(\omega) + \Omega_2^X(\omega) + \cdots + \Omega_N^X(\omega)$, and $\Omega_n^X(\omega)$ is an excitation operator of the form

$$
\Omega_n^X = {\sum_{\mu_n}}' O_{\mu_n}^X(\omega) \mu_n, \tag{22}
$$

where ${\sum}'_{\mu_n}$ stands for restricted summation over nonredundant excitations for double excitations $ai \geq bj$ and for triple excitations $ai \geq bj \geq ck$. Using the transformation from the molecular orbital basis to the Jacobian basis

$$
\mu_n = \sum_M \mathcal{L}_{\mu_n M}^\star r_M, \qquad \widetilde{\mu}_n^\star = \sum_M \mathcal{R}_{\mu_n M}^\star l_M^\star, \tag{23}
$$

$\Omega^X(\omega)$ can be written as

$$\Omega^X(\omega) = \sum_M \sum_{n=1}^{N} \sum_{\mu_n}{}' \mathcal{L}^\star_{\mu_n M} O^X_{\mu_n}(\omega) r_M = \sum_M O^X_M(\omega) r_M. \tag{24}$$

Equation (21) takes then the form

$$\langle l_M|[e^{-T}He^T, r_M]\rangle O^X_M(\omega) + \omega O^X_M(\omega) + \langle l_M|e^{-T}Xe^T\rangle = 0, \tag{25}$$

where $\langle l_M|[e^{-T}He^T, r_M]\rangle$ is the Mth excitation energy ω_M, and we used the biorthonormality condition $\langle l_M|r_K\rangle = \delta_{MK}$. The $O^X_M(\omega)$ reads

$$O^X_M(\omega) = -\frac{\langle l_M|e^{-T}Xe^T\rangle}{\omega_M + \omega}. \tag{26}$$

We will now translate Eq. (20) into a computationally transparent form. The action of the projection superoperator $\hat{\mathcal{P}} = \hat{\mathcal{P}}_1 + \hat{\mathcal{P}}_2 + \cdots + \hat{\mathcal{P}}_N$ on the commutator expansion of $e^{S^\dagger}\Omega^X(\omega)e^{-S^\dagger}$ produces a sum of multiply nested commutators

$$\hat{\mathcal{P}}\left(\sum_{n=1}^{N}\sum_{\mu_n}{}'\sum_{k=0}^{n-1}\frac{1}{k!}[S^\dagger, O^X_{\mu_n}(\omega)]_k\right) = \sum_{n=1}^{N}\sum_{\mu_n}{}' O^X_{\mu_n}\sum_{k=0}^{n-1}\frac{1}{k!}\sum_{\Gamma}[S^\dagger_{n_1}, [\cdots[S^\dagger_{n_{k-1}}, [S^\dagger_{n_k}, \mu_n]\cdots]], \tag{27}$$

where the last summation runs over all sequences satisfying the condition

$$\Gamma : k \le n_1 + \cdots + n_k \le n-1. \tag{28}$$

Using Eq. (27), the polarization propagator in the molecular orbital basis takes the form

$$\langle\langle X; Y\rangle\rangle_\omega = \sum_{n=1}^{N}\sum_{\mu_n}{}' O^X_{\mu_n}(\omega)\gamma^Y_{\mu_n} + \text{g.c.c.}, \tag{29}$$

where we use the shorthand notation for $\gamma^Y_{\mu_n}$ and $\eta(\mu_n)$, respectively,

$$\gamma^Y_{\mu_n} = \langle e^{S^\dagger}e^{-T}Ye^Te^{-S^\dagger}\eta(\mu_n)\rangle, \qquad \eta(\mu_n) = \sum_{k=0}^{n-1}\frac{1}{k!}\sum_{\Gamma}[S^\dagger_{n_1}, [\cdots[S^\dagger_{n_{k-1}}, [S^\dagger_{n_k}, \mu_n]\cdots]]. \tag{30}$$

Transformation of Eq. (29) to the Jacobian basis leads to the following expression:

$$\langle\langle X; Y\rangle\rangle_\omega = -\sum_M \frac{\langle l_M|e^{-T}Xe^T\rangle\langle e^{S^\dagger}e^{-T}Ye^Te^{-S^\dagger}\eta(r_M)\rangle}{\omega_M+\omega} + \text{g.c.c.} = -\sum_M\frac{\xi^X_M\gamma^Y_M}{\omega_M+\omega} + \text{g.c.c.}, \tag{31}$$

where

$$\begin{aligned}\xi^X_M &= \langle l_M|e^{-T}Xe^T\rangle = \sum_{n=1}^{N}\sum_{\mu_n}{}'\mathcal{L}_{\mu_n M}\langle\mu_n|e^{-T}Xe^T\rangle = \sum_{n=1}^{N}\sum_{\mu_n}{}'\mathcal{L}_{\mu_n M}\xi^X_{\mu_n},\\ \gamma^Y_M &= \langle e^{S^\dagger}e^{-T}Ye^Te^{-S^\dagger}\eta(r_M)\rangle = \sum_{n=1}^{N}\sum_{\mu_n}{}'\mathcal{R}_{\mu_n M}\langle e^{S^\dagger}e^{-T}Ye^Te^{-S^\dagger}\eta(\mu_n)\rangle = \sum_{n=1}^{N}\sum_{\mu_n}{}'\mathcal{R}_{\mu_n M}\gamma^Y_{\mu_n}.\end{aligned} \tag{32}$$

The transition strength matrices are computed as the residues of the XCC linear response function

$$S^{0K}_{XY} = -\sum_{K'}\gamma^Y_{K'}\xi^X_{K'} \qquad S^{K0}_{XY} = \sum_{K'}(\gamma^Y_{K'})^\star(\xi^X_{K'})^\star. \tag{33}$$

The line strengths are connected by the relation of antihermiticity, Eq. (19), which comes up naturally in the XCC formalism. As our formulas for the transition strength matrices are exclusively expressed in terms of commutators, they are automatically size intensive, regardless of any truncation of the T or S operators.

We now present the scheme of approximations to the product

$$\gamma^Y_K\xi^X_K = \sum_{n=1}^{N}\sum_{\mu_n}{}'\mathcal{R}_{\mu_n M}\gamma^Y_{\mu_n}\sum_{m=1}^{N}\sum_{\mu_m}{}'\mathcal{L}_{\mu_m M}\xi^X_{\mu_m}. \tag{34}$$

The explicit expressions for γ^Y_μ and ξ^X_μ in the CC3 approximation are

$$\begin{aligned}(\gamma^Y_{\mu_1})^{\text{CC3}} &= \langle(Y + [S^\dagger_1, Y] + [S^\dagger_2, Y] + [S^\dagger_2, [Y, T_1]] + [S^\dagger_2, [Y, T_2]] + [S^\dagger_3, [Y, T_2]])\mu_1\rangle,\\ (\xi^X_{\mu_1})^{\text{CC3}} &= \langle\mu_1|X + [X, T_1] + [X, T_2]\rangle,\\ (\gamma^Y_{\mu_2})^{\text{CC3}} &= \langle([S^\dagger_2, Y] + [S^\dagger_3, Y] + [S^\dagger_2, [S^\dagger_1, Y]] + [S^\dagger_2, [Y, T_1]] + [S^\dagger_3, [Y, T_2]])\mu_2\rangle + \langle(Y + [S^\dagger_2, Y])[S^\dagger_1, \mu_2]\rangle,\\ (\xi^X_{\mu_2})^{\text{CC3}} &= \langle\mu_2|[X, T_2] + [X, T_3] + [[X, T_1], T_2]\rangle,\\ (\gamma^Y_{\mu_3})^{\text{CC3}} &= \langle([S^\dagger_3, Y] + [S^\dagger_2, [S^\dagger_1, Y]] + \frac{1}{2}[S^\dagger_2, [S^\dagger_2, Y]])\mu_3\rangle + \langle[S^\dagger_2, Y][S^\dagger_1, \mu_3]\rangle, + \langle(Y + [S^\dagger_1, Y] + [S^\dagger_2, Y])[S^\dagger_2, \mu_3]\rangle,\\ (\xi^X_{\mu_3})^{\text{CC3}} &= \langle\mu_3|[X, T_3] + \frac{1}{2}[[X, T_2], T_2] + [[X, T_1], T_2]\rangle.\end{aligned} \tag{35}$$

The expressions for γ_μ^Y and ξ_μ^X contain contributions up to and including the third order of MBPT. In $\gamma_{\mu_2}^Y$ and $\gamma_{\mu_3}^Y$, we have omitted the third order terms $\frac{1}{2}\langle[S_2^\dagger, [S_2^\dagger, [Y, T_2]]]\mu_2\rangle$ and $\frac{1}{2}\langle[S_2^\dagger, [S_2^\dagger, [Y, T_2]]]\mu_3\rangle$ as they are computationally much more demanding than the rest of the contributions. The S_1 and S_2 operators are correct through the third order, and the S_3 operator contains only the leading term correct through the second order, Eq. (13).

All the implementation-ready formulas presented in this work have been derived with the assistance of the `Paldus` program developed in our laboratory. `Paldus` is a program for an automated implementation of any level of theory expressible through the products of singlet orbital replacement operators. The formulas obtained with `Paldus` program are automatically optimized and incorporated into the parallelized, standalone `Fortran` code.

III. NUMERICAL RESULTS AND DISCUSSION

A. First-order properties at the CC3 level of theory

We present the results for the ground-state dipole moments of diatomic molecules calculated at the XCC3 level of theory. The geometries of the diatomic molecules are kept at their equilibrium values.[28] Comparison is done with the experimental data[29] and with the LRCC3 results. For all the molecules we employ the def2-QZVPP basis set.[30]

Figs. 1–3 show the unsigned percentage error of the dipole moment relative to the experimental value $\Delta_{\text{rel}} := |\delta q|/|q_{\text{exp}}| \times 100\%$ as a function of the highest-order term included in Eq. (15). In each plot, separate lines represent approximations to the auxiliary operator S, denoted as XCC3S(m). Thus, there are two levels of approximation: one for the expectation value formula, Eq. (15), and one for the operator S, Eq. (14).

In each case, the convergence of the expectation value defined by Eq. (15) is achieved after including the terms up to and including the fifth order. However, the inclusion of the higher-order terms does not introduce much additional computational costs. The most time consuming terms that scale as $\mathcal{N}^8$ appear in the fourth and higher orders. Introduction of intermediates reduces the scaling of all such terms to $\mathcal{N}^7$. As the most expensive terms appear already in the fourth order, computing the full sum, Eq. (15), is essentially of the same cost as computing only the partial sums.

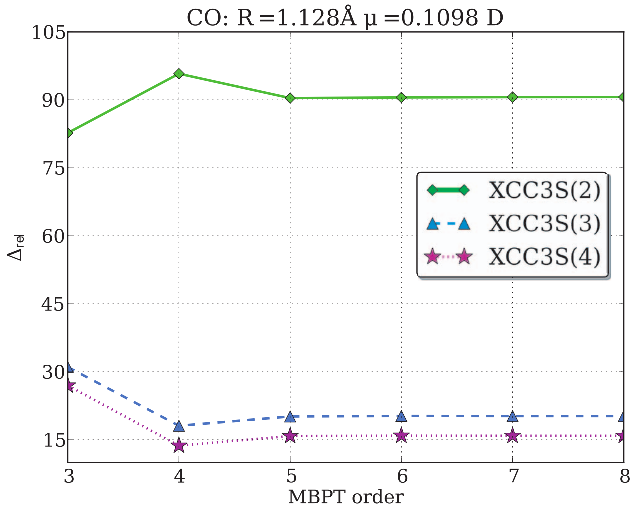

FIG. 2. Δ_{rel} of the dipole moment of CO.

An inspection of Figs. 1–3 shows that in all three cases the use of XCC3S(3) brings an improvement over XCC3S(2) relative to the experimental values. The most challenging case is the CO molecule. For this system, the XCC3S(2) level of theory is unacceptable with Δ_{rel} reaching 90%. A huge reduction of this error is observed for XCC3S(3) and XCC3S(4).

Importantly, in every case improving the accuracy of S improves the accuracy of the results. However, going from XCC3S(3) to XCC3S(4) brings only a negligible improvement not worth the corresponding increase in the computational complexity, from $\mathcal{N}^7$ to $\mathcal{N}^8$. We thus recommend the XCCS(3) level of theory; this will be the approximation of S employed to compute second order properties.

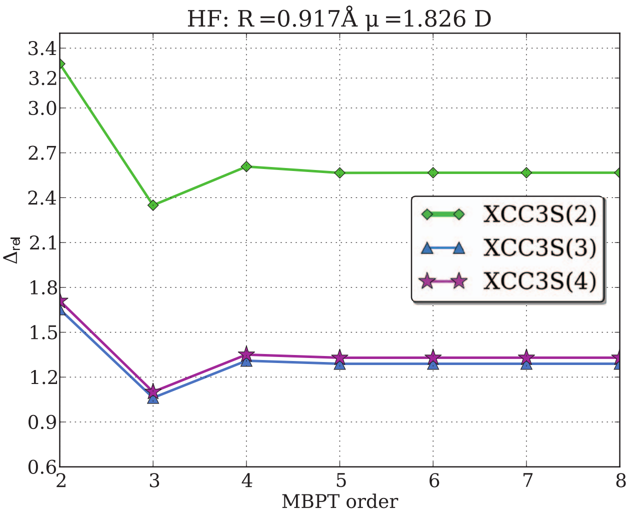

FIG. 1. Δ_{rel} of the dipole moment of HF.

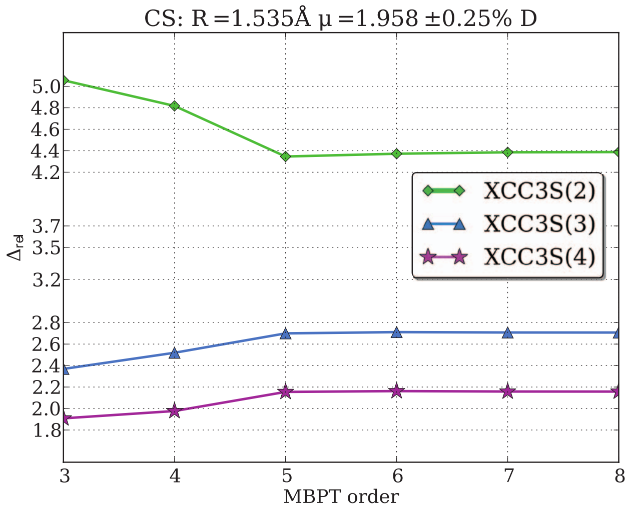

FIG. 3. Δ_{rel} of the dipole moment of CS.

TABLE I. Dipole moments computed with the XCC3S(3) and LRCC3 methods. The def2-QZVPP basis set was employed for molecules at equilibrium geometries. The experimental data are given in Debye, and the computed values are given as an signed error $\Delta_{\text{method}} = \mu_{\text{exp}} - \mu_{\text{method}}$.

Molecule	Exp.	$\Delta_{\text{XCC3S(3)}}$	Δ_{LRCC3}
LiH	5.884	0.0400	0.0463
HF	1.826	0.0235	0.0071
LiF	6.3274	0.0179	0.0879
CO	0.1098	0.0222	−0.0264
NaLi	0.463	−0.0107	−0.0263
HCl	1.1086	0.0169	−0.0216
NaF	8.156	−0.0015	0.0812
CS	1.958	0.0530	0.0055

We compare our method with the Lagrangian technique of Hald and Jørgensen.[13] Table I shows the signed absolute errors of both methods applied to the dipole moments of the test set of diatomics with the experimental data. On the average, the XCC3S(3) method is only slightly better than LRCC3. Indeed, the mean absolute error for XCC3S(2) is equal to 0.023 and for LRCC3 is equal to 0.038.

This result is encouraging since the XCC3 method is conceptually simpler and computationally less demanding than the LRCC3 approach. While both methods employ the same model for the ground-state wave function (that scales as v^4o^3, where v and o stand for the number of the virtual and occupied orbitals, respectively), the difference lies in the computation of the auxiliary operators required for the one-electron properties, i.e., the Lagrangian multipliers in the case of the LRCC approach and the operator S in the case of the XCC method. The equations for the singles and doubles Lagrangian multipliers are solved iteratively and each iteration scales like v^4o^2, whereas the amplitudes of the S_1 and S_2 operators are computed directly in a single step that scales as v^3o^3. Moreover, S_3 can efficiently be approximated by T_3, whereas the most expensive, triples Lagrange multipliers in the LRCC3 approach have to be computed separately. The computational complexity of assembling the density matrices from the auxiliary amplitudes, ground-state amplitudes, and molecular integrals is the same in both approaches and scales as v^4o^3.

B. Transition probabilities

We have performed computations of the electric dipole transition probabilities between the ^{1}S and ^{1}P states for the Mg, Ca, Sr, and Ba atoms, and of the quadrupole transition probabilities between the ^{1}S and ^{1}D states for the Ca and Ba atoms.

The line strength of the dipole transition is defined as

$$S_d = \sum_{K,K'} |\langle K|\mathbf{d}|K'\rangle|^2, \tag{36}$$

where K and K' run over all degenerate states, and $\mathbf{d}$ is the dipole moment operator. The dipole transition probability $A_{^1\text{P}^1\text{S}}$ is related to the line strength by the relation[31]

$$A_{^1\text{P}^1\text{S}} = \frac{1}{3}\frac{16\pi^3}{3h\epsilon_0\lambda^3} S_d^{^1\text{P}^1\text{S}}, \tag{37}$$

where SI units are used for $A_{^1\text{P}^1\text{S}}$, S_d, and λ: s^{-1}, m^{2}C^2, and m, respectively.

The strength of a quadrupole transition is defined as[32]

$$S_q = \sum_{K,K'} |\langle K|\mathbf{Q}|K'\rangle|^2, \tag{38}$$

where $\mathbf{Q}$ is the traceless quadrupole moment operator in Shortley's convention,[32] and the transition probability reads

$$A_{^1\text{D}^1\text{S}} = \frac{1}{5}\frac{32\pi^6}{5h\lambda^5} S_q^{^1\text{D}^1\text{S}}, \tag{39}$$

where SI units are used for $A_{^1\text{D}^1\text{S}}$, S_q, and λ: s^{-1}, m^{4}C^2, and m, respectively. A_{ki} will be used as a shorthand notation for both dipole and quadrupole transition probabilities.

1. Dipole transition probabilities

Table II shows the atomic transition probabilities A_{ki} for the ^{1}S -^{1}P transitions in Mg, Ca, Sr, and Ba atoms. The results are compared with the available spectroscopic data. In each case, we performed calculations with the XCC3S(2), XCC3S(3), and LRCC3 methods. To illustrate the convergence of the computed dipole transition probabilities with the basis set size, we use a progression of basis sets.

We also performed computations with the multireference configuration interaction (MRCI) method restricted to single and double excitations in order to compare our method with approaches based on different models of the wave function. Numerical results for the dipole transition probabilities are presented in the last two columns of Table II. The MRCI results were obtained with the Molpro program.[33] In all cases, except for the Ba atom, the agreement with the experiment of the MRCI data is by an order of magnitude worse than of the results obtained with the XCC and LRCC methods.

Except for the Ba case, the results converge quickly to the experimental benchmarks with the increase of the basis set size. In all other cases, for the largest bases employed, the results are well within the experimental error bars. For the Ba atom no improvement of the XCC, LRCC, or the MRCI values is observed with the enlargement of the basis. This can probably be attributed to the use of the pseudopotential that treats the core-electron correlation in an approximate way. In the case of Mg, Ca, and Sr atoms the use of XCC3S(3) shows a significant improvement over XCC3S(2). This corroborates the choice of XCC3S(3) as the recommended approach. The comparison of XCC3S(3) with LRCC3 shows that the transition probabilities are of the same quality.

Although the transition probabilities obtained with the XCC3 and LRCC3 methods are of equivalent quality, the computational steps required to obtain these properties differ, with XCC3 being the simplest approach. From the computational point of view, the major additional cost of LRCC3 is the calculation of the matrix $F^X_{\mu\nu} = \langle\Lambda[[X,\mu]\nu]|\Psi\rangle$ and obtaining the **F**-transformed vectors.[19,21,34] Moreover, the LRCC3 approach involves (as in the case of ground-state properties) an iterative computation of the Lagrange multipliers, while the XCC3 method requires only a single step calculation of the S amplitudes. The remaining steps, i.e., the

TABLE II. Dipole transition probabilities obtained with the XCC3, LRCC, and MRCI methods. All A_{ki} values given in $10^8 \mathrm{s}^{-1}$. $\Delta = A_{ki}^{\mathrm{exp}} - A_{ki}^{\mathrm{comp}}$. T = def2-TZVP,[30] Q = def2-QZVP,[30] 5 = cc-pV5Z,[35,36] E46 = ECP46MDF.[37]

				Mg $3s^2 - 3s3p$: $A_{ki}^{\mathrm{exp}} = 4.95(15)$[29,38]				
	$A_{ki}^{\mathrm{S(2)}}$	$\Delta^{\mathrm{S(2)}}$	$A_{ki}^{\mathrm{S(3)}}$	$\Delta^{\mathrm{S(3)}}$	A_{ki}^{LR}	Δ^{LR}	A_{ki}^{MR}	Δ^{MR}
T	5.808	−0.858	5.876	−0.926	5.882	−0.932	6.04	1.09
Q	4.777	0.173	4.833	0.117	4.843	0.107	4.80	−0.15
5	4.796	0.154	4.853	0.097	4.864	0.086	4.83	−0.12
				Ca $4s^2 - 4s4p$: $A_{ki}^{\mathrm{exp}} = 2.20(4)$[38,39]				
	$A_{ki}^{\mathrm{S(2)}}$	$\Delta^{\mathrm{S(2)}}$	$A_{ki}^{\mathrm{S(3)}}$	$\Delta^{\mathrm{S(3)}}$	A_{ki}^{LR}	Δ^{LR}	A_{ki}^{MR}	Δ^{MR}
T	2.352	−0.152	2.385	−0.185	2.386	−0.186	2.71	0.51
Q	2.183	0.017	2.211	−0.011	2.212	−0.012	2.64	0.44
5	2.159	0.041	2.184	0.016	2.184	0.016	2.62	0.42
				Sr $5s^2 - 5s5p$: $A_{ki}^{\mathrm{exp}} = 2.01(3)$[38,40]				
	$A_{ki}^{\mathrm{S(2)}}$	$\Delta^{\mathrm{S(2)}}$	$A_{ki}^{\mathrm{S(3)}}$	$\Delta^{\mathrm{S(3)}}$	A_{ki}^{LR}	Δ^{LR}	A_{ki}^{MR}	Δ^{MR}
T	2.067	−0.057	2.089	−0.079	2.089	−0.079	2.17	0.16
Q	1.971	0.039	1.994	0.016	1.993	0.017	2.39	0.38
				Ba $6s^2 - 6s6p$: $A_{ki}^{\mathrm{exp}} = 1.19(4)$[38,41]				
	$A_{ki}^{\mathrm{S(2)}}$	$\Delta^{\mathrm{S(2)}}$	$A_{ki}^{\mathrm{S(3)}}$	$\Delta^{\mathrm{S(3)}}$	A_{ki}^{LR}	Δ^{LR}	A_{ki}^{MR}	Δ^{MR}
T	1.285	−0.095	1.295	−0.105	1.290	−0.100	1.65	0.46
Q	1.312	−0.122	1.324	−0.134	1.323	−0.133	1.81	0.62
E46	1.305	−0.115	1.319	−0.129	1.312	−0.122	1.87	0.68

diagonalization of the Jacobian matrix and solution of the response equation Eq. (21), are the same for both methods.

2. Quadrupole transition probabilities

Electric quadrupole transitions are difficult to observe due to the very long lifetimes of the atomic D states. For closed-shell atoms only the calcium and barium atomic ^{1}D states are directly connected with the ground ^{1}S states through the E2 transition. For the calcium atom two measurements of the quadrupole transition probabilities were reported[42,43] with error bars that exclude one the other. Thus, accurate theoretical determination can discriminate between the two measurements. For barium the (old) experimental result[44] with relatively large error bars does not agree with any theoretical determination.[45–47] Thus, the present results will shed some light on the accuracy of the measurements and calculations.

For Ca, we computed the $4s^2 - 3s^1 4s^1$ quadrupole transition probability with the XCC3S(3) method in the def2-QZVPP basis set.[30] The experimentally measured energy is 21849.63 cm^{-1}.[48] As the energy in Eqs. (37) and (39) is present in third and fifth power, respectively, small error in the computed energy introduces a large error in the transition probability. Therefore, we present the transition probabilities computed with both theoretical and experimental energy input.

Table III shows the result for the calcium E2 transition that have been published to date. In the second and third columns, T stands for theoretically and E for experimentally obtained value for the line strength and energy, respectively. The present theoretical results are well within the error bars of the 2003 measurement[43] and outside the error bars of the older 1982 measurement.[42] Note that the XCC3 and LRCC3 results are very close to each other despite quite different theoretical approaches that are on the basis of these methods. Thus, we can conclude that the present study supports the experimental result from 2003.[43]

We also computed the quadrupole transition probabilities for the calcium atom with the MRCI method as this approach is based on a different model of the wave function. The results obtained with both the theoretical and experimental excitation energies are outside the error bars of the experiment from 2003. However, the value of the quadrupole transition probability calculated with the experimental excitation energy differs only by 1% from the experimental result of Beverini

TABLE III. Quadrupole transition probabilities for Ca. The XCC3 and LRCC3 computations were performed in the cc-pV5Z basis set.[35,36]

A s^{-1}	S	E	Year	Ref.
87	T	T	1980	49
40 ± 8	E	E	1982	42
81	T	T	1981	50
39.6	T	T	1985	51
60.2	T	T	1983	52
70.5	T	T	1991	53
54.4 ± 4	E	E	2003	43
49.42	T	T	2008	54
66.44	T	T	2014	MRCI
58.56	T	E	2014	MRCI
56.08	T	T	2014	LRCC3
51.11	T	E	2014	LRCC3
56.05	T	T	2014	XCC3S(3)
51.08	T	E	2014	XCC3S(3)

TABLE IV. Quadrupole transition probabilities for barium.

A s^{-1}	S	E	Year	Ref.
3.2	T	T	1974	45
2.98	T	T	1984	46
3.381	T	T	1990	47
3.880	T	E	1990	47
8 ± 3	E	E	1981	44
2.47	T	T	2014	MRCI
1.42	T	E	2014	MRCI
3.49	T	T	2014	LRCC3
2.85	T	E	2014	LRCC3
3.52	T	T	2014	XCC3S(3)
2.87	T	E	2014	XCC3S(3)

et al.[43] which confirms once more that the experimental result from 2003 is more probable.

There are only a few theoretical values[45–47] for the $6s^2 - 6s5d$ transition in Ba, and only one experimental result.[44] The experimental transition energy is equal to 11395.35 cm^{-1}.[48] We have employed the ECP46MDF pseudopotential and the corresponding *spdfg* basis.[37,55] Table IV compiles the published results for the $6s^2 - 6s5d$ Ba quadrupole transition. None of the earlier theoretical results as well as the present XCC3 and LRCC3 results, are within the experimental error. One should notice though that the experimental value error bars show a huge uncertainty. The MRCI transition probabilities, both with the theoretical and experimental excitation energies, are also far from the experimental value. Note also that for the Ba atom the MRCI results are significantly different from both the LRCC3 and XCC3 results.

IV. CONCLUSIONS

We have presented an extension of the coupled cluster method designed for the computation of the ground state properties and transition probabilities. In order to test the performance of our method, we have computed dipole moments for several diatomic molecules. The results were compared to the experimental data. A comprehensive analysis showed that the best compromise between accuracy and computational cost is achieved for the XCC3S(3) variant, i.e., for the third-order approximation to the auxiliary operator.

We have reported the expressions for the transition density matrices computed from the Hermitian formulation of the polarization propagator in the XCC3 approximation. In contrast to the LRCC3 method, the correct time-reversal symmetry of the line strength is guaranteed by the algebraic construction of the polarization propagator in the XCC theory and its approximate variants.

The results of the transition probabilities computed with both the XCC3 and LRCC3 methods are of the same quality, though XCC is computationally less demanding. The results of the transition probabilities computed with both the XCC3 and LRCC3 methods are of the same quality, though XCC is computationally less demanding. The same conclusion holds for the XCC3 and LRCC3 dipole moments.

The computed dipole and quadrupole transition probabilities were compared with the experimental data, and in most cases the results were in a perfect agreement with the experiment. Our results for the quadrupole transition probabilities in the calcium atom with both the XCC3 and LRCC3 methods strongly favor the new measurement of 2003.[43] Our results for the Ba atom are consistent with all the other theoretical data, suggesting that the experimental determination should be reconsidered.

The code for transition moments from the ground state will be incorporated in the KOŁOS: A general purpose *ab initio* program for the electronic structure calculation with Slater orbitals, Slater geminals, and Kołos-Wolniewicz functions.

ACKNOWLEDGMENTS

This work was supported by the Polish Ministry of Science and Higher Education within Grant Nos. NN204 215539 and NN204 182840. R.M. thanks the Foundation for Polish Science for support within the MISTRZ program.

APPENDIX: BIORTHONORMAL, NONREDUNDANT BASIS FOR THE TRIPLY EXCITED MANIFOLD

The general bra and ket vectors in the triply exited manifold are denoted as $\left\langle\begin{smallmatrix}a_1a_2a_3\\ i_1i_2i_3\end{smallmatrix}\right|$ and $\left|\begin{smallmatrix}a_1a_2a_3\\ i_1i_2i_3\end{smallmatrix}\right\rangle$, where the sequence of virtual-occupied electron pair indices is decreasing from left to right. In the case where all indices are different ($a_1 > a_2 > a_3$ and $i_1 > i_2 > i_3$), the biorthonormal set is defined as

$$
\begin{aligned}
v_1 &= \left|\begin{smallmatrix}a_1a_2a_3\\ i_1i_3i_2\end{smallmatrix}\right\rangle, \quad v_2 = \left|\begin{smallmatrix}a_1a_2a_3\\ i_2i_1i_3\end{smallmatrix}\right\rangle, \quad v_3 = \left|\begin{smallmatrix}a_1a_2a_3\\ i_2i_3i_1\end{smallmatrix}\right\rangle,\\
v_4 &= \left|\begin{smallmatrix}a_1a_2a_3\\ i_3i_1i_2\end{smallmatrix}\right\rangle, \quad v_5 = \left|\begin{smallmatrix}a_1a_2a_3\\ i_3i_2i_1\end{smallmatrix}\right\rangle,\\
\widetilde{v}_1 &= \frac{\left\langle\begin{smallmatrix}a_1a_2a_3\\ i_1i_3i_2\end{smallmatrix}\right|}{4} + \frac{\left\langle\begin{smallmatrix}a_1a_2a_3\\ i_2i_1i_3\end{smallmatrix}\right|}{12} + \frac{\left\langle\begin{smallmatrix}a_1a_2a_3\\ i_2i_3i_1\end{smallmatrix}\right|}{6} + \frac{\left\langle\begin{smallmatrix}a_1a_2a_3\\ i_3i_1i_2\end{smallmatrix}\right|}{6} + \frac{\left\langle\begin{smallmatrix}a_1a_2a_3\\ i_3i_2i_1\end{smallmatrix}\right|}{12},\\
\widetilde{v}_2 &= \frac{\left\langle\begin{smallmatrix}a_1a_2a_3\\ i_1i_3i_2\end{smallmatrix}\right|}{12} + \frac{\left\langle\begin{smallmatrix}a_1a_2a_3\\ i_2i_1i_3\end{smallmatrix}\right|}{4} + \frac{\left\langle\begin{smallmatrix}a_1a_2a_3\\ i_2i_3i_1\end{smallmatrix}\right|}{6} + \frac{\left\langle\begin{smallmatrix}a_1a_2a_3\\ i_3i_1i_2\end{smallmatrix}\right|}{6} + \frac{\left\langle\begin{smallmatrix}a_1a_2a_3\\ i_3i_2i_1\end{smallmatrix}\right|}{12},\\
\widetilde{v}_3 &= \frac{\left\langle\begin{smallmatrix}a_1a_2a_3\\ i_1i_3i_2\end{smallmatrix}\right|}{6} + \frac{\left\langle\begin{smallmatrix}a_1a_2a_3\\ i_2i_1i_3\end{smallmatrix}\right|}{6} + \frac{\left\langle\begin{smallmatrix}a_1a_2a_3\\ i_2i_3i_1\end{smallmatrix}\right|}{3} + \frac{\left\langle\begin{smallmatrix}a_1a_2a_3\\ i_3i_1i_2\end{smallmatrix}\right|}{6} + \frac{\left\langle\begin{smallmatrix}a_1a_2a_3\\ i_3i_2i_1\end{smallmatrix}\right|}{6},\\
\widetilde{v}_4 &= \frac{\left\langle\begin{smallmatrix}a_1a_2a_3\\ i_1i_3i_2\end{smallmatrix}\right|}{6} + \frac{\left\langle\begin{smallmatrix}a_1a_2a_3\\ i_2i_1i_3\end{smallmatrix}\right|}{6} + \frac{\left\langle\begin{smallmatrix}a_1a_2a_3\\ i_2i_3i_1\end{smallmatrix}\right|}{6} + \frac{\left\langle\begin{smallmatrix}a_1a_2a_3\\ i_3i_1i_2\end{smallmatrix}\right|}{3} + \frac{\left\langle\begin{smallmatrix}a_1a_2a_3\\ i_3i_2i_1\end{smallmatrix}\right|}{6},\\
\widetilde{v}_5 &= \frac{\left\langle\begin{smallmatrix}a_1a_2a_3\\ i_1i_3i_2\end{smallmatrix}\right|}{12} + \frac{\left\langle\begin{smallmatrix}a_1a_2a_3\\ i_2i_1i_3\end{smallmatrix}\right|}{12} + \frac{\left\langle\begin{smallmatrix}a_1a_2a_3\\ i_2i_3i_1\end{smallmatrix}\right|}{6} + \frac{\left\langle\begin{smallmatrix}a_1a_2a_3\\ i_3i_1i_2\end{smallmatrix}\right|}{6} + \frac{\left\langle\begin{smallmatrix}a_1a_2a_3\\ i_3i_2i_1\end{smallmatrix}\right|}{4}.
\end{aligned}
\tag{A1}
$$

The vectors in Eq. (A1) satisfy $\langle \widetilde{v}_k | v_l \rangle = \delta_{kl}$. Note that in this case there are only five linearly independent bra/ket vectors. If some of the indices are equal, there are three cases to consider:

1. A single equality among the occupied indices (either $i_1 = i_3$ or $i_2 = i_3$),

$$
\left\langle\begin{smallmatrix}\widetilde{a_1a_2}a_3\\ i_1i_2i_3\end{smallmatrix}\right| = \frac{1}{3}\left\langle\begin{smallmatrix}a_1a_2a_3\\ i_1i_2i_3\end{smallmatrix}\right| + \frac{1}{6}\left\langle\begin{smallmatrix}a_1a_2a_3\\ i_2i_1i_3\end{smallmatrix}\right|. \tag{A2}
$$

2. A single equality among the virtual indices (and an additional constraint on the occupied indices: $\neg(i_1 > i_2 > i_3)$),

$$\left\langle \begin{smallmatrix} \widetilde{a_1 a_2 a_3} \\ i_1 i_2 i_3 \end{smallmatrix} \right| = \frac{1}{3} \left\langle \begin{smallmatrix} a_1 a_2 a_3 \\ i_1 i_2 i_3 \end{smallmatrix} \right| + \frac{1}{6} \left\langle \begin{smallmatrix} a_1 a_2 a_3 \\ i_3 i_2 i_1 \end{smallmatrix} \right|. \tag{A3}$$

3. A single equality among the occupied indices and among the virtual ones (the equalities are indicated by repeating labels; additionally, the strict inequalities $a_1 > a_2$ and $i_1 > i_2$ hold),

$$\begin{aligned} \left\langle \begin{smallmatrix} \widetilde{a_1 a_1 a_2} \\ i_1 i_2 i_1 \end{smallmatrix} \right| &= \frac{1}{2} \left\langle \begin{smallmatrix} a_1 a_1 a_2 \\ i_1 i_2 i_1 \end{smallmatrix} \right|, \quad \left\langle \begin{smallmatrix} \widetilde{a_1 a_1 a_2} \\ i_1 i_2 i_2 \end{smallmatrix} \right| = \frac{1}{2} \left\langle \begin{smallmatrix} a_1 a_1 a_2 \\ i_1 i_2 i_2 \end{smallmatrix} \right|, \\ \left\langle \begin{smallmatrix} \widetilde{a_1 a_2 a_2} \\ i_2 i_1 i_2 \end{smallmatrix} \right| &= \frac{1}{2} \left\langle \begin{smallmatrix} a_1 a_2 a_2 \\ i_2 i_1 i_2 \end{smallmatrix} \right|, \quad \left\langle \begin{smallmatrix} \widetilde{a_1 a_2 a_2} \\ i_1 i_1 i_2 \end{smallmatrix} \right| = \frac{1}{2} \left\langle \begin{smallmatrix} a_1 a_2 a_2 \\ i_1 i_1 i_2 \end{smallmatrix} \right|. \end{aligned} \tag{A4}$$

All vectors that do not fit into the above defined templates are deemed linearly dependent and discarded from the basis. Note that this is one of the possible choices of the biorthonormal nonredundant basis.

[1] F. Coester, Nucl. Phys. **7**, 421 (1958).
[2] J. Čížek, Adv. Chem. Phys. **14**, 35 (1969).
[3] J. Paldus and J. Čížek, Adv. Quantum Chem. **9**, 105 (1975).
[4] R. J. Bartlett, J. Phys. Chem. **93**, 1697 (1989).
[5] T. D. Crawford and H. F. Schaefer, Rev. Comput. Chem. **14**, 33 (2000).
[6] R. Bartlett in *Modern Electronic Structure Theory, Part I*, edited by D. Yarkony (World Scientific, Singapore, 1995), p. 1047.
[7] R. J. Bartlett and M. Musiał, Rev. Mod. Phys. **79**, 291 (2007).
[8] P. Čárskỳ, J. Paldus, and J. Pittner, *Recent Progress in Coupled Cluster Methods: Theory and Applications* (Springer, New York, 2010), p. 455.
[9] D. I. Lyakh, M. Musiał, V. F. Lotrich, and R. J. Bartlett, Chem. Rev. **112**, 182 (2012).
[10] O. Christiansen, H. Koch, and P. Jørgensen, Chem. Phys. Lett. **243**, 409 (1995).
[11] H. Koch, O. Christiansen, P. Jørgensen, A. M. Sanchez De Merás, and T. Helgaker, J. Chem. Phys. **106**, 1808 (1997).
[12] A. Halkier, H. Koch, O. Christiansen, P. Jørgensen, and T. Helgaker, J. Chem. Phys. **107**, 849 (1997).
[13] K. Hald and P. Jørgensen, Phys. Chem. Chem. Phys. **4**, 5221 (2002).
[14] B. Jeziorski and R. Moszynski, Int. J. Quantum Chem. **48**, 161 (1993).
[15] R. Moszynski and A. Ratkiewicz, J. Chem. Phys. **99**, 8856 (1993).
[16] R. Moszynski, B. Jeziorski, S. Rybak, K. Szalewicz, and H. L. Williams, J. Chem. Phys. **100**, 5080 (1994).
[17] T. Korona and B. Jeziorski, J. Chem. Phys. **125**, 184109 (2006).
[18] T. Korona, M. Przybytek, and B. Jeziorski, Mol. Phys. **104**, 2303 (2006).
[19] H. Koch and P. Jørgensen, J. Chem. Phys. **93**, 3333 (1990).
[20] H. Koch, R. Kobayashi, A. S. de Meras, and P. Jørgensen, J. Chem. Phys. **100**, 4393 (1994).
[21] T. B. Pedersen and H. Koch, J. Chem. Phys. **106**, 8059 (1997).
[22] R. Moszynski, P. S. Żuchowski, and B. Jeziorski, Coll. Czech. Chem. Commun. **70**, 1109 (2005).
[23] T. Korona and B. Jeziorski, J. Chem. Phys. **128**, 144107 (2008).
[24] J. Paldus and B. Jeziorski, Theor. Chim. Acta **73**, 81 (1988).
[25] H. Sekino and R. J. Bartlett, Int. J. Quantum Chem. **26**, 255 (1984).
[26] T. Helgaker, P. Jorgensen, and J. Olsen, *Molecular Electronic-Structure Theory* (Wiley, New York, 2013).
[27] J. Oddershede, Adv. Chem. Phys. **69**, 201 (1987).
[28] F. J. Lovas, E. Tiemann, J. S. Coursey, S. A. Kotochigova, J. Chang, K. Olsen, and R. A. Dragoset, *NIST Diatomic Spectral Database* (NIST, Baltimore, 2011).
[29] D. Liede and W. M. Haynes, *CRC Handbook of Chemistry and Physics* (CRC, Boca Raton, FL, 2010).
[30] F. Weigend and R. Ahlrichs, Phys. Chem. Chem. Phys. **7**, 3297 (2005).
[31] G. W. Drake, *Springer Handbook of Atomic, Molecular, and Optical Physics* (Springer, New York, 2006).
[32] G. H. Shortley, Phys. Rev. **57**, 225 (1940).
[33] H.-J. Werner, P. J. Knowles, G. Knizia, F. R. Manby, M. Schütz *et al.*, MOLPRO, version 2012.1, a package of *ab initio* programs, 2012, see http://www.molpro.net.
[34] O. Christiansen, A. Halkier, H. Koch, P. Jørgensen, and T. Helgaker, J. Chem. Phys. **108**, 2801 (1998).
[35] K. A. Peterson and T. H. Dunning, Jr., J. Chem. Phys. **117**, 10548 (2002).
[36] J. Koput and K. A. Peterson, J. Phys. Chem. A **106**, 9595 (2002).
[37] I. S. Lim, H. Stoll, and P. Schwerdtfeger, J. Chem. Phys. **124**, 034107 (2006).
[38] J. E. Sansonetti and W. C. Martin, J. Phys. Chem. Ref. Data **34**, 1559 (2005).
[39] D. C. Morton, Astrophys. J. Suppl. Ser. **149**, 205 (2003).
[40] J. Sansonetti and G. Nave, J. Phys. Chem. Ref. Data **39**, 033103 (2010).
[41] J. Klose, J. R. Fuhr, and W. Wiese, J. Phys. Chem. Ref. Data **31**, 217 (2002).
[42] K. Fukuda and K. Ueda, J. Phys. Chem. **86**, 676 (1982).
[43] N. Beverini, E. Maccioni, F. Sorrentino, V. Baraulia, and M. Coca, Eur. Phys. J. D **23**, 223 (2003).
[44] I. Klimovskii, P. Minaev, and A. Morozov, Opt. Spectrosc. **50**, 464 (1981).
[45] P. McCavert and E. Trefftz, J. Phys. B **7**, 1270 (1974).
[46] C. Bauschlicher, Jr., S. Langhoff, R. Jaffe, and H. Partridge, J. Phys. B **17**, L427 (1984).
[47] J. Migdalek and W. Baylis, Phys. Rev. A **42**, 6897 (1990).
[48] S. Lias, J. Bartmess, J. Liebman, J. Holmes, R. Levin, and W. Mallard, in *NIST Chemistry WebBook, NIST Standard Reference Database*, edited by P. Linstrom and W. Mallard (NIST, Baltimore, 2013).
[49] L. Pasternack, D. Yarkony, P. Dagdigian, and D. Silver, J. Phys. B **13**, 2231 (1980).
[50] R. Diffenderfer, P. Dagdigian, and D. Yarkony, J. Phys. B **14**, 21 (1981).
[51] C. W. Bauschlicher, Jr., S. R. Langhoff, and H. Partridge, J. Phys. B **18**, 1523 (1985).
[52] D. Beck and C. A. Nicolaides, J. Phys. B **16**, L627 (1983).
[53] N. Vaeck, M. Godefroid, and J. Hansen, J. Phys. B **24**, 361 (1991).
[54] J. Mitroy and J.-Y. Zhang, J. Chem. Phys. **128**, 134305 (2008).
[55] M. Krych, W. Skomorowski, F. Pawłowski, R. Moszynski, and Z. Idziaszek, Phys. Rev. A **83**, 032723 (2011).

Appendix B Paper II: J. Chem. Phys. 146, 034108 (2017)

THE JOURNAL OF CHEMICAL PHYSICS **146**, 034108 (2017)

Transition moments between excited electronic states from the Hermitian formulation of the coupled cluster quadratic response function

Aleksandra M. Tucholska,[a] Michał Lesiuk, and Robert Moszynski[b]
Faculty of Chemistry, University of Warsaw, Pasteura 1, 02-093 Warsaw, Poland

(Received 30 September 2016; accepted 30 December 2016; published online 20 January 2017)

We introduce a new method for the computation of the transition moments between the excited electronic states based on the expectation value formalism of the coupled cluster theory [B. Jeziorski and R. Moszynski, Int. J. Quantum Chem. **48**, 161 (1993)]. The working expressions of the new method solely employ the coupled cluster operator T and an auxiliary operator S that is expressed as a finite commutator expansion in terms of T and $T^\dagger$. In the approximation adopted in the present paper, the cluster expansion is limited to single, double, and linear triple excitations. The computed dipole transition probabilities for the singlet-singlet and triplet-triplet transitions in alkali earth atoms agree well with the available theoretical and experimental data. In contrast to the existing coupled cluster response theory, the matrix elements obtained by using our approach satisfy the Hermitian symmetry even if the excitations in the cluster operator are truncated, but the operator S is exact. The Hermitian symmetry is slightly broken if the commutator series for the operator S are truncated. As a part of the numerical evidence for the new method, we report calculations of the transition moments between the excited triplet states which have not yet been reported in the literature within the coupled cluster theory. Slater-type basis sets constructed according to the correlation-consistency principle are used in our calculations. *Published by AIP Publishing.* [http://dx.doi.org/10.1063/1.4973978]

I. INTRODUCTION

Response of a system to external perturbations is described by linear, quadratic, and higher-order response functions.[1–3] Many physical observables such as transition probabilities, dynamic polarizabilities, hyperpolarizabilities, and lifetimes are defined through the response functions or can be derived from the response functions. Until recently, properties of the excited electronic states were not easily available in high-resolution experiments, but with the advances of new spectroscopic techniques in the hot pipe[4–8] and ultracold experiments,[9–13] more and more accurate experimental data become available and possibly need theoretical interpretation. Theoretical information about the transition moments between the excited states is also necessary to propose new routes to obtain molecules in the ground rovibrational state (see, e.g., Ref. 14). Last but not least, the excited state properties define the asymptotics of the excited state interaction potentials[15] and play an unexpectedly important role in the dynamics of nuclear motions in the presence of external fields.[16]

The properties of the excited states, e.g., polarizabilities, transition strengths, and lifetimes, can be obtained from the limited multiconfiguration interaction theory, but this approach inherently suffers from the size inconsistency problem. Applying the size consistent coupled cluster (CC) formalism to the response function opens up a possibility of an accurate description of molecular properties with an affordable computational cost for medium size molecules. In the 1990s, Jørgensen and collaborators formulated the CC response theory,[17,18] based on the coupled cluster generalization of the Hellmann-Feynman theorem where the average value is replaced by a transition expectation value with respect to the coupled cluster state. However, in this theory, the necessary Hermiticity condition required from the transition moments is not satisfied, and in some cases this leads to unphysical numerical results.

In the present study, we focus on the molecular properties that can be obtained from the quadratic response function, $\langle\langle X; Y, Z\rangle\rangle_{\omega_Y,\omega_Z}$. The latter describes the response of an observable X to perturbations Y and Z oscillating with the frequencies ω_Y and ω_Z, respectively. In the exact case, the transition moment $\mathcal{T}^X_{LM}$ between the excited states L and M can be computed from the double residue of the quadratic response function

$$\lim_{\omega_Y\to-\omega_L}(\omega_L+\omega_Y)\lim_{\omega_Z\to\omega_M}(\omega_M-\omega_Z)\langle\langle X; Y, Z\rangle\rangle_{\omega_Y,\omega_Z} = \mathcal{T}^Y_{0L}(\mathcal{T}^X_{LM}-\delta_{LM}\langle\Psi_0|X|\Psi_0\rangle)\mathcal{T}^Z_{M0}, \tag{1}$$

where $\mathcal{T}^Y_{0L}$ and $\mathcal{T}^Z_{M0}$ are transition moments between the ground and excited sates, and ω_K is the excitation energy of the state K. Note that the Kronecker delta term δ_{LM} appearing in the above expression is responsible for the cancellation of the disconnected terms in the quadratic response function as in the standard third-order perturbation theory. When $L \neq M$, and this is always the case, this term simply vanishes. For different L and M states, the transition strength $\mathcal{S}_{LM}$ is defined as

$$\mathcal{S}_{LM} = |\mathcal{T}_{LM}|^2. \tag{2}$$

The transition moments are necessary to compute the transition probabilities[19]

[a]Electronic mail: tuchol@tiger.chem.uw.edu.pl
[b]Also at Kavli Institute for Theoretical Physics, University of California, Santa Barbara, CA 93106-4030, USA.

$$A_{LM} = \frac{1}{3}\frac{16\pi^3}{3h\epsilon_0\lambda^3}S_{LM}, \tag{3}$$

where ϵ_0 is the vacuum permittivity, λ is the wavelength, h is the Planck constant, and S_{LM} is the transition strength. The lifetime[19] of a state L is defined as

$$\tau_L = \frac{1}{\sum_K A_{LK}}. \tag{4}$$

There exist two coupled cluster approaches for the computation of the transition moments between the ground and excited states, the linear response coupled cluster theory (LRCC) of Koch *et al.*[17,18,20,21] and the coupled cluster expectation value formulation of the linear response function (XCC) of Tucholska *et al.*[22] As already stated above, for the transition moments between the excited states, the only available approach is based on the quadratic response coupled cluster (QRCC) theory of Koch *et al.*[17,18,20,21] In the present work, we generalize the approach of Refs. 22 and 23 to the calculation of transition properties between the excited states. The transition moments, $\mathcal{T}^X_{LM}$, where L and M denote the singlet or triplet excited states, are extracted from the response function to compute lifetimes and transition probabilities.

In the exact theory, the transition moments are Hermitian

$$\mathcal{T}^X_{LM} = (\mathcal{T}^X_{ML})^\star, \tag{5}$$

but this relation is violated by the existing QRCC method, in some cases to a large degree, when the cluster operator is truncated at some excitation level. In extreme cases, this leads to non-physical, negative transition strengths which will be discussed in detail in the remaining part of this work. Recently, a new approach to the problem has been proposed, where molecular properties are computed as derivatives of the eigenvalues of a Hermitian eigenproblem.[24] This approach should apparently remove the inaccuracies and inconsistencies of the QRCC theory. However, numerical results for this method are not yet available and we cannot assess its accuracy. Therefore, we will restrict our comparisons to the original QRCC theory.

This paper is organized as follows. In Sections II A and II B, we derive the formula for the XCC transition moments between the excited states. In Section II C, we present the truncations and approximations used in this work. In Section III, we report numerical results for the transition moments and lifetimes of the Mg and Sr atoms, and for the Mg_2 molecule. First, we present the comparison of our results with the QRCC method (Subsection III B), next, we compare our results with the available theoretical and experimental data (Subsection III C), and finally, we investigate the Hermiticity violation in the XCC and QRCC methods (Subsection III D). In Section IV, we conclude our paper.

II. THEORY

A. Basic definitions

In the CC theory, the ground state wave function Ψ_0 is represented by the exponential ansatz $\Psi_0 = e^T\Phi$, where the cluster operator T is given by the sum of n-tuple excitation operators T_n,

$$T = \sum_{n=1}^{N} T_n, \tag{6}$$

$$T_n = \frac{1}{n!}\sum_{\mu_n}^{N} t_{\mu_n}\mu_n, \tag{7}$$

where $\mu_n = E_{ai}E_{bj}\ldots E_{fm}$ is the product of spin-free excitation operators. Φ is the Slater determinant built from the occupied orbitals, and N is the number of electrons. Throughout the work, the indices $a, b, c \ldots$ and $i, j, k \ldots$ denote the virtual and occupied orbitals, respectively, and $p, q, r \ldots$ are used in summations over all orbitals. In practical applications, the operator T is truncated to make the CC calculation computationally feasible.

The expectation value of an observable X in the XCC theory is given by the explicitly connected, size-consistent expression introduced by Jeziorski and Moszynski[25]

$$\frac{\langle e^T\Phi|X|e^T\Phi\rangle}{\langle e^T\Phi|e^T\Phi\rangle} = \langle\Phi|e^{S^\dagger}e^{-T}Xe^{T}e^{-S^\dagger}\Phi\rangle. \tag{8}$$

See also the seminal work of Čížek[26,27] and other formulations of the CC expectation value problem.[28–35] The auxiliary operator S is defined as

$$|e^S\Phi\rangle = \frac{|e^Te^{T^\dagger}\Phi\rangle}{\langle e^T\Phi|e^T\Phi\rangle}, \qquad S = S_1 + S_2 + \cdots + S_N, \tag{9}$$

and S_n is expressed as[25]

$$\begin{aligned} S_n = T_n &- \frac{1}{n}\hat{\mathcal{P}}_n\left(\sum_{k=1}\frac{1}{k!}[\widetilde{T}^\dagger, T]_k\right) \\ &- \frac{1}{n}\hat{\mathcal{P}}_n\left(\sum_{k=1}\sum_{m=0}\frac{1}{k!}\frac{1}{m!}[[\widetilde{S}, T^\dagger]_k, T]_m\right), \end{aligned} \tag{10}$$

where

$$\widetilde{T} = \sum_{n=1}^{N} nT_n, \qquad \widetilde{S} = \sum_{n=1}^{N} nS_n, \tag{11}$$

and $[A, B]_k$ is a k-tuply nested commutator. The superoperator $\hat{\mathcal{P}}_n(X)$ yields the n-tuple excitation part of X,

$$\hat{\mathcal{P}}_n(X) = \frac{1}{n!}\sum_{\mu_n}\langle\widetilde{\mu_n}|X\rangle\,\mu_n, \tag{12}$$

where for simplicity we introduce the following notation $\langle A|B\rangle = \langle A\Phi|B\Phi\rangle$. The symbol $\widetilde{\mu_n}$ is used to indicate the use of the biorthonormal basis $\langle\widetilde{\mu_n}|\nu_m\rangle = \delta_{\mu_n\nu_m}$. For the single and double excitation manifolds, we use the basis proposed by Helgaker, Jørgensen, and Olsen,[36] and for the triply excited manifold, we employ the basis proposed by Tucholska *et al.*[22]

The formula for S is a finite expansion, though it contains terms of high order in the fluctuation potential.[25] To find the exact S operator, one requires an iterative procedure. However, S can efficiently be approximated while retaining the size-consistency. In our previous work,[22] we presented a hierarchy of approximations and assessed their accuracy. Let $S_n(m)$ denote the n-electron part of S, where all available contributions up to the order m in the fluctuation potential are accounted for. In the computations based on the CC3 model (single, double, and linear triple excitations), we employ

$$\begin{aligned} S_1(3) &= T_1 + \hat{\mathcal{P}}_1\left([T_1^\dagger, T_2]\right) + \hat{\mathcal{P}}_1\left([T_2^\dagger, T_3]\right), \\ S_2(3) &= T_2 + \frac{1}{2}\hat{\mathcal{P}}_2\left([[T_2^\dagger, T_2], T_2]\right), \\ S_3(2) &= T_3, \end{aligned} \tag{13}$$

where the CC3 equations for T_1, T_2, and T_3 are given by Koch *et al.*[37] It should be noted that we take $S_3 = T_3$ from the CC3 theory and no additional terms from Eq. (10); hence we only include terms of the second-order in S_3. In the instances where the underlying model of the wave function is CCSD (coupled cluster limited to single and double excitations), we employ $S = S_1(3) + S_2(3)$ neglecting the terms including T_3.

The exact quadratic response function can be written as the sum over states

$$\langle\langle X;Y,Z\rangle\rangle_{\omega_Y,\omega_Z} = P_{XYZ}\sum_{\substack{K=1\\N=1}} \frac{\langle\Psi_0|Y|K\rangle\,\langle K\,|X-\langle\Psi_0|X|\Psi_0\rangle\,|N\rangle\,\langle N|Z|\Psi_0\rangle}{(\omega_K+\omega_Y)(\omega_N-\omega_Z)}, \tag{14}$$

where K and N run over all possible excitations, and $|\Psi_0\rangle$ is the ground state. The action of the permutation operator P_{XYZ} yields six distinct contributions to $\langle\langle X;Y,Z\rangle\rangle_{\omega_Y,\omega_Z}$ with the indices X, Y, and Z being interchanged.

B. XCC transition moments

The exact transition moment between the excited states L and M ($L \neq M$) can be identified from the double residue of the quadratic response function[21]

$$\begin{aligned}\lim_{\omega_Y\to-\omega_L}(\omega_L+\omega_Y)\lim_{\omega_z\to\omega_M}(\omega_M-\omega_Z)\langle\langle X;Y,Z\rangle\rangle_{\omega_Y,\omega_Z} &= \langle\Psi_0|Y|L\rangle\,\langle L|X-\langle\Psi_0|X|\Psi_0\rangle\,|M\rangle\,\langle M|Z|\Psi_0\rangle\\ &= \mathcal{T}^Y_{0L}\mathcal{T}^X_{LM}\mathcal{T}^Z_{M0}.\end{aligned} \tag{15}$$

To obtain $\mathcal{T}^X_{LM}$ in the XCC theory, we express $\langle\langle X;Y,Z\rangle\rangle_{\omega_Y,\omega_Z}$ by using the XCC formalism and take the limit of Eq. (15).

Let us introduce the coupled cluster parametrization of the quadratic response function. The first order wave function $\Psi^{(1)}(\omega)$ is expressible through the resolvent $\mathcal{R}_\omega$,

$$\Psi^{(1)}(\omega_V) = \mathcal{R}_\omega V|\Psi_0\rangle, \qquad V = Y \text{ or } Z, \tag{16}$$

$$\mathcal{R}_\omega = \sum_{N=1}\frac{|N\rangle\langle N|}{\omega_N+\omega}. \tag{17}$$

Using these definitions, the expression for the quadratic response function, Eq. (14), can be reformulated as follows:

$$\langle\langle X;Y,Z\rangle\rangle_{\omega_Y,\omega_Z} = P_{XYZ}\langle\Psi^{(1)}(\omega_Y)|X_0|\Psi^{(1)}(-\omega_Z)\rangle, \tag{18}$$

where $X_0 = X - \langle X\rangle$ and $\langle X\rangle = \langle\Psi_0|X|\Psi_0\rangle$. The normalized ground state wave function in the coupled cluster parametrization is given by

$$|\Psi_0\rangle = \frac{|e^T\Phi\rangle}{\langle e^T\Phi|e^T\Phi\rangle^{\frac{1}{2}}}. \tag{19}$$

The first order wave function $\Psi^{(1)}(\omega)$ in the coupled cluster parametrization is given by the operator $\Omega(\omega) = \Omega_1(\omega) + \Omega_2(\omega) + \cdots$, of the same structure as the operator T, acting on Ψ_0,[23]

$$|\Psi^{(1)}(\omega)\rangle = (\Omega_0+\Omega(\omega))\frac{|e^T\Phi\rangle}{\langle e^T\Phi|e^T\Phi\rangle^{\frac{1}{2}}},\ \Omega_0 = -\langle\Psi_0|\Omega(\omega)\Psi_0\rangle, \tag{20}$$

where Ω_0 is a number to ensure the orthogonality of $\Psi^{(1)}$ to Ψ_0. The excitation operator $\Omega(\omega)$ can be found from the following equation:[23,38]

$$\left\langle\mu|[e^{-T}He^T,\Omega(\omega)] + \omega\Omega(\omega) + e^{-T}Xe^T\right\rangle = 0. \tag{21}$$

We express the excitation operator $\Omega^Y(\omega)$ in the basis of the right eigenvectors r_N of the CC Jacobian matrix $A_{\mu_n\nu_m} = \langle\widetilde{\mu}_n|[e^{-T}He^T,\nu_m]\rangle$, using the transformation from the molecular orbital basis μ_n to the Jacobian basis r_N,

$$\mu_n = \sum_N \mathcal{L}^\star_{\mu_n N} r_N, \tag{22}$$

$$\Omega^Y(\omega) = \sum_N\sum_{n=1}\sum_{\mu_n}{}' \mathcal{L}^\star_{\mu_n N} O^Y_{\mu_n}(\omega) r_N = \sum_N O^Y_N(\omega) r_N, \tag{23}$$

where $\sum'_{\mu_n}$ stands for restricted summation over non-redundant double excitations $ai \geq bj$ and triple excitations $ai \geq bj \geq ck$. We obtain the amplitudes $O^Y_N(\omega)$ in terms of the right eigenvector r_N, by projecting Eq. (21) onto the left eigenvector l_N of the Jacobian

$$O^Y_N(\omega_Y) = -\frac{\langle l_N|e^{-T}Ye^T\rangle}{\omega_N+\omega_Y}. \tag{24}$$

By inserting Eq. (20) into Eq. (18), we arrive at

$$\begin{aligned}\langle\langle X;Y,Z\rangle\rangle^{XCC}_{\omega_Y,\omega_Z} &= P_{XYZ}\Bigg(\langle(\Omega^Y_0+\Omega^Y(\omega_Y))\Psi_0|X_0|(\Omega^Z_0+\Omega^Z(-\omega_Z))\Psi_0\rangle\\ &= \frac{\langle\Omega^Y(\omega_Y)e^T|e^T\rangle}{\langle e^T|e^T\rangle}\frac{\langle e^T|\Omega^Z(-\omega_Z)e^T\rangle}{\langle e^T|e^T\rangle}\frac{\langle e^T|X_0|e^T\rangle}{\langle e^T|e^T\rangle}\\ &\quad-\frac{\langle\Omega^Y(\omega_Y)e^T|e^T\rangle}{\langle e^T|e^T\rangle}\frac{\langle e^T|X_0|\Omega^Z(-\omega_Z)e^T\rangle}{\langle e^T|e^T\rangle}\\ &\quad-\frac{\langle e^T|\Omega^Z(-\omega_Z)e^T\rangle}{\langle e^T|e^T\rangle}\frac{\langle\Omega^Y(\omega_Y)e^T|X_0|e^T\rangle}{\langle e^T|e^T\rangle}\\ &\quad+\frac{\langle\Omega^Y(\omega_Y)e^T|X_0|\Omega^Z(-\omega_Z)e^T\rangle}{\langle e^T|e^T\rangle}\Bigg),\end{aligned} \tag{25}$$

where $\Omega^V(\omega_V)$ is the solution of Eq. (21) with $X = V$ and $\omega = \omega_V$. Further algebraic manipulations are carried out by using the following identities:

$$[e^T,\Omega] = 0, \tag{26}$$

$$e^{-S^\dagger}\Phi = \Phi, \tag{27}$$

$$X\Phi = \langle X\rangle\Phi + \hat{\mathcal{P}}(X)\Phi, \tag{28}$$

$$\frac{\langle e^T|X|e^T\rangle}{\langle e^T|e^T\rangle} = \langle e^{S^\dagger}e^{-T}Xe^Te^{-S^\dagger}\rangle, \tag{29}$$

so that the final expression for $\langle\langle X;Y,Z\rangle\rangle^{XCC}_{\omega_Y,\omega_Z}$ reads

$$\langle\langle X;Y,Z\rangle\rangle^{XCC}_{\omega_Y,\omega_Z} = P_{XYZ}\Big(\langle(\hat{\mathcal{P}}(e^{-S}e^{T^\dagger}\Omega^Y(\omega_Y)e^{-T^\dagger}e^S)|e^{S^\dagger}e^{-T}(X_0)e^Te^{-S^\dagger}\hat{\mathcal{P}}(e^{-S^\dagger}\Omega^Z(-\omega_Z)e^{S^\dagger})\rangle\Big). \tag{30}$$

Therefore, by using the eigenvectors and eigenvalues of the CC Jacobian, one can express $\langle\langle X;Y,Z\rangle\rangle^{XCC}_{\omega_Y,\omega_Z}$ as follows:

$$\begin{aligned}\langle\langle X;Y,Z\rangle\rangle^{XCC}_{\omega_Y,\omega_Z} &= P_{XYZ}\sum_{\substack{K=1\\N=1}}\left(O^Y_K(\omega_Y)\right)^\star O^Z_N(-\omega_Z)\langle\kappa(r_K)|e^{S^\dagger}e^{-T}X_0e^{T}e^{-S^\dagger}|\eta(r_N)\rangle\\ &= \sum_{\substack{K=1\\N=1}}\frac{\langle e^{-T}Ye^{T}|l_K\rangle}{\omega_K+\omega_Y}\frac{\langle l_N|e^{-T}Ze^{T}\rangle}{\omega_Z-\omega_N}\langle\kappa(r_K)|e^{S^\dagger}e^{-T}X_0e^{T}e^{-S^\dagger}|\eta(r_N)\rangle,\end{aligned}\tag{31}$$

where

$$\kappa(r_N)=\hat{\mathcal{P}}\left(e^{-S}e^{T^\dagger}r_Ne^{-T^\dagger}e^{S}\right),\quad \eta(r_N)=\hat{\mathcal{P}}\left(e^{S^\dagger}r_Ne^{-S^\dagger}\right).\tag{32}$$

Finally, the double residue from the quadratic response function is given by

$$\begin{aligned}&\mathcal{T}^Y_{0L}\mathcal{T}^X_{LM}\mathcal{T}^Z_{M0}\\ &\quad=\lim_{\omega_Y\to-\omega_L}(\omega_L+\omega_Y)\lim_{\omega_Z\to\omega_M}(\omega_M-\omega_Z)\langle\langle X;Y,Z\rangle\rangle_{\omega_Y,\omega_Z}\\ &\quad=\langle e^{-T}Ye^{T}|l_L\rangle\langle\kappa(r_L)|e^{S^\dagger}e^{-T}X_0e^{T}e^{-S^\dagger}|\eta(r_M)\rangle\langle l_M|e^{-T}Ze^{T}\rangle.\end{aligned}\tag{33}$$

We derived our formula for the residue of the quadratic response function, so we have to consider the whole right hand side of Eq. (33). Thus, we cannot identify the middle factor on the right hand side of Eq. (33) as $\mathcal{T}^X_{LM}$. To extract $\mathcal{T}^X_{LM}$ from Eq. (33), we divide both sides by $\left|\mathcal{T}^Y_{0L}\mathcal{T}^Z_{M0}\right|=\sqrt{|\mathcal{T}^Y_{0L}|^2|\mathcal{T}^Z_{M0}|^2}$, where

$$|\mathcal{T}^Y_{0L}|^2=\langle e^{-T}Ye^{T}|l_L\rangle\langle\kappa(r_L)|\eta(r_L)\rangle\langle l_L|e^{-T}Ye^{T}\rangle.\tag{34}$$

Eq. (34) is derived by taking the double residue of $\langle\Psi^{(1)}(\omega_Y)|X|\Psi^{(1)}(-\omega_Z)\rangle$ with $L=M$ and $Y=Z$. For the exact wave function $|\mathcal{T}^Y_{0L}|^2=\langle 0|Y|L\rangle\langle L|Y|0\rangle$. This quantity is then used to extract $\mathcal{T}^X_{LM}$ from the double residue of the quadratic response function

$$\mathcal{T}^X_{LM}=\pm\frac{\langle 0|Y|L\rangle\langle L|X_0|M\rangle\langle M|Z|0\rangle}{\sqrt{\langle 0|Y|L\rangle\langle L|L\rangle\langle L|Y|0\rangle\langle 0|Z|M\rangle\langle M|M\rangle\langle M|Z|0\rangle}}=\pm\frac{\lim_{\omega_Y\to-\omega_L}(\omega_L+\omega_Y)\lim_{\omega_z\to\omega_M}(\omega_M-\omega_Z)\langle\langle X;Y,Z\rangle\rangle_{\omega_Y,\omega_Z}}{\sqrt{|\mathcal{T}^Y_{0L}|^2|\mathcal{T}^Z_{M0}|^2}}.\tag{35}$$

The $\pm$ sign results from taking the square root of $|\mathcal{T}^Y_{0L}|^2$. This fact is of no concern as both $\mathcal{T}^X_{LM}$ and $\mathcal{T}^X_{ML}$ have identical denominators, and we compute the transition strengths which are products $\mathcal{T}^X_{LM}\mathcal{T}^X_{ML}$.

The final expression for T^X_{LM} in the XCC theory is given by

$$\begin{aligned}\mathcal{T}^X_{LM}&=\pm\frac{\xi^Y_L\langle\kappa(r_L)|e^{S^\dagger}e^{-T}X_0e^{T}e^{-S^\dagger}\eta(r_M)\rangle\xi^Z_M}{\sqrt{\xi^Y_L\langle\kappa(r_L)|\eta(r_L)\rangle(\xi^Y_L)^\star\xi^Z_M\langle\kappa(r_M)|\eta(r_M)\rangle(\xi^Z_M)^\star}}\\ &=\pm\frac{\langle\kappa(r_L)|e^{S^\dagger}e^{-T}X_0e^{T}e^{-S^\dagger}\eta(r_M)\rangle}{\sqrt{\langle\kappa(r_L)|\eta(r_L)\rangle\langle\kappa(r_M)|\eta(r_M)\rangle}},\end{aligned}\tag{36}$$

where

$$\xi^Z_M=\langle l_M|e^{-T}Ze^{T}\rangle.\tag{37}$$

Note that our formula for $\mathcal{T}^X_{LM}$ is expressible solely in terms of commutators. Therefore, it is automatically size-consistent no matter the level of truncation of the T and S operators.

Alternatively, one can use the identities (26)–(29) to obtain

$$\tilde{\mathcal{T}}^X_{LM}=\pm\frac{\langle\eta(r_L)|e^{-S}e^{T^\dagger}X_0e^{-T^\dagger}e^{S}\kappa(r_M)\rangle}{\sqrt{\langle\kappa(r_L)|\eta(r_L)\rangle\langle\kappa(r_M)|\eta(r_M)\rangle}}.\tag{38}$$

It is easy to note that as long as

$$\mathcal{T}^X_{LM}=\tilde{\mathcal{T}}^X_{LM},\tag{39}$$

the Hermiticity relation $\mathcal{T}^X_{LM}=(\mathcal{T}^X_{ML})^\star$ is satisfied. Eq. (39) is true for any truncated T operator and the exact S operator. This follows from the fact that in the derivation of the expression for $\mathcal{T}^X_{LM}$, we used the definition from Eq. (9) which is valid only for the exact S operator.[25] Thus, the Hermiticity relation does not hold for an approximate S operator. However, the deviations from the exact symmetry are very small (see Section III D).

C. Approximations

In order to obtain computationally tractable expressions for the transition moments, we employ several levels of

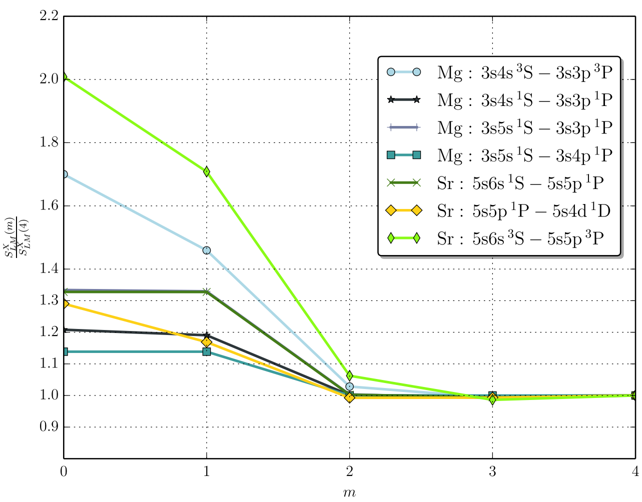

FIG. 1. Convergence of the XCC transition strengths with the MBPT order (m) for transition dipole strengths for Mg and Sr atoms. The T amplitudes are at the CC3/CCSD level of theory.

TABLE I. Singlet and triplet energy levels (cm^{-1}) of the magnesium atom computed using Gaussian (G) and Slater (S) basis sets. E_{exp} is given as an absolute value, and the computed energies are given as deviations from the experimental energy.

Level	E_{exp}	XCCSD(G)[a]	XCC3(G)[a]	XCCSD(S)[b]	XCC3(S)[b]	XCCSD(S)[c]	XCC3(S)[c]
$3p^1P^\circ$	350 51	246	269	13	111	69	87
$4s^1S$	435 03	421	413	103	115	37	92
$3d^1D$	464 03	497	356	194	132	241	121
$4p^1P^\circ$	493 46	394	363	413	443	11	56
$5s^1S$	525 56	214	186	...	...	261	168
$3p^3P^\circ$	218 91	525	...	241	...	292	...
$4s^3S$	411 97	447	...	118	...	110	...
$4p^3P^\circ$	478 48	399	...	10	...	46	...
$3d^3D$	479 57	1325	...	...	...	85	...

[a]Gaussian basis set: d-aug-cc-pVQZ.[41,42]
[b]Slater basis set: mg-dawtcc4d basis of Lesiuk *et al.*[40,43,44] with a similar number of basis functions as the Gaussian basis set.
[c]Slater basis set: mg-dawtcc5d basis of Lesiuk *et al.*[40,43,44]

TABLE II. Transition strengths $\mathcal{S}_{LM}^X$ (a.u.) in the XCC and QRCC methods for the Mg atom.

Transition	XCCSD(G)[a]	XCC3(G)[a]	QRCCSD(G)[a]	QRCC3(G)[a]	XCCSD(S)[b]	XCC3(S)[b]
$3s4s^1S$-$3s3p^1P^\circ$	16.2	16.0	18.3	18.3	16.0	15.8
$3s4p^1P^\circ$-$3s4s^1S$	70.4	69.9	73.7	69.6	71.6	70.8
$3s5s^1S$-$3s4p^1P^\circ$	101.8	101.7	101.6	101.6	97.8	98.2
$3s5s^1S$-$3s3p^1P^\circ$	0.3	0.3	0.4	0.4	0.3	0.3
$3s3d^1D$-$3s3p^1P^\circ$	12.7	12.2	10.3	10.0	23.7	20.3
$3s4p^1P^\circ$-$3s3d^1D$	41.8	42.4	43.0	...[c]	86.2	79.6

[a]Gaussian basis set: d-aug-cc-pVQZ.[41,42]
[b]Slater basis set: mg-dawtcc5d basis of Lesiuk *et al.*[40,43,44]
[c]Non-physical value. For details, see Section III D.

approximations to Eq. (36). There are three issues that we need to address in this equation: the level of truncation of the operator T, operator S, and of the multiply nested commutators resulting from the Baker-Campbell-Hausdorff expansion. We already stated that we employ the operator T from the CCSD/CC3 theory, and that we employ the approximate operator S defined by Eq. (13). To establish the best approximation of the multiply nested commutators, we performed the following procedure. We derived the orbital expressions separately for $S_{LM}^X(m) = (\mathcal{T}_{LM}^X \mathcal{T}_{ML}^X)(m)$, $m \in (0, 1, 2, 3, 4)$, where m is the leading-order in the many-body perturbation theory (MBPT). We computed the transition strength $S_{LM}^X(m)/S_{LM}^X(4)$ for the selected singlet and triplet transitions in the Mg and Sr atoms. In Fig. 1, we plotted the obtained transition strengths (normalized to $S_{LM}^X(4)$ for more clear view) versus the MBPT order m. We studied the behavior of the numerical values of the transition strength with the increase of the MBPT order and concluded that in every case the results converge to the numerical limit with the inclusion of third-order terms. Therefore in all our computations, we approximate the XCC transition strength to the third order in MBPT. It should also be mentioned that due to the computational limits for larger basis sets we discarded terms that scaled as N,[7] with N being a measure of the system size. We tested that those terms were of negligible importance. We want to clearly state here that the only approximation responsible for the possible Hermiticity violation in the XCC transition strength expression is the truncation of the operator S.

III. NUMERICAL RESULTS

A. Basis sets

Slater-type orbitals (STOs) used in this work were constructed according to the correlation-consistency principle,[39] similarly as by Lesiuk *et al.*[40] for the beryllium atom. The only difference in the procedure is that the exponents ζ were chosen according to the well-tempered formula, ($\zeta_{il} = \alpha_l + \beta_l i + \gamma_l i^2/n + \delta_l i^3/n^2$), where n is the number of basis set functions for a given angular momentum, l. After some numerical experimentation, the value of δ_l was set equal to zero for $l > 2$. A detailed composition of the STO basis sets is available from the authors upon request. The STO basis sets are usually significantly smaller when compared with the Gaussian-type basis sets of a comparable quality. Therefore there is a strong reason

TABLE III. Transition strengths $\mathcal{S}_{LM}^X$ (a.u.) for the Mg atom.

Transition	XCC3(G)[a]	XCC3(S)[b]	Chang	Fischer	Zheng
$3s4s^1S$-$3s3p^1P^\circ$	16.0	15.8	17.9	18.1	18.8
$3s4p^1P^\circ$-$3s4s^1S$	69.9	70.8	69.9	65.4	77.2
$3s5s^1S$-$3s4p^1P^\circ$	101.8	98.2	91.7	92.3	87.4
$3s5s^1S$-$3s3p^1P^\circ$	0.3	0.3	0.4	0.3	0.9
$3s3d^1D$-$3s3p^1P^\circ$	12.2	20.3	21.5	21.4	61.5
$3s4p^1P^\circ$-$3s3d^1D$	42.4	79.6	76.6	81.9	83.7

[a]Gaussian basis set: d-aug-cc-pVQZ.[41,42]
[b]Slater basis set: mg-dawtcc5d basis of Lesiuk *et al.*[40,43,44]

TABLE IV. Lifetimes (in ns) of the singlet excited states of the magnesium atom.

Reference	3s3p 1P°	3s4s ^{1}S	3s3d ^{1}D	3s4p ^{1}P°	3s5s^{1}S
			Experiment		
Gratton[49]	...	46.2 ± 2.6	74.8 ± 3	14.3	101.0 ± 3.5
Chantepie[51]	2.3	44.0 ± 5	72.0 ± 4	13.4 ± 0.5	102.0 ± 5
Jönsson[52]	...	47.0 ± 3	81.0 ± 6	...	100.0 ± 5
Schaefer[50]	...	...	57.0 ± 4	...	163.0 ± 8
			Theory		
Fischer[46]	2.1	44.8	77.2	13.8	102.0
Chang[47]	2.1	45.8	79.5	14.3	100.0
Zheng[48]	...	42.3	27.4	...	65.3
QRCC3(G)[a]	2.1	47.0	200	...[b]	99.8
XCC3(G)[a]	2.1	53.8	163.9	14.6	91.9
XCC3(S)[c]	2.1	51.7	79.7	14.1	111.9

[a]Gaussian basis set: d-aug-cc-pVQZ.[41,42]
[b]Not converged.
[c]Slater basis set: mg-dawtcc5d basis of Lesiuk *et al.*[40,43,44]

TABLE V. Lifetimes (in ns) of the triplet excited states for the Mg atom.

Reference	3s4s ^{3}S	3s5s ^{3}S	3s4p ^{3}P	3s3d ^{3}D
		Experiment		
Aldenius[53]	11.5 ± 1.0	29.0 ± 0.3	...	5.9 ± 0.4
Kwiatkowski[54]	9.7 ± 0.6	...	...	5.9 ± 0.4
Andersen[55]	10.1 ± 0.8	...	...	6.6 ± 0.5
Schaefer[50]	14.8 ± 0.7	25.6 ± 2.1	...	11.3 ± 0.8
Ueda[56]	9.9 ± 1.25	...	...	5.93
Havey[57]	9.7 ± 0.5	...	...	...
Gratton[49]	9.8 ± 0.3	25.6 ± 2.1	...	...
		Theory		
Fischer[46]	9.86	26.8	74.5	6.18
Moccia[58]	9.7	26.5	81.0	5.8
Victor[59]	9.07	...	...	6.25
Chang[47]	9.98	27.5	77.0	5.89
Mendoza[60]	9.79	...	...	...
Zheng[48]	...	...	78.49	...
XCCSD(S)[a]	12.7	29.87	70.44	5.33

[a]Slater basis set: mg-dawtcc5d basis of Lesiuk *et al.*[40,43,44]

to use them in the computationally demanding coupled cluster theory.

In Table I, we demonstrate how the underlying coupled cluster approximation (CCSD/CC3) and the basis set (Gaussian/Slater) affect the calculated excitation energies for the magnesium atom. While including the connected triple amplitudes is important, the use of the Slater-type orbitals (STOs) yields a dramatic improvement in the accuracy of the excited state energies.

B. Comparison with the QRCC theory

Let us compare our results with the QRCC results obtained with the Dalton program package.[45] Although both methods originate from the coupled cluster theory, their working expressions are different, and in general, they are not expected to give identical results. We computed the first few singlet-singlet transition moments for the Mg atom with both methods. The results are given in Table II. One can see a relatively good agreement between the two methods.

It is clear from Table II that the CC3 approximation has a little effect on the transition strength values. Yet we use the CC3 approximation as it gives better excitation energies, necessary for the lifetime computations. We also present the results obtained with the Slater orbitals to emphasize the influence of this basis on the computed transition strengths. It is worth noting that the use of the Slater orbitals leads in some cases to substantially different results.

TABLE VI. Transition probabilities (10^6 s^{-1}) of the Sr atom.

Reference	5s6s^{1}S-5s5p^{1}P°	5s5p^{1}P°-5s4d^{1}D	5s6s^{3}S-5s5p^{3}P°	5s4d^{3}D-5s5p^{3}P°
		Experiment		
Hunter[62]	...	0.0039 ± 0.0016	...	...
Jönsson[52]	...	...	66.0 ± 4	...
Brinkmann[64]	...	...	91.0 ± 2.5	...
Havey[57]	...	...	77.0 ± 4.5	...
Borisov[65]	...	...	...	0.24 ± 0.04
Miller[66]	...	...	...	0.29 ± 0.03
		Theory		
Werij[61]	18.6	0.0017	71.3	4.32
Vaeck[67]	...	0.0048	...	...
Porsev[63]	...	...	70.9	0.41
XCC3(G)[a]	15.1	0.0027	47	0.70
QRCC3(G)[a]	20.4	...[b]	...[c]	...[c]

[a]Gaussian basis set: [8s8p5d4f1g] basis augmented by a set of [1s1p1d1f3g] diffuse functions and the ECP28MDF pseudopotential.[9,41,42,68]
[b]Not converged.
[c]Not implemented.

C. Comparison with the available theoretical and experimental data

In Table III, we present a comparison of our computed transition strengths with other theoretical approaches, the relativistic multiconfigurational Hartree–Fock approximation,[46] the CI approximation with the *B*-spline basis,[47] and the semi-empirical weakest bound electron potential model.[48] The $\mathcal{S}^X_{LM}$ values of Chang and Tang were derived from A^X_{LM} with the experimental excitation energies.

The XCC3(S) results are in a much better agreement with the results calculated with other theoretical methods than the results obtained with the XCC3(G) and QRCC3(G) methods. The most dramatic improvement is observed for the 3d^{1}D-3p^{1}P° and 4p^{1}P°-3d^{1}D transitions.

The combination of the XCC3 method and the STO basis set results in lifetimes of the excited states of the Mg atom in a very good agreement with the available experimental and theoretical data (Tables IV and V). For the singlet states, we find an excellent agreement with the most recent experimental data[49] but not with the older experiment of Schaefer.[50] The mean absolute percentage error of our results for the singlet states is about 8% relative to the data of Gratton[49] and the largest error, slightly above 10%, is found for the 3s4s^1 S state. Our results are also consistent with the lifetimes computed by Fischer[46] and Chang,[47] but they are in significant disagreement with the semi-empirical values of Zheng.[48] Note parenthetically that no experimental uncertainty is attributed to some of the values given in Tables IV and V, and thus it is difficult to access their reliability in several cases.

All the computed lifetimes for the triplet states of Mg agree well with the existing experimental and theoretical results (Table V). Remarkably, the XCCSD(S) results are close to the most recent experimental data of Aldenius[53] for all states where the data are available. The mean absolute percentage deviation from this data is about 8%, and the largest error is found for the 3s4s ^{3}S state. For the 3s5s ^{3}S state, other theoretical results support the older values of Schaefer[50] and Gratton.[49] Similarly, in the case of the 3s4s ^{3}S state, the lifetimes calculated at the XCCSD(S) level are slightly larger than the other theoretical results, yet in an excellent agreement with the Aldenius experiment.[53] For the 3s4p ^{3}P state, there are no experimental results available, but all the theoretical lifetimes, including the XCCSD(S) one, are consistent within 10% at worst. The triplet-triplet transition dipole moments which are necessary to compute the lifetimes of the triplet states are not available in the QRCC implementation. Therefore, no comparison with the QRCC method is possible.

In Table VI, we present transition probabilities for the Sr atom. For the singlet states, we note a good agreement with the Werij[61] results. For the 5s5p^{1}P°-5s4d^{1}D transition, our result is also within the experimental error of Hunter, Walker, and Weiss.[62] In the case of 5s6s^{3}S-5s5p^{3}P° transition, our result deviates significantly from other theoretical and experimental results. The 5s4d^{3}D-5s5p^{3}P° transition strengths vary between different theories and experiments to a large degree. Our result is in reasonable agreement with the latest theoretical result of Porsev *et al.*[63]

TABLE VII. $\mathcal{T}^X_{LM}$ and $(\mathcal{T}^X_{ML})^\star$ computed with the QRCC and XCC methods for the Mg atom.

Transition	$\mathcal{T}^X_{LM}$ (QRCC)	$(\mathcal{T}^X_{ML})^\star$ (QRCC)	$\mathcal{T}^X_{LM}$ (XCC)	$(\mathcal{T}^X_{ML})^\star$ (XCC)
		aug-cc-pVQZ		
3s4s^{1}S-3s3p^{1}P°	4.3	4.26	4.00	4.01
3s4p^{1}P°-3s4s^{1}S	8.39	8.30	8.36	8.36
		d-aug-cc-pVQZ		
3s5s^{1}S-3s4p^{1}P°	10.12	10.04	10.08	10.09
3s5s^{1}S-3s3p^{1}P°	0.60	0.60	0.51	0.51
3s3d^{1}D-3s3p^{1}P°	0.67	−0.40	1.40	1.43
3s4p^{1}P°-3s3d^{1}D	−1.18	0.72	2.64	2.63

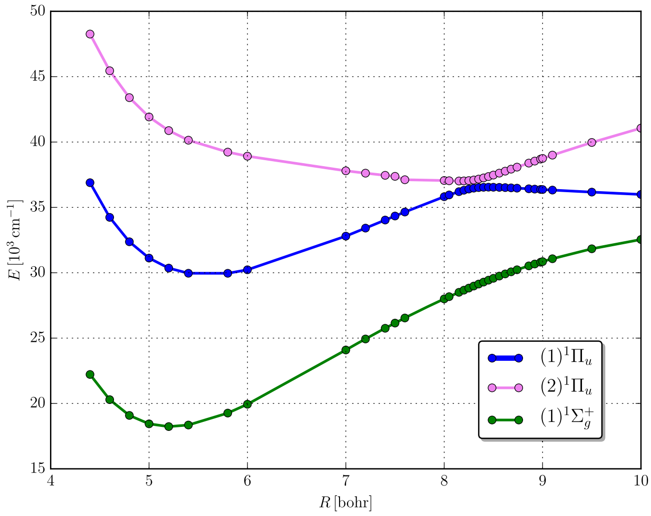

FIG. 2. Potential energy curves for Mg_2 states.

D. Possible Hermiticity violation and its consequences

The exact transition moment $\mathcal{T}^X_{LM}$ is Hermitian, i.e., it satisfies the relation given by Eq. (5). This implies that the

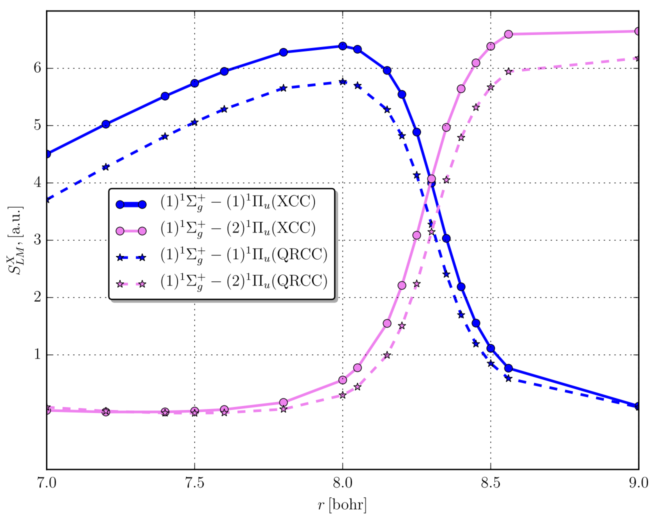

FIG. 3. Transition strengths for Mg_2 computed with the XCCSD(G) and QRCCSD(G) methods for R = 7-9 a.u.

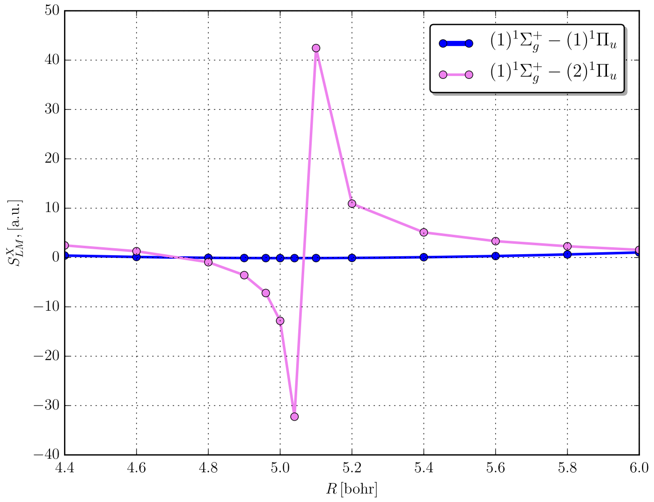

FIG. 4. Transition strengths for Mg_2 computed with the QRCC3(G) method.

transition strength $\mathcal{S}_{LM}^X$, Eq. (2), cannot be negative. This condition is not satisfied in the QRCC theory as well as in the approximate XCC theory. However, in the XCC theory, this violation of the Hermiticity originates solely from the truncation of the S operator, while in the QRCC method it has a more fundamental origin. Therefore, the lack of the Hermiticity is expected to be a fairly minor issue in our method, by contrast to the QRCC theory.

For the purpose of this study, we investigate some problematic transitions in the Mg atom and Mg_2 molecule which have been encountered beforehand.[6] We found that the transition strengths for the $3d^1D$-$3p^1P°$, $3d^1D$-$4p^1P°$, and $3d^1D$-$5p^1P°$ transitions computed with the QRCC code exhibited a non-physical behavior, i.e., some of the contributions were negative. No such artifacts were found in any transition strength contributions with the XCC theory. In Table VII, we present the differences between $\mathcal{T}_{LM}^X$ and $(\mathcal{T}_{ML}^X)^\star$ computed with the QRCC and XCC theories. In QRCC, these differences are significant, especially in situations where one is positive and the other is negative. Although in the XCC method, the Hermiticity is also violated, we do not observe such strong deviations.

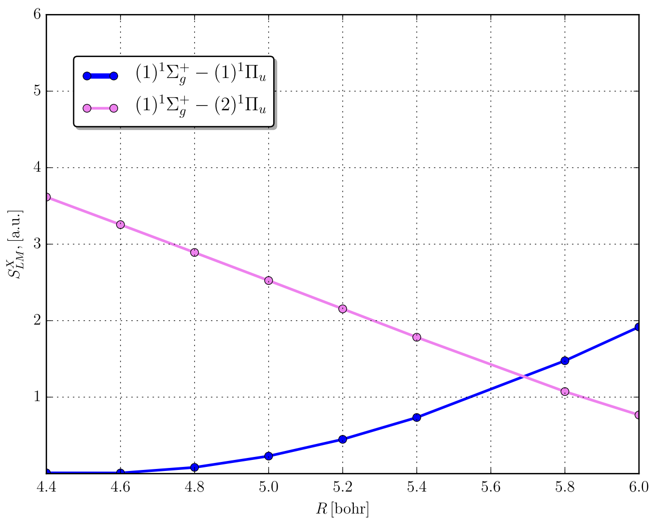

FIG. 5. Transition strengths for Mg_2 computed with the XCCSD method.

A different problem is found for the Mg_2 molecule. In Fig. 2, we present potential energy curves for $(1)^1\Pi_u$, $(2)^1\Pi_u$, and $(1)^1\Sigma_g^+$ states of Mg_2 computed with the EOM-CCSD approximation. We also present a set of transition strengths for various interatomic distances R computed with the XCCSD(G) and QRCCSD(G) methods, Fig. 3. For R ranging from 7 to 9 bohr, both methods give similar results. However, the QRCCSD(G) method exhibits problems at small distances where we obtained negative transition strengths that by definition (2) should always be positive. In Fig. 4, we see a pole-like structure which is clearly an artifact, as no such structure should be observed for the transition strengths. By contrast, no such difficulties were found in the XCCSD(G) theory, see Fig. 5. This suggests that the adopted truncation scheme for the S operator has a negligible impact on the behavior of the XCC transition moments.

IV. CONCLUSIONS

We have presented a novel coupled cluster approach to the computation of the transition moments between the excited electronic states. In contrast to the existing CC approaches, our method approximately obeys the Hermiticity relation $(\mathcal{T}_{LM}^X) = (\mathcal{T}_{ML}^X)^\star$, and the deviations from this symmetry are negligible. There are three levels of approximations in our formulas for $\mathcal{T}_{LM}^X$

1. the underlying model for the CC amplitudes (CCSD/CC3),
2. approximations of the auxiliary operator S employed in the computation of the expectation values with the CC ground state wave function,
3. choice of the commutators included in the expansion of the XCC formula for $\mathcal{T}_{LM}^X$.

In trouble-free situations, i.e., when the existing QRCC approach satisfies the Hermiticity relation to a good approximation, both methods yield transition moments of a similar quality. However, in certain cases, the QRCC method violates the Hermiticity relation to an unacceptable degree and gives unphysical values of the transition strengths. The XCC method does not suffer from this problem. Clearly, this can be viewed as an important improvement over the existing QRCC approach.

We have presented numerical examples for several singlet-singlet and triplet-triplet dipole transitions in the Mg and Sr atoms, and the Mg_2 molecule. Lifetimes derived from the transition moments computed with our method are, in most cases, very close to the available experimental data and to other theoretical results. We have assessed the performance of our method in the STO basis set and obtained results of significantly better quality than with the available Gaussian basis sets. In certain cases, the use of STO basis set was the game-changer.

In two of the forthcoming papers, we will consider calculations of the radial and angular nonadiabatic coupling matrix elements and of the spin-orbit coupling matrix elements between the excited states within the XCC theory. Both works are in preparation.

The code for transition moments between the excited states will be incorporated in the KOŁOS: A general purpose *ab initio* program for the electronic structure calculation with Slater orbitals, Slater geminals, and Kołos-Wolniewicz functions.

ACKNOWLEDGMENTS

This research was supported in part by the National Science Foundation under Grant No. NSF PHY-1125915 and by the National Science Centre (NCN) under Grant No. 2016/21/N/ST4/03734.

[1] D. Zubarev, Usp. Fiz. Nauk **3**, 320 (1960).
[2] J. Linderberg and Y. Öhrn, *Propagators in Quantum Chemistry* (John Wiley & Sons, 2004).
[3] J. Oddershede, Adv. Chem. Phys. **69**, 201 (1987).
[4] L. Rybak, Z. Amitay, S. Amaran, R. Kosloff, M. Tomza, R. Moszynski, and C. P. Koch, Faraday Discuss. **153**, 383 (2011).
[5] L. Rybak, S. Amaran, L. Levin, M. Tomza, R. Moszynski, R. Kosloff, C. P. Koch, and Z. Amitay, Phys. Rev. Lett. **107**, 273001 (2011).
[6] S. Amaran, R. Kosloff, M. Tomza, W. Skomorowski, F. Pawłowski, R. Moszynski, L. Rybak, L. Levin, Z. Amitay, J. M. Berglund, D. M. Reich, and C. P. Koch, J. Chem. Phys. **139**, 164124 (2013).
[7] L. Levin, W. Skomorowski, L. Rybak, R. Kosloff, C. P. Koch, and Z. Amitay, Phys. Rev. Lett. **114**, 233003 (2015).
[8] R. M. Wilson, Phys. Today **68**, 19 (2015).
[9] W. Skomorowski, F. Pawłowski, C. P. Koch, and R. Moszynski, J. Chem. Phys. **136**, 194306 (2012).
[10] B. McGuyer, M. McDonald, G. Iwata, M. Tarallo, W. Skomorowski, R. Moszynski, and T. Zelevinsky, Nat. Phys. **11**, 32 (2015).
[11] M. McDonald, B. McGuyer, F. Apfelbeck, C.-H. Lee, I. Majewska, R. Moszynski, and T. Zelevinsky, Nature **534**, 122 (2016).
[12] B. McGuyer, C. Osborn, M. McDonald, G. Reinaudi, W. Skomorowski, R. Moszynski, and T. Zelevinsky, Phys. Rev. Lett. **111**, 243003 (2013).
[13] B. McGuyer, M. McDonald, G. Iwata, W. Skomorowski, R. Moszynski, and T. Zelevinsky, Phys. Rev. Lett. **115**, 053001 (2015).
[14] M. Tomza, M. H. Goerz, M. Musiał, R. Moszynski, and C. P. Koch, Phys. Rev. A **86**, 043424 (2012).
[15] W. Skomorowski and R. Moszynski, J. Chem. Phys. **134**, 124117 (2011).
[16] M. Tomza, W. Skomorowski, M. Musiał, R. González-Férez, C. P. Koch, and R. Moszynski, Mol. Phys. **111**, 1781 (2013).
[17] H. Koch and P. Jørgensen, J. Chem. Phys. **93**, 3333 (1990).
[18] T. B. Pedersen and H. Koch, J. Chem. Phys. **106**, 8059 (1997).
[19] G. W. Drake, *Springer Handbook of Atomic, Molecular, and Optical Physics* (Springer, New York, 2006).
[20] H. Koch, R. Kobayashi, A. S. de Meras, and P. Jørgensen, J. Chem. Phys. **100**, 4393 (1994).
[21] O. Christiansen, P. Jørgensen, and C. Hättig, Int. J. Quantum Chem. **68**, 1 (1998).
[22] A. M. Tucholska, M. Modrzejewski, and R. Moszynski, J. Chem. Phys. **141**, 124109 (2014).
[23] R. Moszynski, P. S. Żuchowski, and B. Jeziorski, Collect. Czech. Chem. Commun. **70**, 1109 (2005).
[24] F. Pawłowski, J. Olsen, and P. Jørgensen, J. Chem. Phys. **142**, 114109 (2015).
[25] B. Jeziorski and R. Moszynski, Int. J. Quantum Chem. **48**, 161 (1993).
[26] J. Čížek, J. Chem. Phys. **45**, 4256 (1966).
[27] J. Čížek, J. Paldus, and L. Šroubková, Int. J. Quantum Chem. **3**, 149 (1969).
[28] J. Noga and M. Urban, Theor. Chim. Acta **73**, 291 (1988).
[29] H. J. Monkhorst, Int. J. Quantum Chem. **12**, 421 (1977).
[30] J. Arponen, R. Bishop, and E. Pajanne, Phys. Rev. A **36**, 2519 (1987).
[31] J. Arponen, Ann. Phys. **151**, 311 (1983).
[32] S. Pal, Theor. Chim. Acta **66**, 151 (1984).
[33] S. Pal, Theor. Chim. Acta **68**, 379 (1985).
[34] S. Pal, Phys. Rev. A **33**, 2240 (1986).
[35] S. Pal, Phys. Rev. A **42**, 4385 (1990).
[36] T. Helgaker, P. Jørgensen, and J. Olsen, *Molecular Electronic-Structure Theory* (Wiley, New York, 2013).
[37] H. Koch, O. Christiansen, P. Jørgensen, A. M. Sanchez De Merás, and T. Helgaker, J. Chem. Phys. **106**, 1808 (1997).
[38] T. Korona, M. Przybytek, and B. Jeziorski, Mol. Phys. **104**, 2303 (2006).
[39] T. H. Dunning, Jr., J. Chem. Phys. **90**, 1007 (1989).
[40] M. Lesiuk, M. Przybytek, M. Musiał, B. Jeziorski, and R. Moszynski, Phys. Rev. A **91**, 012510 (2015).
[41] D. Feller, J. Comput. Chem. **17**, 1571 (1996).
[42] K. L. Schuchardt, B. T. Didier, T. Elsethagen, L. Sun, V. Gurumoorthi, J. Chase, J. Li, and T. L. Windus, J. Chem. Inf. Model. **47**, 1045 (2007).
[43] M. Lesiuk and R. Moszynski, Phys. Rev. E **90**, 063318 (2014).
[44] M. Lesiuk and R. Moszynski, Phys. Rev. E **90**, 063319 (2014).
[45] K. Aidas, C. Angeli, K. L. Bak, V. Bakken, R. Bast, L. Boman, O. Christiansen, R. Cimiraglia, S. Coriani, P. Dahle *et al.*, Wiley Interdiscip. Rev.: Comput. Mol. Sci. **4**, 269 (2014).
[46] C. F. Fischer, Can. J. Phys. **53**, 338 (1975).
[47] T. Chang, Phys. Rev. A **34**, 4550 (1986).
[48] N. W. Zheng, T. Wang, R. Y. Yang, T. Zhou, D. X. Ma, Y. G. Wu, and H. T. Xu, At. Data Nucl. Data Tables **79**, 109 (2001).
[49] R. G. Gratton, E. Carretta, R. Claudi, S. Lucatello, and M. Barbieri, Astron. Astrophys. **404**, 187 (2003).
[50] A. Schaefer, Astrophys. J. **163**, 411 (1971).
[51] M. Chantepie, B. Cheron, J. Cojan, J. Landais, B. Laniepce, A. Moudden, and M. Aymar, J. Phys. B **22**, 2377 (1989).
[52] G. Jönsson, C. Levinson, A. Persson, and C.-G. Wahlström, Z. Phys. A **316**, 255 (1984).
[53] M. Aldenius, J. D. Tanner, S. Johansson, H. Lundberg, and S. G. Ryan, Astron. Astrophys. **461**, 767 (2007).
[54] M. Kwiatkowski, U. Teppner, and P. Zimmermann, Z. Phys. A **294**, 109 (1980).
[55] T. Andersen, L. Molhave, and G. Sorensen, Astrophys. J. **178**, 577 (1972).
[56] K. Ueda, M. Karasawa, and K. Fukuda, J. Phys. Soc. Jpn. **51**, 2267 (1982).
[57] M. Havey, L. Balling, and J. Wright, J. Opt. Soc. Am. **67**, 488 (1977).
[58] R. Moccia and P. Spizzo, J. Phys. B **21**, 1133 (1988).
[59] G. Victor, R. Stewart, and C. Laughlin, Astrophys. J., Suppl. Ser. **31**, 237 (1976).
[60] C. Mendoza, J. Phys. B **14**, 397 (1981).
[61] H. Werij, C. H. Greene, C. Theodosiou, and A. Gallagher, Phys. Rev. A **46**, 1248 (1992).
[62] L. Hunter, W. Walker, and D. Weiss, Phys. Rev. Lett. **56**, 823 (1986).
[63] S. Porsev, A. D. Ludlow, M. M. Boyd, and J. Ye, Phys. Rev. A **78**, 032508 (2008).
[64] U. Brinkmann, J. Goschler, A. Steudel, and H. Walther, Z. Phys. **228**, 427 (1969).
[65] E. N. Borisov, N. P. Penkin, and T. P. Redko, Opt. Spectrosc. **63**, 475 (1987).
[66] D. Miller, L. You, J. Cooper, and A. Gallagher, Phys. Rev. A **46**, 1303 (1992).
[67] N. Vaeck, M. Godefroid *et al.*, Phys. Rev. A **38**, 2830 (1988).
[68] I. S. Lim, H. Stoll, and P. Schwerdtfeger, J. Chem. Phys. **124**, 034107 (2006).